# Surface Circulation in the Tropical Indian Ocean Using Multi-Mission Altimeter Data

Thesis submitted to the
## Cochin University of Science and Technology

*In partial fulfillment of the requirement for the Degree of*

## Doctor of Philosophy
in
## Oceanography

By

## AKULA RAGHUNADHA RAO

## Naval Physical & Oceanographic Laboratory
**Defence Research and Development Organisation**
**Ministry of Defence, Government of India**
**Thrikkakara, Kochi-682021**

to my beloved
parents..

# DECLARATION

I hereby declare that the thesis entitled '***Surface Circulation in the Tropical Indian Ocean Using Multi-Mission Altimeter Data'*** is a genuine record of research work carried out by me and no part of the thesis has been submitted to any University or Institution for the award of any Degree or Diploma.

<div align="right">

A RAGHUNADHA RAO

Naval Physical and Oceanographic Laboratory

Thrikkakara

Kochi-682021
</div>

Kochi
1 July 2008

# CERTIFICATE

This is to certify that the thesis entitled *'Surface Circulation in the Tropical Indian Ocean Using Multi-Mission Altimeter Data'* is a *bona fide* record of research work done by Shri. A. Raghunadha Rao, scientist, Naval Physical and Oceanographic Laboratory. He carried out the study reported in this thesis independently under my supervision. I also certify that the subject matter of the thesis has not formed the basis for the award of any degree or diploma of any University or Institution.

This is to certify that Shri A. Raghunadha Rao has passed the Ph.D qualifying examination conducted by the Cochin University of Science and Technology in November 2005.

**Basil Mathew**
(Supervising guide)

Kochi
1 July 2008

# ACKNOWLEDGEMENTS

# PREFACE

Oceans play an important role in the development of mankind. History tells us civilizations evolved with the availability of resources. Initially knowledge on surface currents in the ocean is used effectively for navigation. Latter the role of ocean circulation in redistributing energy and in driving atmosphere is recognized. Because of oceans vastness and vagaries it is impossible to observe entire ocean on synoptic time scales on regular basis. Most of the knowledge on surface currents is the compilation of sparsely collected data sets. Well organized International Indian Ocean Expedition to World Ocean Circulation experiment there has been tremendous improvement. The advent of satellite altimetry changed the line of research and given an ample opportunity to the researchers to observe global oceans on weekly interval.

This study made use of such dataset generated using constellations of satellites carrying altimeters. Geostrophic surface currents is computed using Sea Surface Height parameter derived from altimeter data available on regular grids. Studies during WOCE period proved geostrophic component of currents is the most dominant on seasonal time scales except along the coasts and some parts of equator. In this study surface circulation is described using geostrophic currents derived from the altimeter data on seasonal and interannual time scales.

In the first chapter introduction is given. Unique geographical setup of Indian Ocean and the previous studies on circulation is described in the beginning. In latter sections the concept of altimeter and methodology for calculating geostrophic currents is given. Finally the objective of the study is defined.

In the second chapter seasonal variability is described using monthly climatology computed using 12 year multi-mission altimeter data. Months of season described together for better understanding.

In the third chapter interannual variability is described using monthly means of 12 years data. In the initial sections year to year variability is presented. To identify the dominant areas of such variability spatial Empirical Orthogonal Functions are used. In latter sections the role of wind has been examined in such dominant areas using wavelet analysis on time series of wind data.

In the fourth chapter the role of planetary waves on the circulation is presented. Initially the presence and variability of planetary waves is described. Latter based on two case studies one in the Arabian Sea and another in the Bay of Bengal the role of planetary waves on the circulation is described.

Finally the summary and conclusions are presented in the fifth chapter

**CHAPTER I**

**Introduction**

**1.1 Importance of circulation**

One of the key factors in understanding oceans is to study its circulation which charecterises its properties in spatio-temporal domain. The principle energy source for driving ocean circulation is the uneven distribution of the incoming solar radiation. Oceans have the capacity to hold large amounts of heat due to high specific heat of sea water, but their temperatures never rise beyond a certain level. This occurs because of the circulation in the ocean which redistributes the energy from places of surplus to places of deficit.

**1.2. Factors influencing circulation in the Indian Ocean**

In the world oceans, the Indian Ocean is in several respects unique when compared to the other oceans. The unique geographical setup, seasonally reversing monsoon winds and planetary waves in the Indian Ocean determine the pattern of circulation. The striking uniqueness of the Indian Ocean is briefly mentioned in the following sections.

**1.2.1 Geography of the Indian Ocean**

The Indian Ocean is the smallest and least explored ocean of the world oceans. It occupies aproximately 20% of the world ocean. It is bounded on the north by Asia; on the west by Africa; on the east by the Malay Peninsula, the Sunda Islands, and Australia; and on the south by the Southern Ocean. The Indian subcontinent divides the northern Indian Ocean into two smaller basins, the Arabian Sea in the west and the Bay of Bengal in the east (Fig 1.1). Two marginal seas, the Persian Gulf and Red Sea, join the Arabian Sea. The chain of the Andaman and Nicobar Islands separate the Andaman Sea from the Bay of Bengal.

The Indian Ocean does not extend to the cold climate regions of the northern hemisphere. Such a geographical situation causes asymmetry in its structure and circulation. The land mass of Asia has profound influence on the meteorology and oceanography of this region. The land-ocean contrast forces seasonally reversing winds, the monsoons, over the northern Indian Ocean, which in turn reverses the oceanic circulation. The monsoon winds are southwesterly during the summer monsoon and northeasterly during the winter monsoon. Associated with these seasonally changing winds upwelling occurs only during one season,

in contrast to all other major upwelling areas in the world oceans. Because the monsoon winds are asymmetrical about the equator, the current systems in the Indian Ocean are not symmetrical about the equator. The asymmetrical wind distribution generates convergence in the equatorial Indian Ocean. In other world oceans, divergence is observed near the equatorial regions. Another outgrowth of the geographical and climatological settings is the formation of high salinity waters in the Arabian Sea, the Red Sea and the Persian Gulf. These water masses form a high salinity layer in the Arabian Sea and affect the circulation in the intermediate depth drastically by limiting the water of the southern hemisphere from penetrating into the northern Indian Ocean. However, in the Bay of Bengal effects of precipitation and fresh water river runoff reduce the salinity in the surface layers. Another outgrowth of the peculiar geographical and climatological settings is the equatorward heat transport in the north Indian Ocean. The Indian Ocean has no polar or sub polar northern regions, resulting in a net southward heat export across the equator.
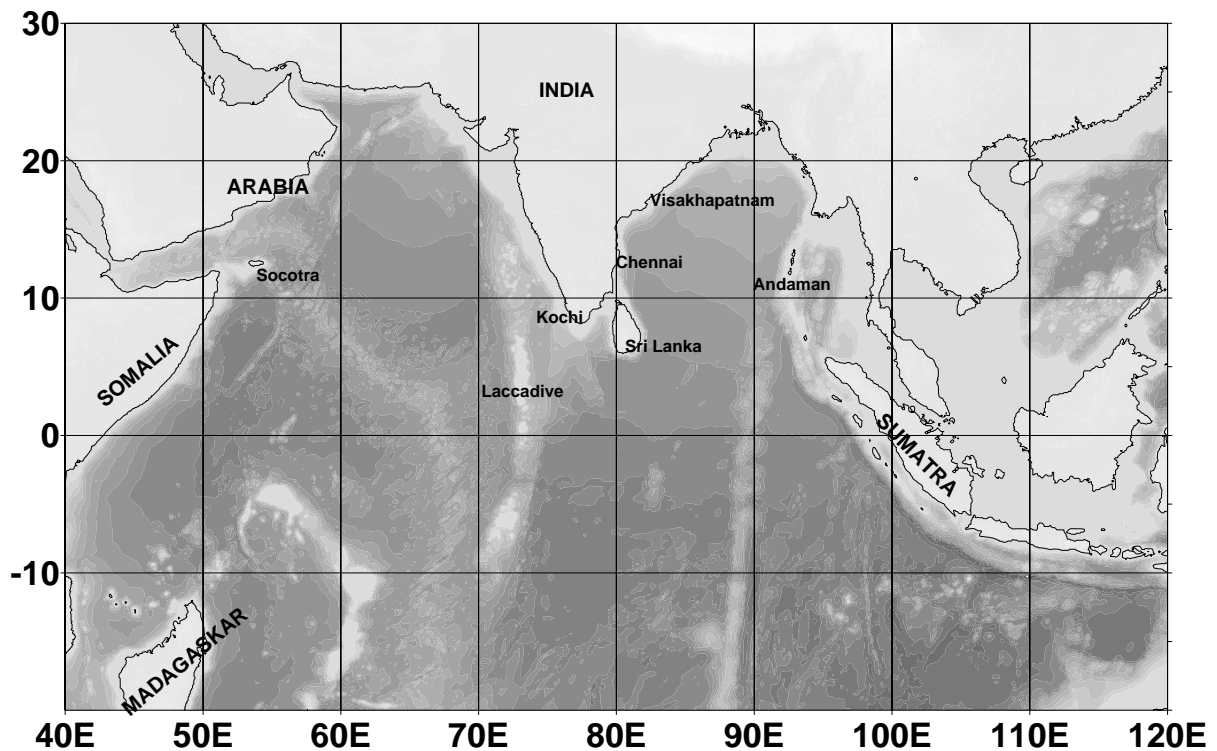


**Fig.1.1 Study area – the tropical Indian Ocean**

### 1.2.2 Geology and bathymetry

Geologically, the Indian Ocean is characterized with the presence of several submarine plateaus, ridges and hot spots. Many of these features trend in a north-south direction, and together with the active ridges and surrounding continents, the Indian Ocean is divided into a number of ocean basins. One of the outgrowths of these peculiar geological features is that the Indian Ocean has deep northward western boundary currents.

### 1.2.3 Winds over the Indian Ocean

Historically, surface wind measurements over the ocean are made primarily from ships. These measurements compiled over several decades are used to compute mean monthly climatology. One such climatology generated by NCEP is used in the present study to describe the observed seasonal cycle over the Indian Ocean. The detailed description of wind variability using different data sets is given in Schott, (2001). The seasonal cycle of the wind field is shown in Fig. 1.2, for January, April, July and October based on NCEP monthly-mean climatology. In the northern hemisphere during winter, the winds are directed away from the Asian continent, causing northeasterly wind stresses over the Arabian Sea and the Bay of Bengal (Fig. 1.2a), whereas during the summer monsoon, the winds are southwesterly over both the basins (Fig. 1.2c). In contrast to the winter situation, southern hemisphere trade winds sweep into the western Arabian Sea in the form of a narrow atmospheric jet called Findlater Jet (Findlater, 1971). South of 10°S, the southeast trades persist throughout the year. They have their seasonal maximum and northernmost extent during southern winter.

A unique wind forcing pattern occurs over the equatorial Indian Ocean, which is in contrast to the patterns in other equatorial oceans. Here the occurrence of semi-annual eastward winds over the equator, during April - June and October - November (Fig. 1.2 d) are observed. These winds generate zonal wind stress (along equator) that is eastward and so mean surface temperatures along the equator are warm due to absence of any significant equatorial upwelling in marked contrast with the other equatorial oceans.
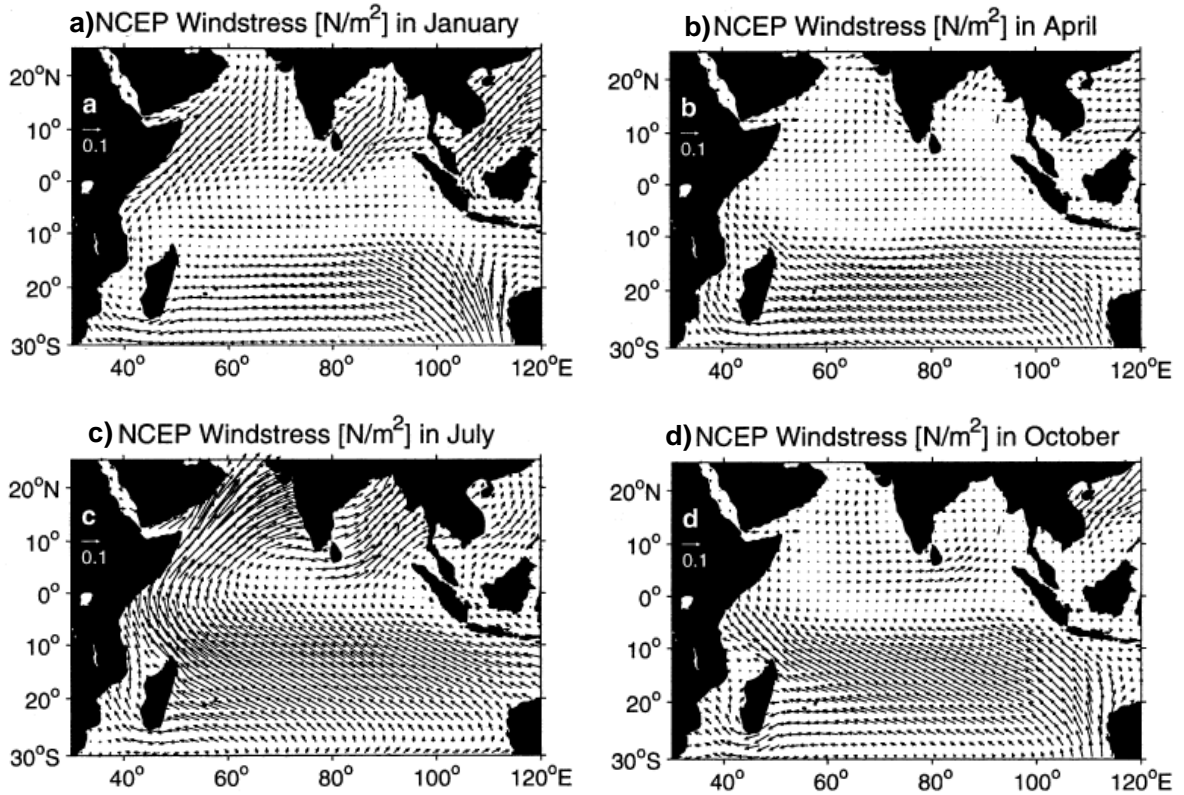
Fig. 1.2    Wind stress using NCEP climatology during a) January; b) April; c) July; d) November.

During April to May, weak alongshore winds occur off Somalia (Fig. 1.2 b). The subsequent onset of the summer monsoon occurs over the Arabian Sea in several different ways (Fieux & Stommel, 1977). In the annual mean the summer monsoon winds overwhelm the winds during the other seasons in the northern hemisphere, and the mean basin scale stress in the Arabian Sea is therefore anticyclonic. Planetary waves also play important role in determining the circulation. The next section gives a brief description on the planetary waves in the Indian Ocean.

## 1.2.4 Role of planetary waves and associated eddies

The seasonal monsoon winds over the equator trigger Kelvin waves and Rossby waves. These planetary waves play a vital role in the surface circulation and currents (Perigaud and Delecluse, 1992; Cipollini et al., 1997; Subrahmanyam et al., 2001; McCreary et al., 1993; 1996). Interestingly with the seasonal reversing monsoons, the surface currents

and boundary currents over the north Indian Ocean also reverse, though they are not in phase with the local winds. These differences with the wind forcing can be attributed to remote forcing by the planetary waves. During the summer monsoon, the circulation in the western Indian Ocean evolves into a complex pattern of mesoscale eddies and gyres. The role of planetary waves in the development of eddy type circulation is evident. Previous studies indicated that the unique geographical setup, seasonal reversing winds and planetary waves in the Indian Ocean determines the pattern of circulation.

## 1.3 Previous studies on circulation

The Indian Ocean was the least studied till the late 1950's. The existence of seasonally reversing currents in the Arabian Sea has been mentioned in the medieval Arab texts (Warren, 1966). The International Indian Ocean Expedition (IIOE) conducted during 1962 – 1965 improved the situation (Duing, 1970; Wyrtki, 1971; Colborn, 1975). Three major international observational experiments were conducted in the Arabian Sea and the Bay of Bengal in the 1970s, namely, ISMEX-73, MONSOON-77 and MONEX-79. These experiments involved four Soviet Union (USSR) ships forming a polygons. Rao et al (1987) explored these experimental data and emphasized the need of intense observational programs in the Indian Ocean. Nevertheless, important ideas did not exist or were not clear when the IIOE atlas was prepared, and the hydrography and circulation of the Indian Ocean still requires much study. The study of the Indian Ocean dynamics was restricted to the analysis of ship drift data and did not reach below the surface layer over a long period of time. Long-term current meter moorings were not deployed till the mid and late seventies (Knox, 1976; Swallow et al., 1983).

The response of the Somali Current system to monsoonal wind forcing was brought out using experimental data sets (Swallow and Bruce, 1966; Swallow et al., 1983). The ocean circulation studies gained momentum since 1995 when a comprehensive survey of the Indian Ocean (Ffield, 1997; Hacker et al., 1998) was undertaken under the World Ocean Circulation Experiment (WOCE). Later on specific observational programs such as the Bay of Bengal Monsoon Experiment (BOBMEX) during 1999 (Bhat et al., 2001) and the Joint Air-Sea Monsoon Interaction Experiment (JASMINE) (Webster et al., 2002) to study monsoon variability were conducted.

Wyrtki (1971) noted that the circulation in the Indian Ocean is complex; the winter monsoon gyre does not close cleanly in the east, with most of the flow from the South Equatorial Counter Current (SECC) flowing into the South Equatorial Current (SEC), and a strong branch of the Winter Monsoon Current (WMC) turning north to flow along the Indian west coast, transporting low-salinity water from the Bay of Bengal into the eastern Arabian Sea. The circulation during the winter monsoon was shallow compared with that during the summer monsoon, when intense upwelling was observed in several places and the circulation penetrated deeper, affecting the movement of water masses below the thermocline, especially in the western Arabian Sea. The complexity of the circulation represented by the hydrographic data was seen in the large number of eddies (Duing, 1970; Wyrtki, 1971), which were found to be connected intimately to the dynamics of the monsoon gyre. The most vigorous of these eddies lay about 300 km offshore of the Somali coast; large parts of the Somali Current were re-circulated around this eddy, known as the 'Great Whirl' (Bruce, 1968).

Shenoi et al (1999a) compared hydrography based on the climatologies of Levitus and Boyer (1994) and Levitus et al., (1994) to currents from surface drifters, and concluded that the role of geostrophy in representing the surface flows varies both geographically and seasonally. The agreement between the drifter data and hydrography was less during the summer monsoon, when the drifters showed southeastward flows all over the Arabian Sea, unlike in the hydrography. Flagg and Kim (1998) discussed relative merits and demerits of insitu measurements, they used ship borne ADCP data collected during JGOFS and showed that the currents in the Arabian Sea are more of geostrophic except along coastal boundaries.

Hydrographic data, however, were also used in later studies (Bruce et al 1994; Bruce et al 1998; Donguy & Meyers, 1995; Murty et al 1992; Murty et al., 2000; Gopalakrishna, Pednekar, & Murty, 1996; Vinayachandran et al., 1999), which showed strong geostrophic flows and transports associated with the monsoon currents. These estimates yield current strengths of ~40 cm/s and transports of ~ 10Sv in the upper 400 or 1000 m, which implies that the geostrophic flows associated with the monsoon currents, are not small. However the surface Ekman flows may become significant in some regions during some seasons. The geostrophic flows estimated by Hastenrath and Greischar (1991) are weak probably because of the poor resolution of the data and the averaging they did to obtain climatological currents

and transports in a region. In contrast, except for the IIOE atlas (Wyrtki, 1971), the hydrographic data are usually from individual cruises. These data, which yield higher estimates for the geostrophic transports, show that the monsoon currents are not found in the same location during a given season or during different years. For example, Vinayachandran et al. (1999) showed that the Summer Monsoon Current (SMC) in the Bay of Bengal intensifies and shifts westwards as the summer monsoon progresses; this westward shift with time is also seen in the surface geostrophic flow inferred from TOPEX/Poseidon altimetry (Eigenheer & Quadfasel, 2000). In spite of these differences, all the observations— hydrography, ship drifts, and from surface drifters— show that the monsoon currents flow across the breadth of the north Indian Ocean. The branches of the SMC and WMC that flow around the Laccadive High and Low in the southeastern Arabian Sea (McCreary et al., 1993; Bruce et al., 1994; Shankar & Shetye, 1997) link the circulations in the Arabian Sea and the Bay of Bengal. The SMC flows eastward south of Sri Lanka and into the Bay. It is fed by a flow from the southwest near the equator and by the flow around the Laccadive Low. East of Sri Lanka, the SMC flows northeastward into the Bay of Bengal. An outflow from it, however, appears to flow southeastward and crosses the equator near Sumatra in the surface-drifter data (Shenoi et al 1999a). Recent hydrographic data (Unnikrishnan et al 2001) also show that the eastward current between 80°E and 88°E flows close to the equator and even to the south of it. The SMC transports high-salinity water (Arabian Sea High Salinity Water) into the Bay (Wyrtki, 1971; Murty et al., 1992; Gopalakrishna et al., 1996; Han & McCreary, 2001). The WMC flows westward south of Sri Lanka, where it divides into two branches, one flowing westward into the southern Arabian Sea, the other flowing around the Lakshadweep High into the West India Coastal Current (WICC). The WMC transports low-salinity water (Bay of Bengal water) into the eastern Arabian Sea, where it is entrained into the Lakshadweep High and spread along the west coast of India by the WICC (Wyrtki, 1971; Bruce et al., 1994; Han, 1999; Shenoi et al  1999b; Shankar & Shetye, 1999; Han & McCreary, 2001; Han, McCreary, & Kohler, 2001; Howden & Murtugudde, 2001).

It is not surprising that the only direct current measurements of the monsoon currents have been made between Sri Lanka and the equator along 80.5°E (Schott, Reppin, Fischer, & Quadfasel, 1994; Reppin, Schott, Fischer, & Quadfasel, 1999). The current meter and ADCP (Acoustic Doppler Current Profiler) observations show that the SMC and WMC transport

~10Sv in the upper 300 m. These direct measurements also confirm hydrographic observations that the monsoon currents are shallow, with most of the variation being restricted to the upper 100 m. The moored array showed upward phase propagation, implying downward propagation of energy. Most striking was the difference between the Equatorial Current and the monsoon currents, even though both flow together through the same bottleneck (Schott et al., 1994; Reppin et al., 1999).

## 1.4 Present study

The seasonal circulation of the Indian Ocean hinges on currents derived from ship drift (Defant, 1961; Varadachari and Sharma 1967, Cuttler and Swallow 1984, Rao, Molinari, & Festa, 1989, Rao et al 1991), from geostrophic computations (Duing 1970, Wyrtki 1971). However these measurements basically suffer from isolated coverage or biased along a few shipping lanes in the Indian Ocean at random. The ocean circulation models have given simulations to comfortably fill in observational gaps (Kantha, 1999; Kantha et al., 1999; and Kantha et al., 2005) and explore the physics behind various processes (McCreary et al., 1993).  Although the circulation models overcame these limitations, their results are to be validated by direct current measurements at sea.

Though considerable advances have been made in the last few decades in understanding the circulation of the Indian Ocean, many aspects such as synoptic scale circulation in the entire Indian Ocean, its interannual variability, influence of propagating waves in modifying the circulation etc are yet to be fully resolved. The data from satellites especially sea surface height anomaly from altimeter provide a good tool to address these problems in much greater detail. The sparsely distributed insitu data gives only coarse synoptic view to interpret variations in the circulation pattern.

However, the above problems can be resolved by satellite measurements with their unique advantages, like near-simultaneous coverage of vast regions of the ocean, repeated coverage of these regions at short time intervals with reasonable resolution and accuracy. The advent of satellite data provides us the higher spatio –temporal mapping of the ocean on ~10 – 30 days for altimeter sea level (Fu et al., 1994). Utilizing satellite altimeter measurements

of Sea Surface Height (SSH) Prasanna Kumar et al (1998) and Ali et al (1998) presented the circulation in the north Indian Ocean.

In the present study, recent and more robust (12-year) T/P+ERS Altimeter Sea Level Anomaly (SLA) data over the Indian Ocean is analysed to describe the circulation features over an annual cycle and its interannual variability.

## 1.4.1 Area of study

The area of study is the Indian Ocean north of 20°S comprises major part of south Indian Ocean (covering the South Equatorial Current (SEC) region), the Arabian Sea and the Bay of Bengal. This is the area in which major seasonal variation in surface flow patterns are seen. In addition, planetary waves generated in the equatorial Indian Ocean and their propagation cause considerable change in the flow pattern in this region.

Taking all these in to account, wide area is selected for this study i.e., $40\text{-}120^0$E and $20^0$S to $30^0$N. This covers the Arabian Sea, the Bay of Bengal, the equatorial Indian Ocean and southern tropical Indian Ocean (Fig. 1.1).

## 1.4.2 Objectives

The main objectives are to study the following using long period satellite multi - mission altimeter data.

1. Describe and explain the observed seasonal variability of geostrophic circulation in the Indian Ocean.
2. Describe and explain the observed interannual variability of geostrophic circulation in the Indian Ocean.
3. Influence of propagating waves on the circulation.

The observational background described in the previous sections give the importance of studying the circulation in larger areas and synoptic time scales. Hence one of the promising data sets for this purpose is obviously from satellites especially from the altimeter. In this study multi-mission high resolution altimeter data has been primarily used to address the objectives.

## 1.5. Data and methodology

Insitu observations are not adequate for the quantitative description of either the mean or the fluctuating components of the global ocean circulation. The satellite altimeter measures the precise height of the sea surface for studying the dynamics of the circulation of the oceans. Other applications are the study of ocean tides, geod and geodynamics, ocean wave height, and wind speed.

### 1.5.1 Data used in this study

In this study all the processed Sea Surface Height (SSH) data on 1/3° grid obtained from AVISO (Archiving, Validating, and Interpretation of Satellite Oceanographic Data) CNES, France is used for computing geostrophic currents. This is a validated, directly usable dataset corrected for all environmental and orbit errors (AVISO User Handbook, 1997). There is one map of SSH every 7 days for a period of more than 11 years (October 1992 to January 2005).

AVISO prepared this dataset by merging data from five satellites i.e., T/P (October 1992 to July 2002), ERS1 (January 1994 and March 1995), ERS2 (June 1996 to June 2003), Jason1 (after July 2002) and Envisat (after June 2003). The details of the processing techniques are well documented by several authors (AVISO/Altimetry, 1996 CLS, 1996; Le Traon and Ogor, 1998; Le Traon et al 1998; Dorandeu and Le Traon, 1999; Ducet et al, 2000; www.jason.oceanobs.com/documents/donnees/duacs/handbook_duacs_uk.pdf ). In the following sections a brief description on satellite altimeter is given.

### 1.5.2 Concept of Altimetry

An altimeter measures the two-way travel time required for a radar pulse emitted by the altimeter antenna, to travel and reflect off the sea surface, and then return to the antenna. Knowing the speed of light, the distance of the sea surface from the altimetry can be calculated. This is termed in the altimeter range. If the height of the satellite above some reference ellipsoid is known then the height of the sea surface above the reference ellipsoid can be calculated. This is termed sea surface height (SSH), which is the term we wish to find out from the satellite altimetry (Figure 1.3).
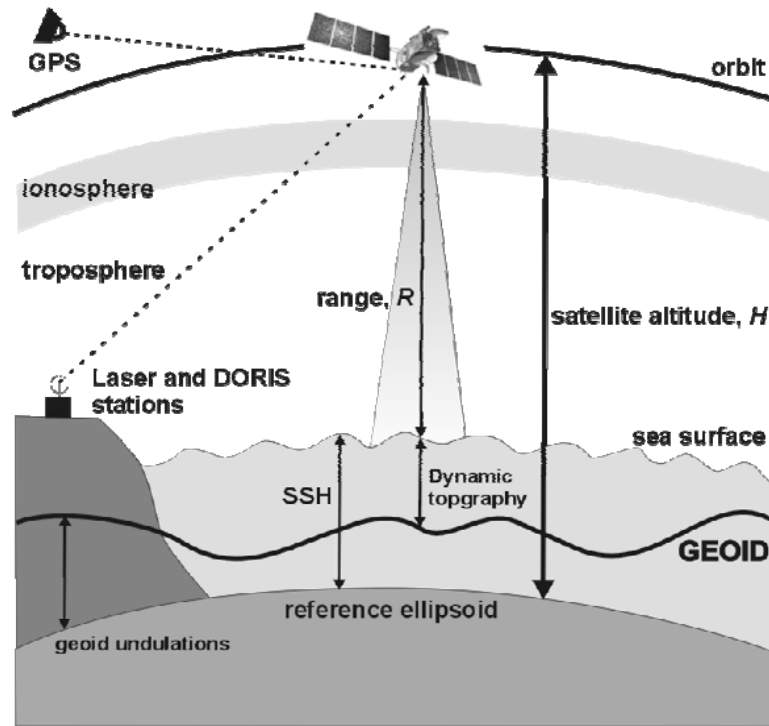
Figure 1.3 Schematic of the principle of altimeter.

The SSH signal has three sources: (1) the geoid caused by the earth's spatially varying gravity field (amplitude of up to 300m), (2) solid earth and ocean tides (amplitude of the order of 1-10 m), and (3) ocean currents (amplitude of order of 10-100 cm). The geoid signal is stationary in time and can be approximated by the mean height signal along repeats of a single ground track. Hence from altimetry the time varying part of the current signal can be determined to a few centimetres. The longer the time series of the altimeter used, the lower the repeat frequency of current variability which can be determined.

### 1.5.3  Error sources in satellite altimetry

To achieve such a measurement accuracy ($< 50$cm) to obtain any useful oceanographic information requires careful instrument design as well as corrections of the intervening atmosphere (Fu et al 1994). The standard corrections applied to the altimeter ranges are troposphere (dry and wet), ionosphere, tide influence, ocean wave influence and inverse barometric effect. The data used in this study are subjected to the above corrections by AVISO before they made available for researchers.

### 1.5.4 Determination of sea surface height from altimeter

The position of the SSH measurements is normally determined relative to some fixed reference i.e. the reference ellipsoid. In order to obtain SSH relative to this reference ellipsoid, it is necessary to know the orbit height. The error in the orbit and the geoid are the dominant terms in the altimetric error budget. The orbit accuracies in the past altimeters were ~10 m for GEOS-3, ~50 cm for GEOSAT, and ~7 cm for ERS-1 (Scharroo and Visser, 1998). The T/P is accurate to 3 cm (Tapley et al, 1994).

In the present study the multi-mission high resolution altimeter data obtained from four different satellites (set of two tandem missions formed as constellation of two) is used. In the next section the advantages of such data will be discussed.

### 1.5.5 Multi mission high-resolution altimetry

The Topex/Poseidon-ERS and Jason-Envisat are fine examples of how altimetry satellites can operate together to get high resolution data. Topex/Poseidon and Jason-1 follow a repeat cycle of ten days designed to monitor ocean variations, so they pass over the same points fairly frequently but their ground tracks are some 315 kilometers apart at the equator- more than the average span of an ocean eddy. On the other hand, ERS-2 and Envisat only revisit the same point on the globe every 35 days but the maximum distance between two tracks at the equator is just 80 kilometers (Fig. 1.4). The typical ground tracks of these two satellites are shown in Fig. 1.4. At least two altimetry satellites are required to map the ocean and monitor its movements precisely, particularly at scales of 100 to 300 kilometers (mesoscale).
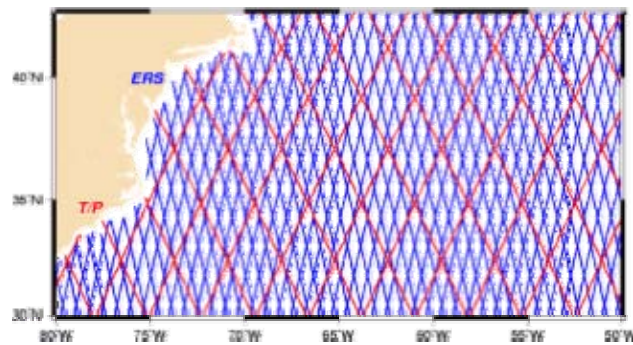


Figure 1.4 Typical ground track overlay of T/P-Jason (red) and ERS-ENVISAT (blue).
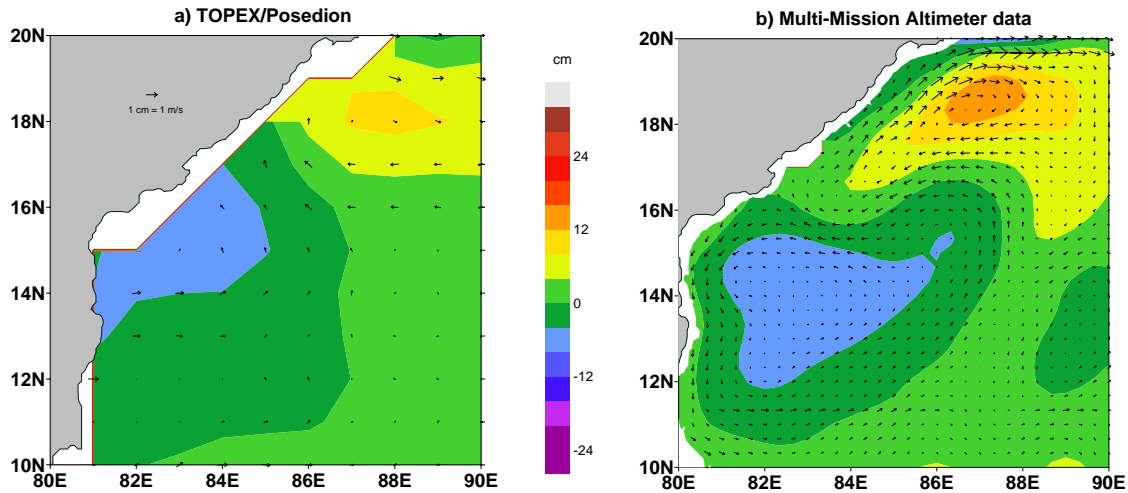
Figure1.5 Geostrophic currents superimposed on Sea Level Anomaly in the Bay of Bengal (a) T/P data only on 1° resolution. (b) Multi mission altimeter data on 1/3° resolution.

High-resolution sampling is needed for many applications. Higher spatial resolution makes it possible to resolve mesoscale processes (Fig. 1.5b), to measure geostrophic velocities in both directions, to better describe the dynamic topography near the shoreline, to describe the variability of high-frequency barotropic signals, transient phenomena at large spatial scales, such as internal waves and to study of sea ice, continental ice, sea state and study of vegetation.

The multi-mission processing of altimeter data was developed by CLS as part of DUACS (Developing Use of Altimetry for Climate Studies), a European Commission 3-year project which started in February 1997.

The multi-mission products developed for the original DUACS project are now widely used by the scientific community. They cover a large spectrum of operational oceanography needs, from mesoscale to climate applications.

## 1.6 Computation of geostrophic currents

The motion of a fluid can be generally described by the Navier-Stokes equation combining the effects of pressure gradient, internal friction, gravity gradient and the Coriolis force originating from the rotation of the earth. Apart from the coastal and equatorial regions and for periods longer than a few days the pressure gradient and the Coriolis force dominate and all other accelerating forces can be neglected (Pond and Pickard, 1983). The resulting

relation between the pressure gradient and the Coriolis force is called the geostrophic balance (Wunsch, 1993):

The surface geostrophic currents are computed using mean monthly SSH of 1/3° grids in the Indian Ocean from the following equations (Kalyanidevasena et al (1995)).

$$u_s = -\frac{g\partial\varsigma}{f\partial y} \quad \text{--------------1.1}$$

$$v_s = \frac{g\partial\varsigma}{f\partial x} \quad \text{------------1.2}$$

Where

$u_s$ $v_s$ – zonal and meridional component of surface current

$\partial\varsigma$- water slope (SSH difference) between two adjacent 1/3° grids

g – gravitational constant

$f$ - Coriolis parameter

The speed (V) and direction ($\theta$) of the geostrophic current was given by

$$V = \sqrt{u_s^2 + v_s^2} \quad \text{-------1.3}$$

$$\theta = \tan^{-1}\left(\frac{v_s}{u_s}\right) \text{--------1.4}$$

We computed surface monthly geostrophic currents from equations (1.3) and (1.4) using mean monthly 1/3° squares SSH slopes ($\partial\varsigma$).

Since the geostrophic approximation fails at the equator geostrophic currents are not computed across 1° on either side of the equator (Lukas, 1984). In fact, Pond and Pickard (1983) suggested 0.5° around the equator as the region of invalid geostrophy.

In the next chapter the seasonal variability of geostrophic currents using multi-mission high resolution data of 12 years is presented.

**Seasonal Variability**

## 2.1. Introduction

In the Indian Ocean, the current measurements are limited and scattered over isolated regions for short periods compared to the Atlantic and the Pacific Oceans. These measurements are inadequate to describe many details of circulation aspects of the Indian Ocean. The present knowledge on the Indian Ocean circulation hinges on currents derived from ship drifts (KNMI, 1952, Varadachari and Sharma 1967, Cutler and Swallow 1984, Rao *et al.*, 1991), from geostrophic computations (Duing, 1970, Wyrtki, 1971) and from surface drift buoy measurements (Molinari *et al.*, 1990, Shenoi et al 1999a). Moreover, the subsurface current measurements were carried out at certain locations during specific observational programs. With the availability of hull mounted Acoustic Doppler Current Profilers (ADCP) considerable improvement have been made in the measurements of currents (Flagg and Kim 1998). However, these measurements basically suffer from isolated coverage at random along a few shipping lanes in the Indian Ocean. Although the circulation models overcome these limitations to a certain extent, most of their results are not validated with direct measurements.

Satellite measurements have unique advantages of simultaneous coverage of vast regions at short time intervals with reasonable resolution and accuracy. However, these are confined to sea surface measurements. Prasanna Kumar et al (1998) reported contrasting circulation features in this region for January and July utilizing 5-year TOPEX/POSEIDON (T/P) satellite altimeter measurements of SLA in the north Indian Ocean.  Ali et al (1998) presented 10-day year-to-year snap shots of SSH from the altimeter measurements of GEOSAT satellite. Raghunadha Rao et al (2001) presented monthly climatology of geostrophic currents using 7 year T/P satellite altimeter data. These studies using TP data alone could not describe the circulation in the shallow water and small scale features due to lack of resolution. Shankar et al  (2002) described general circulation of north Indian Ocean and brought out how various branches of currents evolve as major current system in their mature phase utilizing satellite data (T/P data), ship drift data and model results. Kantha et al

(2008) used model to hindcast currents using satellite SSH data as model input and compared results with the available insitu data. Recently efforts have been made to prepare robust and merged multi-mission altimeter sea level anomaly data (Jason-1 + ENVISAT; T/P + ERS) with a resolution of 1/3° over the Indian Ocean. These data sets are available in the AVISO website. Flagg and Kim (1998) used shipborne ADCP data collected during JGOF and showed that the currents in the Arabian Sea are more of geostrophic except along coastal boundaries. In this chapter geostrophic currents computed using multi-mission altimeter data are used to describe the seasonal variability of the Indian Ocean circulation. Because of the high spatial and temporal resolution, these data sets can provide a better understanding of the prevailing meso-scale circulation features in the Indian Ocean. Hence, for this study, this high resolution data are utilized to describe meso-scale features, some of which are not reported, in the Indian Ocean on an annual cycle (used monthly climatology of geostrophic currents over the Indian Ocean).

## 2. 2. Data and methods

The data used to study the geostrophic currents are obtained from a complete reprocessing of TOPEX/POSEIDON, Jason and ERS-1/2 data. Processed data in 1/3°X1/3° available on the AVISO website. Sea Surface Height (SSH) data are available at every 7 days for a period of more than 12 years (October 1992 to December 2004). The description of data is given in previous Chapter.

## 2. 3. Geostrophic currents

Observations have shown that the large-scale ocean circulation is not perfectly geostrophic, but has slight deviations from geostrophy, especially near land boundaries. Perfect geostrophy ignores the time evolution of the field and the influence of the other forces such as the wind. The total geostrophic current in the ocean is composed of both barotropic and baroclinic components. The current velocities computed from hydrographic data contain only the baroclinic component. Determination of the barotropic component of the flow from the hydrography data is difficult, but the ship drift measurements have the total current (baroclinic and barotropic) velocity. This major problem can be overcome with the use of absolute velocities from the Acoustic Doppler Current Profiler (ADCP) instruments

together with inverse modeling (Saunders and King, 1995). However ship drift currents suffer from errors due to wind drag (Flagg and Kim 1998) and mostly biased to shipping lanes.

The surface geostrophic currents are computed using mean monthly SSH of 1/3° grids in the Indian Ocean using equations 1.1 to 1.4 shown in Chapter-1. However, current vectors presented in the figures (Fig. 2.1 to Fig 2.12) in this Chapter are plotted at 1° interval for better clarity. Since the geostrophic approximation fails at the equator geostrophic currents are not computed within 1° on either side of the equator (Lukas, 1984).

## 2. 4. Results and discussions

It is well known that the currents in the Indian Ocean show large variability on an annual cycle, due to variety of factors. The earlier studies have also indicated large variability in the sea surface height on an annual cycle (Ali et al. 1998). The climatology of surface geostrophic currents in the Indian Ocean is computed for all the months of the year and presented for each 1° grid superimposed on the SSH maps. These SSH maps in the background are useful for interpreting 'highs' and 'lows'.

In this chapter the monthly climatology of currents are presented and described together for periods of three months (Jan – March, April – June, July – September, October – December) for easier understanding of the seasonal evolution of currents. The surface currents in the Indian Ocean are highly variable both in the spatial and temporal domains.

### 2.4.1 January – March

The surface geostrophic currents for the tropical Indian Ocean are shown in Fig. (2.1 – 2.3). In the Bay of Bengal an anti-cyclonic eddy is observed off Visakhapatnam (see Fig. 1.1 for location)) in January. Under its influence, the coastal currents are northeasterly north of Visakhapatnam and along the eastern boundary of the Bay of Bengal the currents flow is southward. For further description the coastal currents in the eastern Bay of Bengal is named as Eastern Bay of Bengal Current (EBBC).

However, south of Visakhapatnam the currents are southerly along the southeast coast. The currents flowing along southeast coast of India is known as the East India Coastal Current (EICC) (Shetye et al., 1991). This suggests that the EICC has different directions

north and south of Visakhapatnam in January (Fig. 2.1). By February (Fig 2.2) the EICC reverses to northerly direction north of 12°N and the currents become very strong (~40cm/s) off Visakhapatnam associated with western boundary current (Legeckis, 1987). A strong (25 - 40cm/s) anti-cyclonic eddy forms off east of Sri Lanka by February which strengthens and moves towards north and a complete anti-cyclonic gyre is well established in the Bay of Bengal by March (Fig. 2.3). Under the influence of two anti- cyclonic eddies in the western Bay of Bengal the currents in the central Bay of Bengal are mainly southerly. Contrary to expectations currents in the central Bay of Bengal are mostly meridional and these currents are described as Central Bay of Bengal Current (CBBC) in the following discussion.

Coastal currents in the entire Arabian Sea forms as a part of basin scale anti-cyclonic gyre in January ( Fig 2.1). The high sea level (25 cm) and consequent anti-cyclonic gyre off the southwest coast of India is due to the Laccadive High (Bruce, 1994). On the other hand an equally strong low sea level (-25 cm) and cyclonic gyre is also observed off Somalia. The Somalia gyre weakens by February – March (Fig. 2.2 and Fig. 2.3). On the other hand, the Laccadive High detached from the southwest coast of India by February and by March it weakens and propagates westward. With the detachment and consequent westward movement of the Laccadive High, West India Coastal Current (WICC) off the southwest coast of India changes its direction to southerly. By February and March the WICC becomes southerly south of 12°N. Further north the currents are weak and northerly, but the Somali current continues to flow southward. Another conspicuous feature of the current pattern is a consistent northward current in the central Arabian Sea sandwiched between the Laccadive High and the cyclonic gyre in the western Arabian Sea, throughout January – March (Fig. 2.1 to Fig. 2.3). This current is described as Central Arabian Sea Current (CASC) in the ongoing discussion.
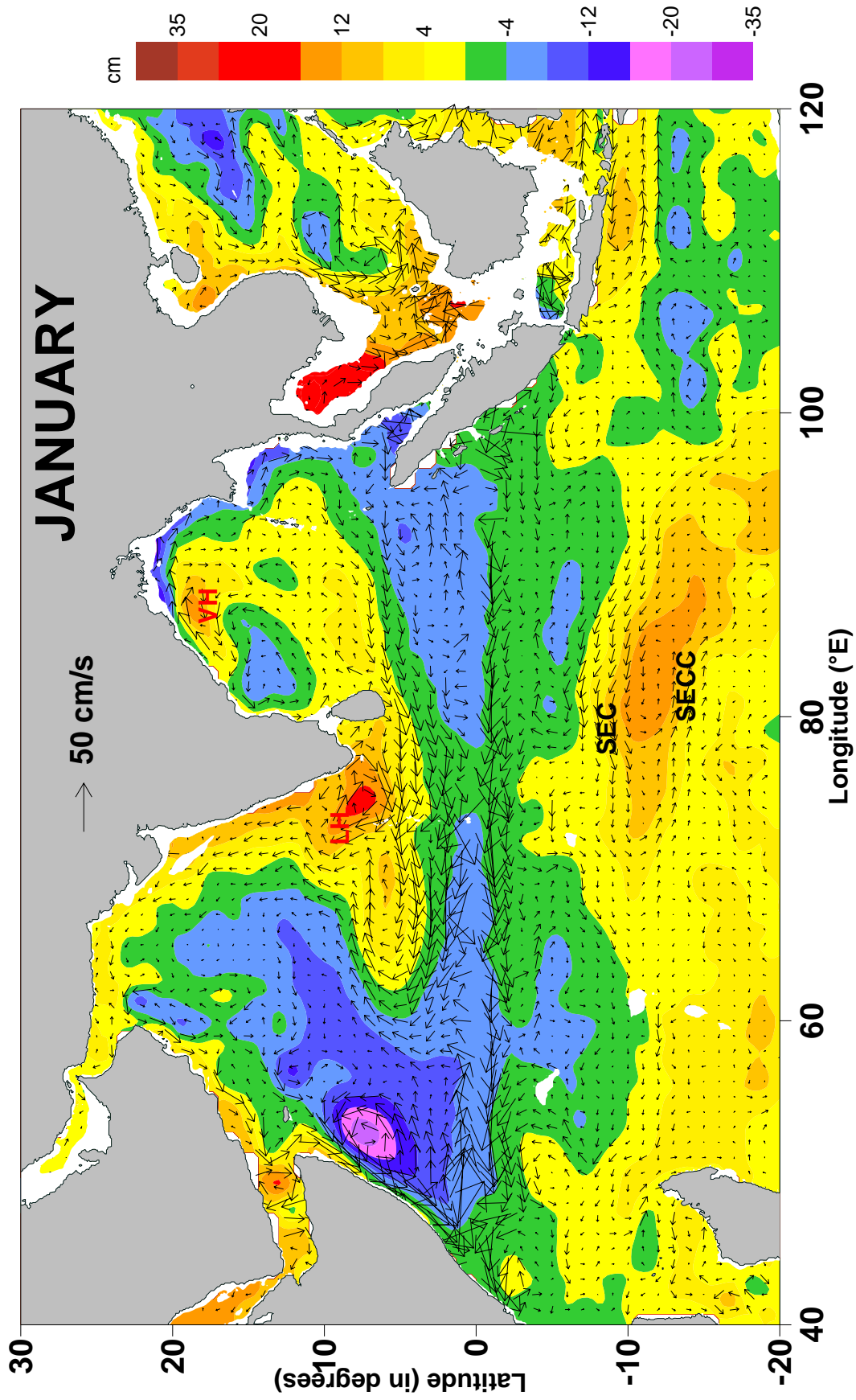
**Fig. 2 .1 January climatology of Surface geostrophic currents overlaid on SSH climatology.**

19
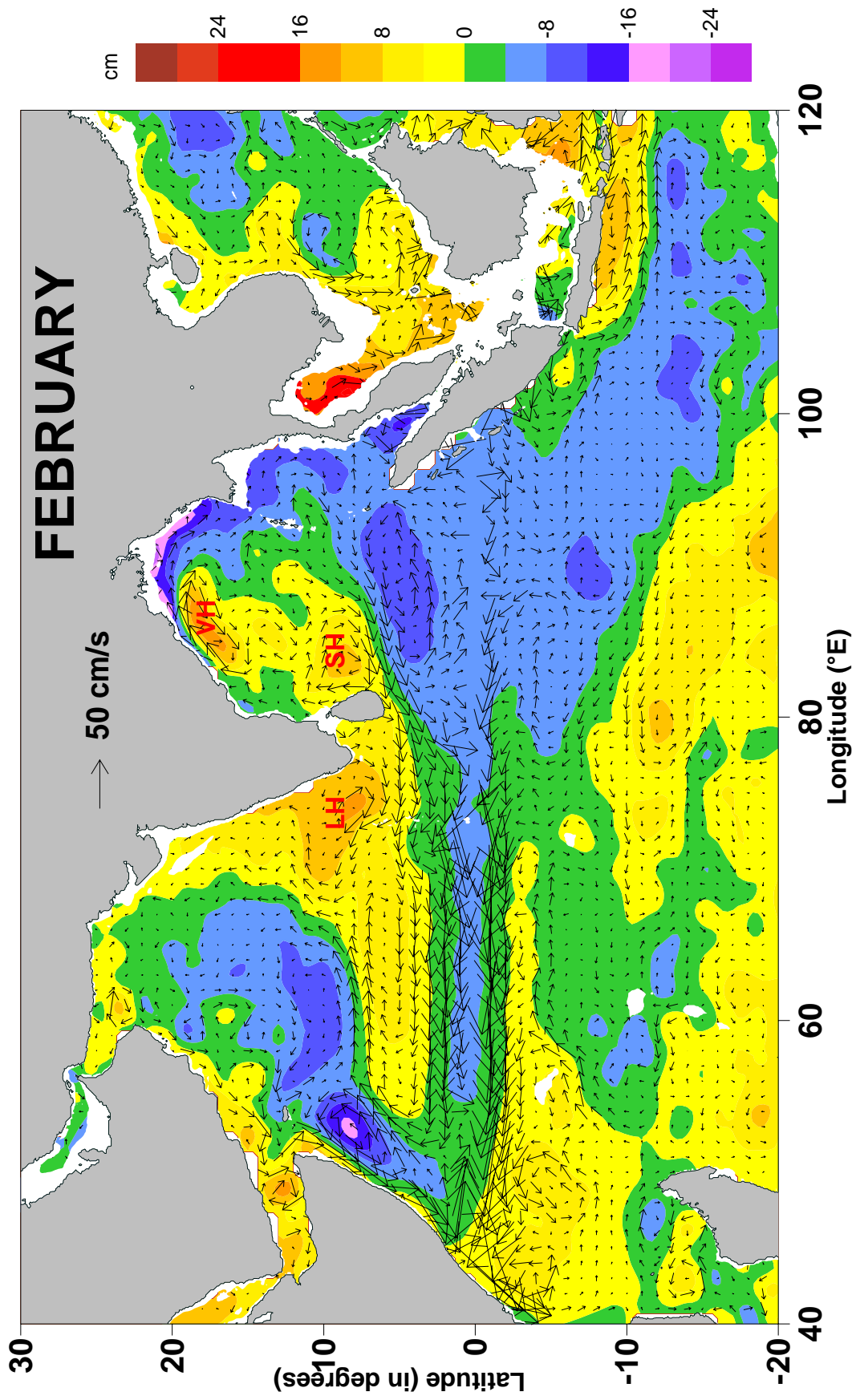
**Fig. 2 .2 February climatology of Surface geostrophic currents overlaid on SSH climatology.**

20
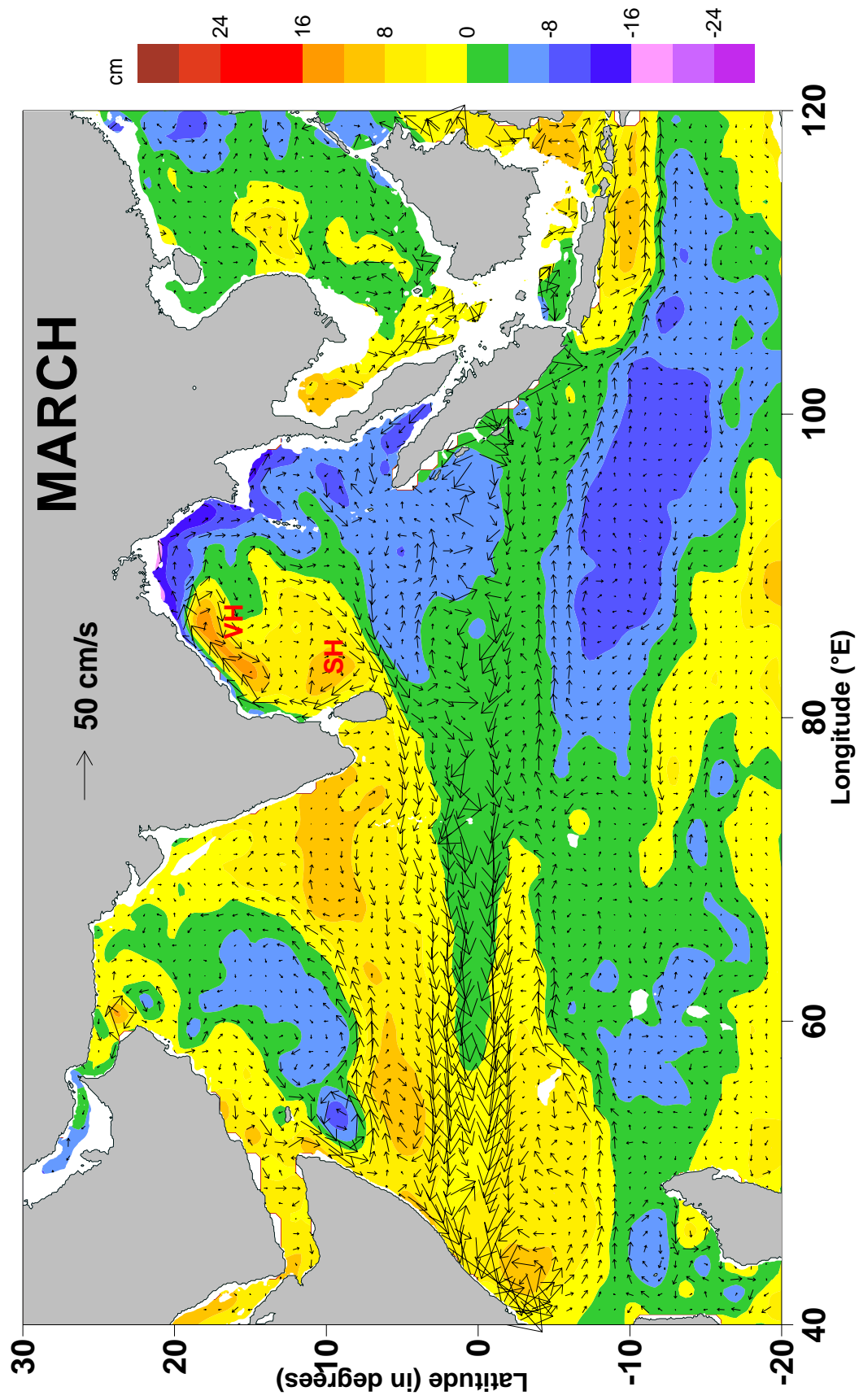
**Fig. 2 .3 March climatology of Surface geostrophic currents overlaid on SSH climatology.**

21

The currents near the equator are mostly westerly during this period (associated with the Winter Monsoon Current which weakens by March. In the southern tropical Indian Ocean an anti-clockwise gyre centered around 15°S, 80 -90°E with in the South Equatorial Current systems is observed during January. This weakens by February – March. On the other hand a clockwise gyre centered around 10°S; 90 – 100°E became prominent by April (Fig. 2.4). In the western equatorial Indian Ocean (close to the African coast) centered around 3°S, 42°E a weak anti-cyclonic eddy in January intensifies by February – March thus producing very strong current. South of Java a positive SSH and consequent easterly current is observed in January – February but by March it gets detached from the coast thus reversing the currents near the coast. The currents in the southwestern Indian Ocean are southerly due to the formation of an anti-clockwise eddy centered around 5°S, 42°E which intensifies and turns into a clockwise eddy by April. Numerical models run with monthly climatological wind forcing alone have reproduced many of the large-scale features of the southern tropical Indian Ocean (Woodberry et al 1989).

### 2.4.2 April – June

The surface geostrophic currents for the period of April – June is presented in Fig. 2.4 – Fig. 2.6). In the Bay of Bengal the EICC is well established and the clockwise eddy off Sri Lanka moved northward and merged with the clockwise eddy off the east coast of India by May (Fig. 2.5). The coastal currents in the entire Bay of Bengal continues to be clockwise in April. The EBBC reverses its direction in the eastern Bay in May and further extends to northern Bay by June (Fig. 2.6). The clockwise eddy in the western Bay of Bengal weakens and moves eastward by June thus weakening the coastal currents. The formation of anti-clockwise eddy off Visakhapatnam and its further intensification by June produces southerly coastal currents in these regions.  Thus the EICC distinctly branched into two major flow patterns, i.e. weak northerly flow south of Visakhapatnam and southerly flow north of Visakhapatnam by May – June.

The situation in the Arabian Sea during this period also shows interesting results. The Laccadive High which is prominent in March almost dissipated by April and the WICC flow southward. By June the SSH off the southwest coast of India becomes negative thus forming

Laccadive Low (LL). The Somali Current continues to be southerly in April, though weakened compared to the previous months. However, by May the currents in the Arabian Sea become cyclonic in general and a strong anti-cyclonic eddy becomes prominent north of Socotra (15°N, 55°E). The northerly CASC weakens by April – May. The northward flowing Somali Current is established by May and intensifies (>50 cm/s) by June with the formation of a strong clockwise eddy (5°N, 53°E) off Somalia named as 'Great Whirl' (GW) (Bruce, 1968, Swallow et al (1983)). The currents in southwestern Indian Ocean turned northerly by May with the formation of cyclonic eddy centered around 5°S, 42°E, which moves northward and dissipates by June.

The equatorial currents especially east of 60°E are strong easterly (~50 cm/s) in April - May associated with the Equatorial Jet (Wyrtki 1973). The mass transport by the Equatorial Jet is high and it causes convergence or deepening of thermocline in the eastern Indian Ocean (Wyrtki, 1973). The SSH shows large positive anomalies of the order of 15cm in the eastern equatorial Indian Ocean there by producing northeasterly/southeasterly currents north/south of equator in May and June. The cyclonic eddy in the SEC in the eastern Indian Ocean is conspicuous during February – May weakens by June.
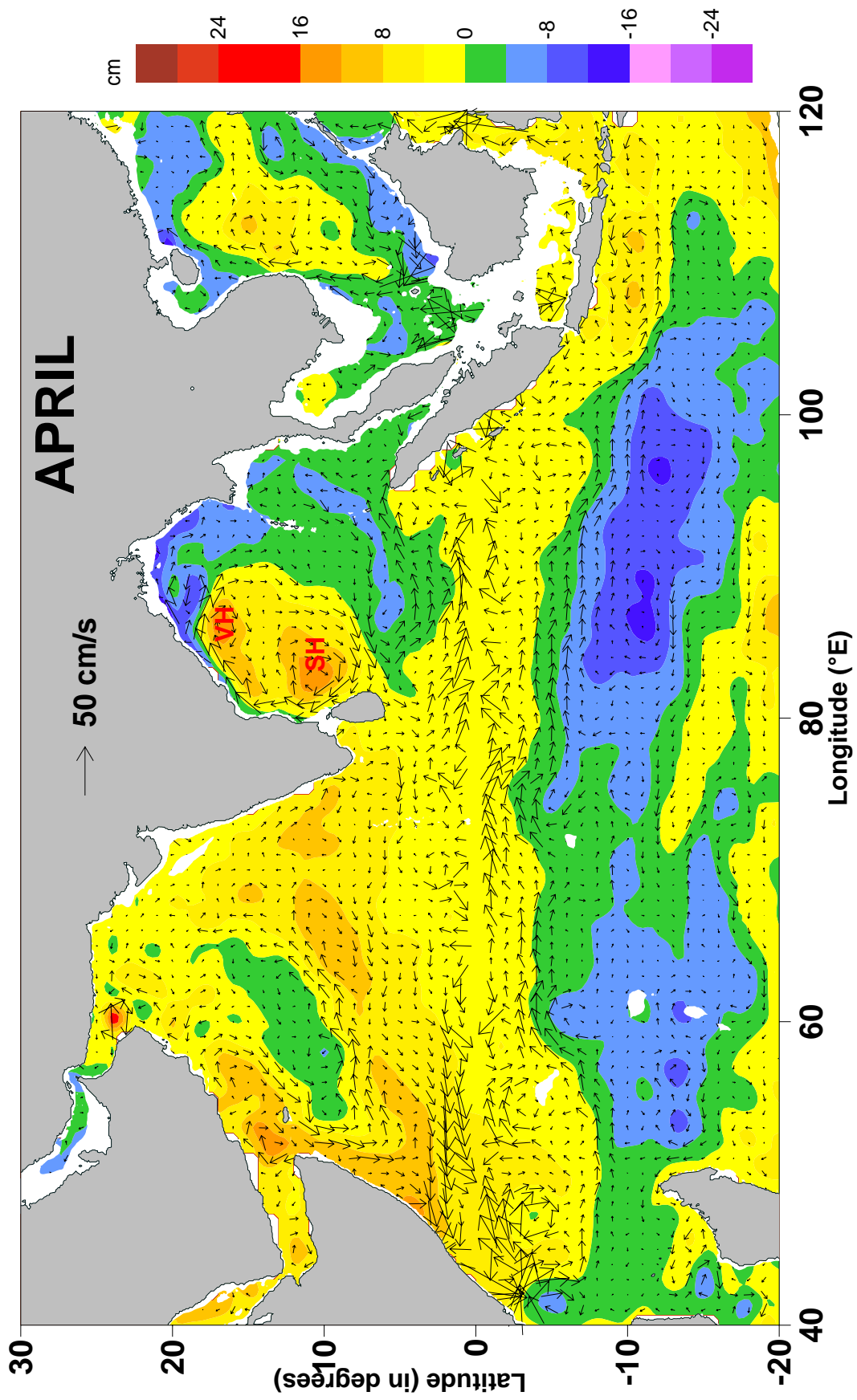
**Fig. 2 .4 April climatology of Surface geostrophic currents overlaid on SSH climatology.**
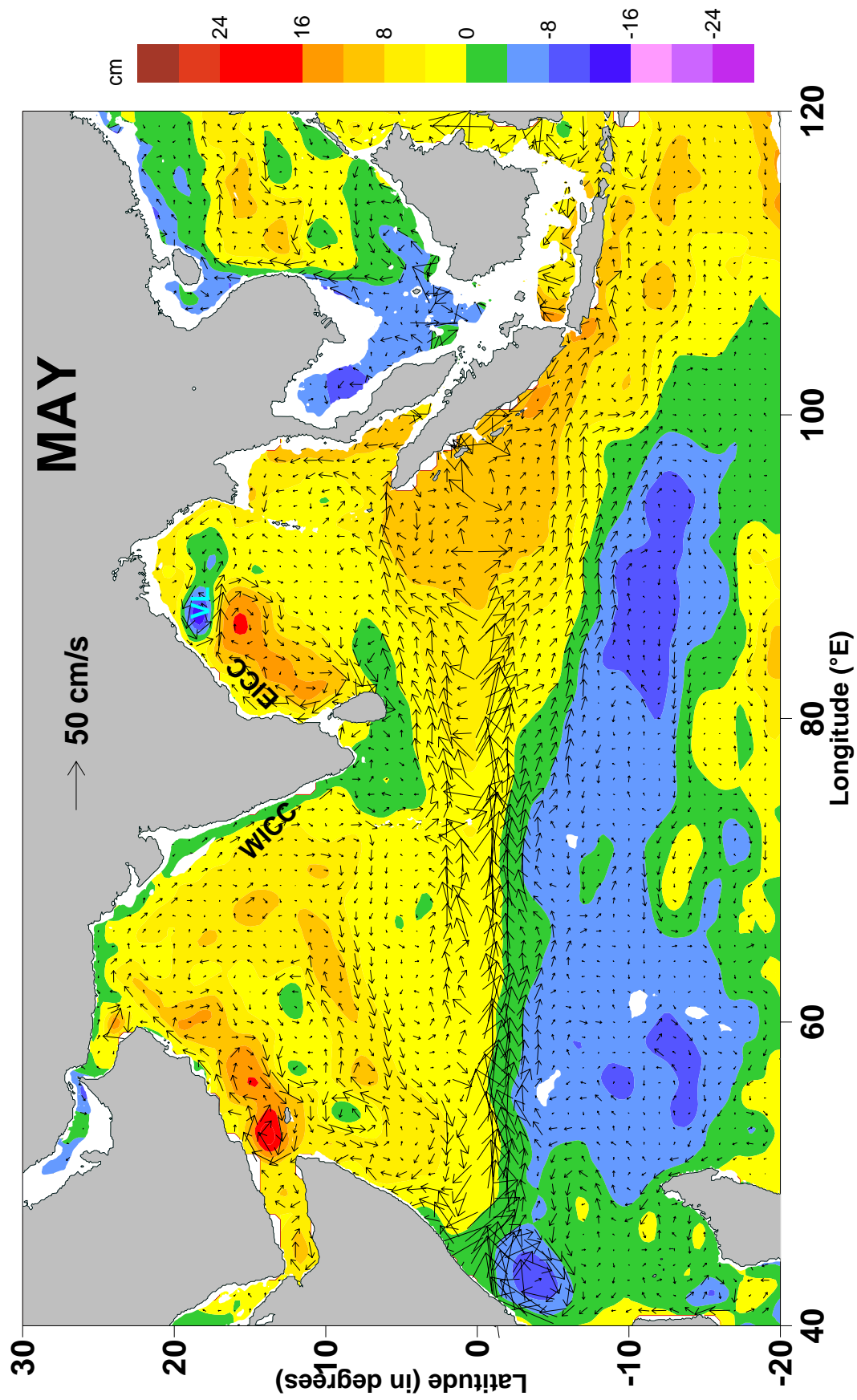
**Fig. 2 .5 May climatology of surface geostrophic currents overlaid on SSH climatology.**
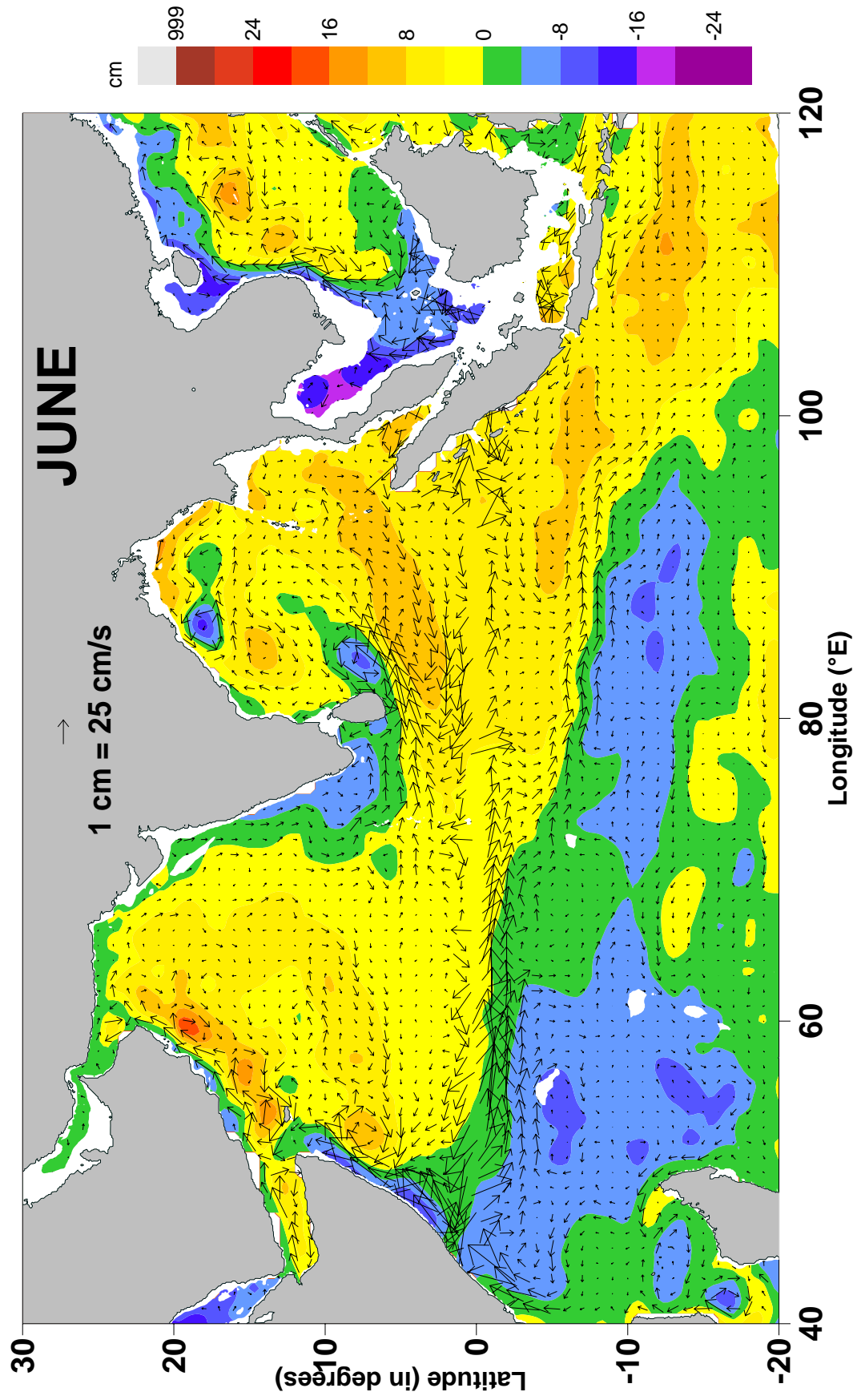
Fig. 2 .6 June climatology of surface geostrophic currents overlaid on SSH climatology.

**2.4.3 July – August – September**

The coastal currents are indicative of a cyclonic gyre in the Bay of Bengal except between 12°N and 17°N where it is weak northerly in July – August and by September the cyclonic gyre is well established in the Bay of Bengal (Fig. 2.7 – 2.9). The cyclonic eddy off Sri Lanka called the Sri Lanka Dome (Vinayachandran and Yamagata 1998) intensifies during this period and moves northwestward, while the cyclonic eddy off Visakhapatnam moves offshore from July to September. A weak anti-cyclonic eddy is sandwiched between these two cyclonic eddies.

In the Arabian Sea an clockwise gyre (basin scale) is well established during this period along with a strong Somali anti-cyclonic eddy. The Socotra eddy disappears by August. Another anti-cyclonic gyre associated with the Laccadive Low is seen off the southwest coast of India. This low detaches from the coast by August, thus forming a anti-clockwise gyre (Laccadive Low) offshore. The surface currents near the southwest coast of India turns northerly (though weak) by September as the Laccadive Low moves away from the coast. The currents in the central Arabian Sea are mainly northerly. The conspicuously low sea level off Arabia is indicative of the large extent of the coastal Arabian Sea upwelling region (Smith and Bottero 1977).

The currents in the equatorial Indian Ocean are highly variable during this period. Currents in the southern tropical Indian Ocean are highly influenced by eddies. A strong anti-clockwise gyre dominates the flow in the southeastern Indian Ocean which intensifies and moves westward from July – September. On the other hand the flow in the western part of southern tropical Indian Ocean is dominated by clockwise eddy in July – August.
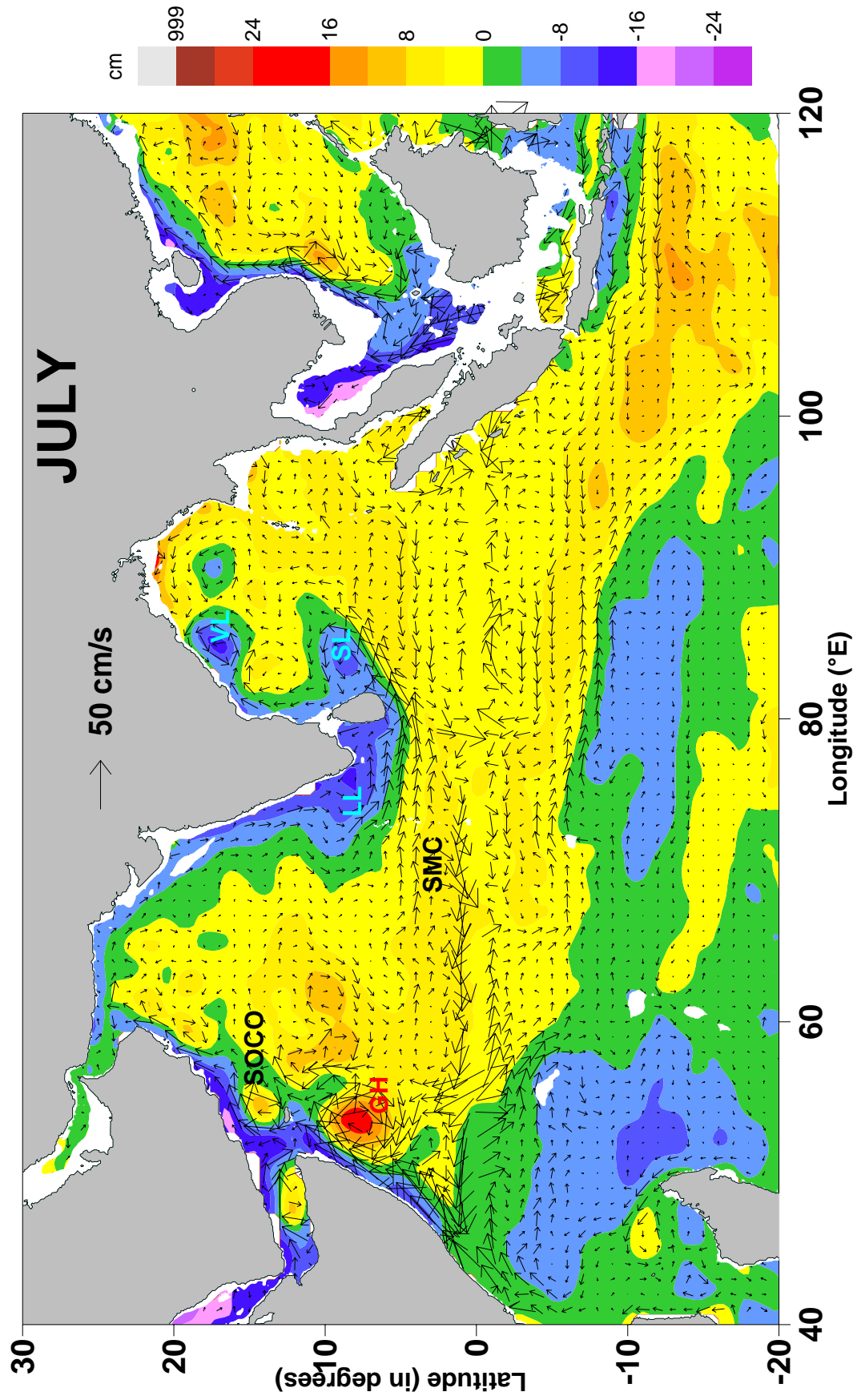
**Fig. 2 .7 July climatology of surface geostrophic currents overlaid on SSH climatology.**

28
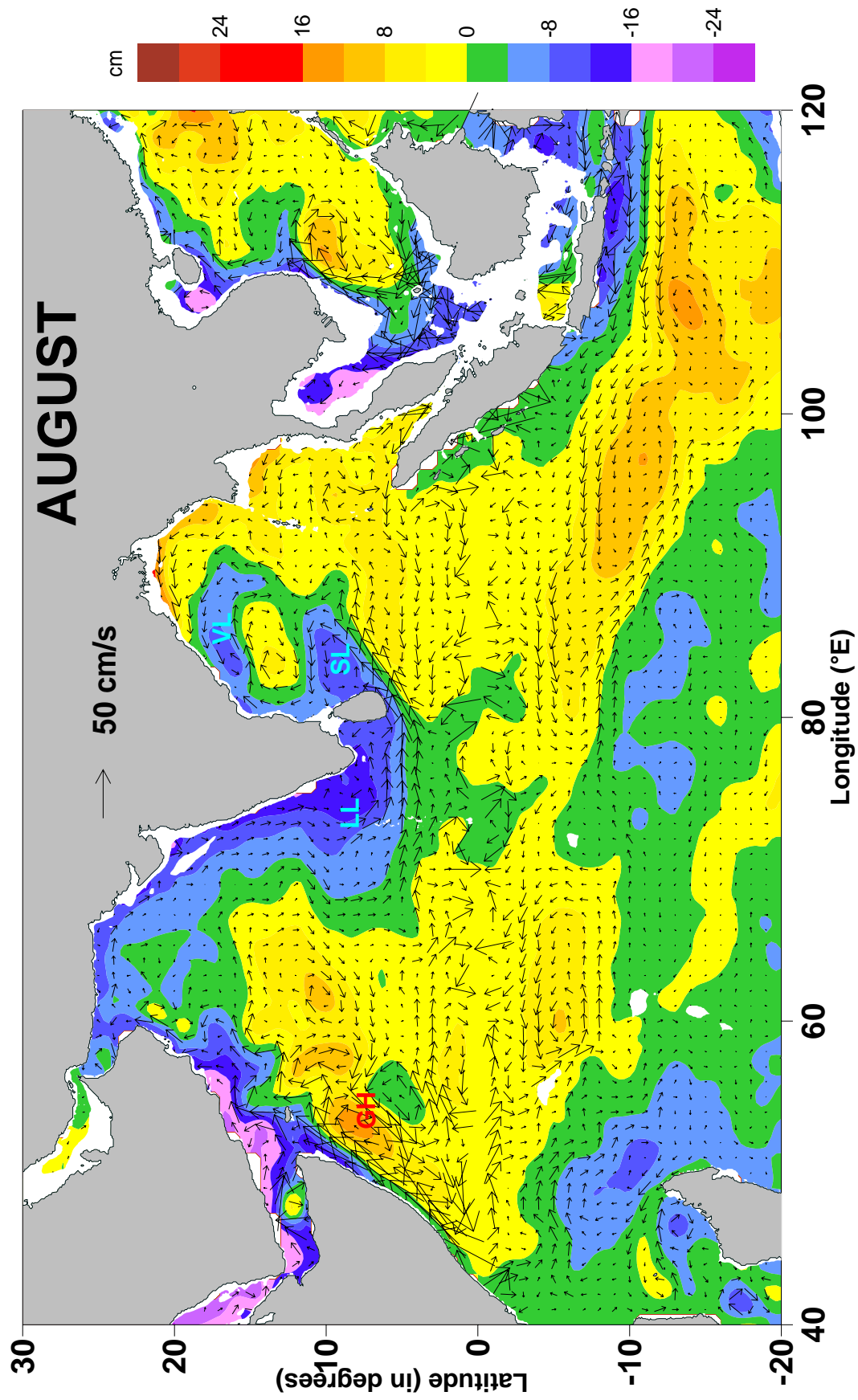
**Fig. 2 .8 August climatology of surface geostrophic currents overlaid on SSH climatology.**
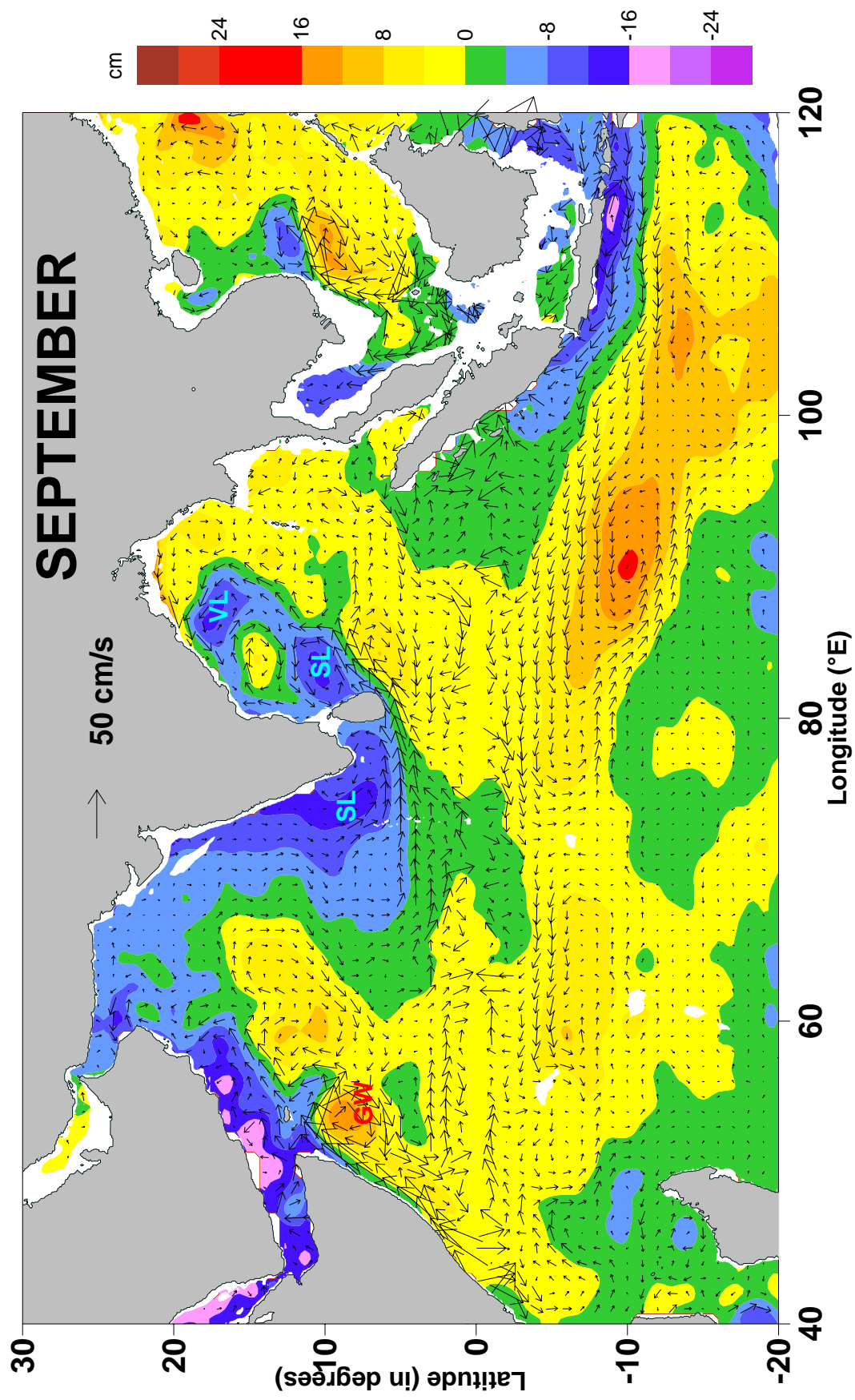
**Fig. 2 .9 September climatology of surface geostrophic currents overlaid on SSH climatology.**

30

South of the equator centered on 60°E another anti-cyclonic eddy is dominant during August - September. The presence and movement of eddies in the South Equatorial Current (SEC) system often produces countercurrent within the westward moving SEC.

By July negative SSH and associated circulation is dominant south of Java which intensifies by August – September. During this period the currents south of Java are predominantly westerly.

### 2.4.4 October – November – December

During October - November a anti-clockwise gyre continues to prevail in the western Bay of Bengal, with the East India Coastal Current particularly strong in October - November. The anti-clockwise eddy off Sri Lanka further moves northward and merges with the anti-clockwise eddy off Visakhapatnam and forms a single large anti-clockwise eddy by October – November. The eddy weakens by December. Northerly currents are seen in the central Bay of Bengal mainly due to the re-circulation of waters in the anti-clockwise eddy. The currents in the eastern Bay of Bengal (EBBC) change its direction by December.

In the Arabian Sea as the Laccadive Low moves westward and the West India Coastal Current becomes northerly and by November a large cyclonic gyre is established in the Arabian Sea. By December the Laccadive Low moves further west thus forming a huge anti-clockwise eddy. The Laccadive High again starts to appear in November and is well established in December. With the formation of Laccadive High a clockwise eddy forms off the southwest coast of India and the currents flow northward along the western boundary of the eddy in the central Arabian Sea. The Somali anti-cyclonic eddy moved northeastward and weakens by October and dissipates by November. One important observation is that the gyres in the Bay of Bengal and the Arabian Sea seem to be independent in October (with little exchange of water between these two basins) but they are well connected in November. Unlike the Laccadive High, the Laccadive Low doesn't spread and dissipate as it moves westward.
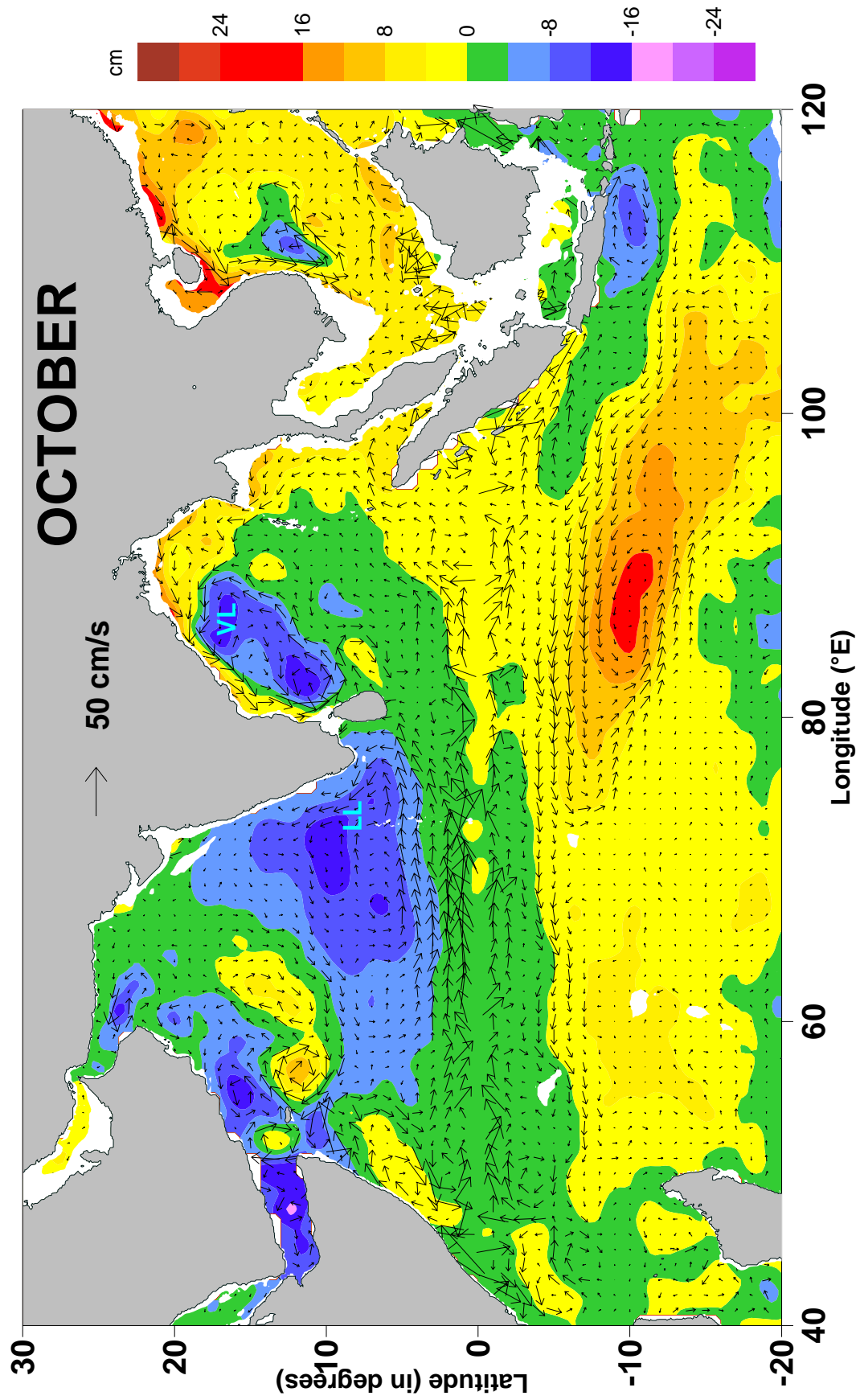
Fig. 2 .10 October september climatology of surface geostrophic currents overlaid on SSH climatology.

32
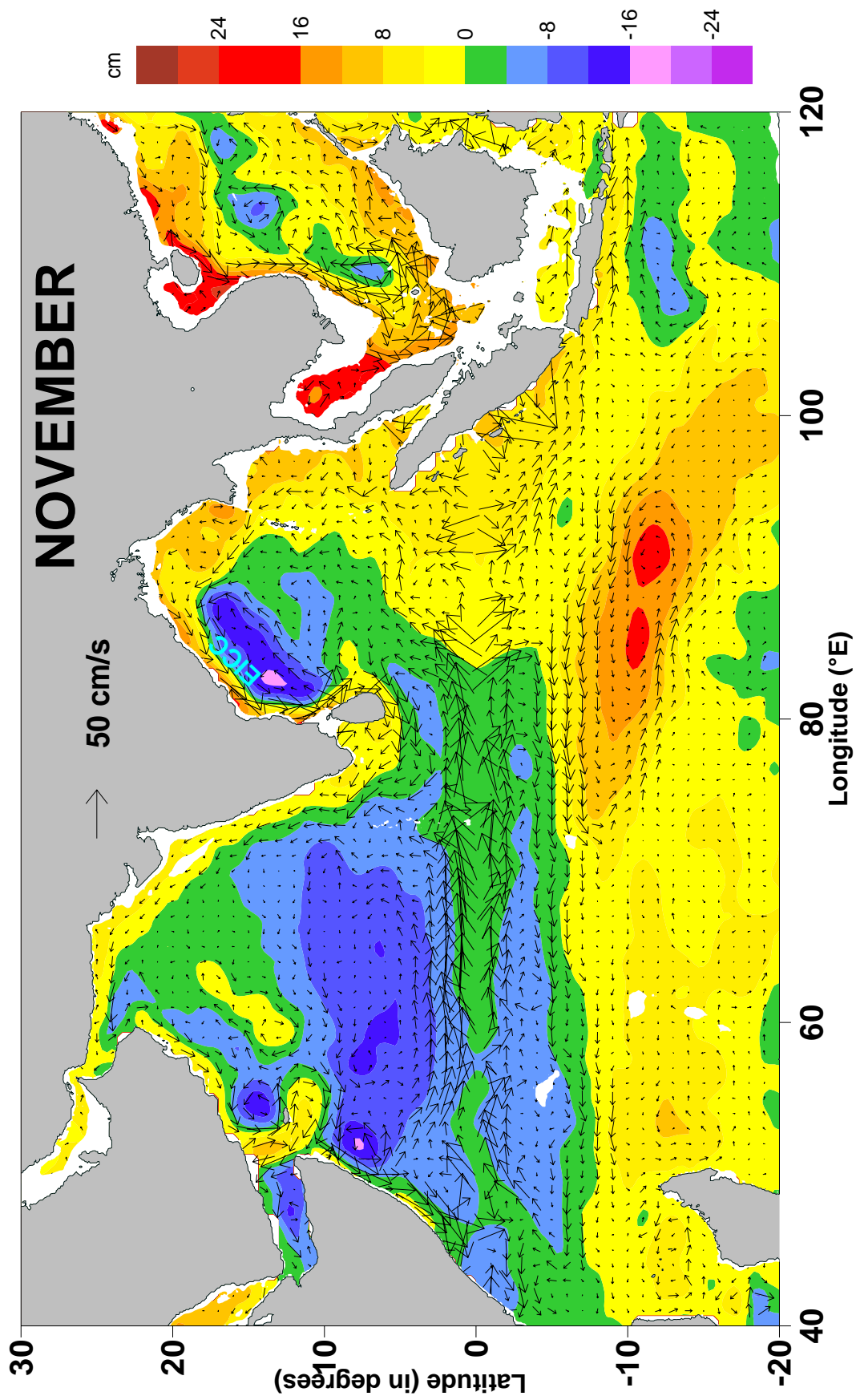
**Fig. 2 .11 November september climatology of surface geostrophic currents overlaid on SSH climatology.**

33
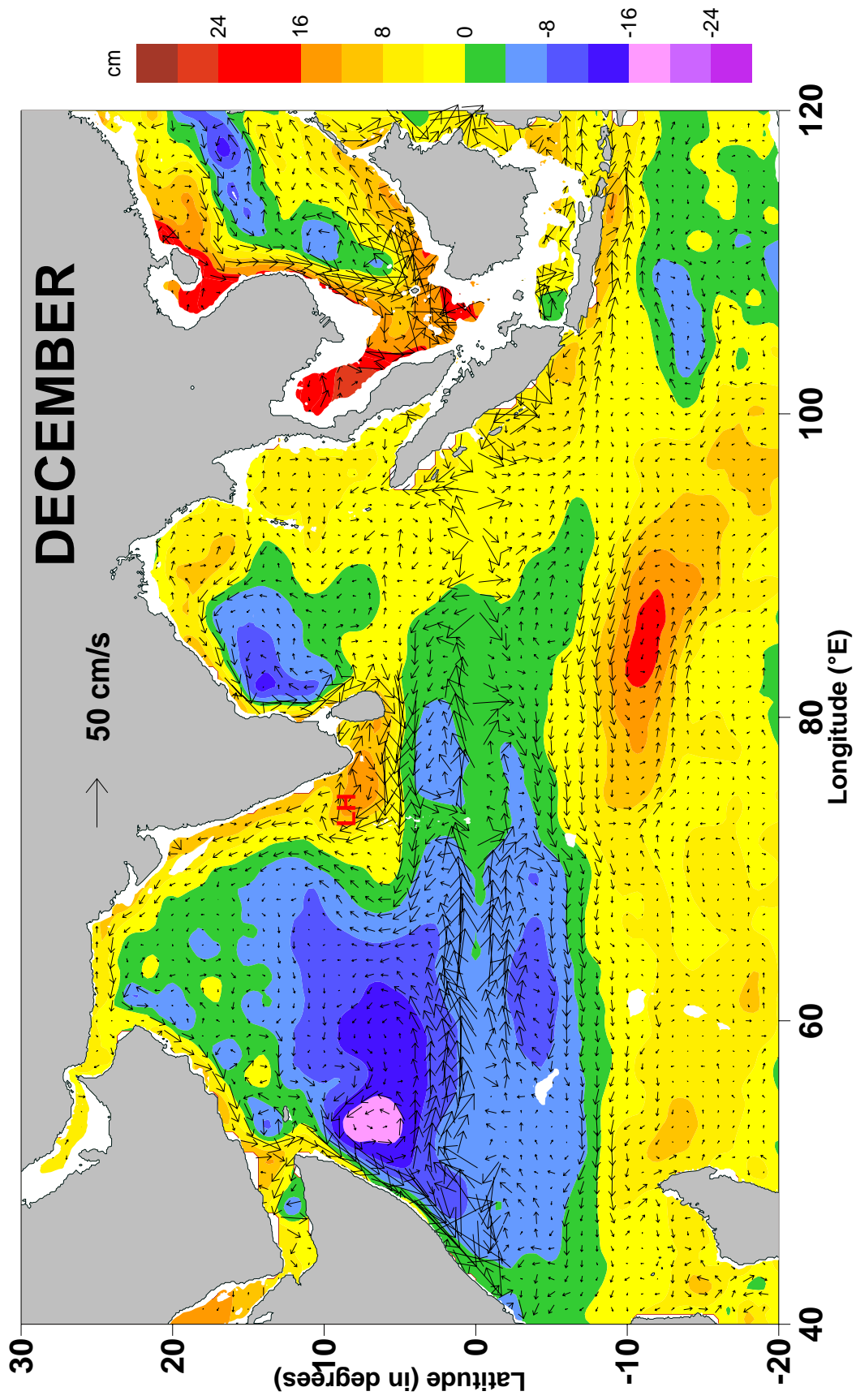
**Fig. 2 .12 December september climatology of surface geostrophic currents overlaid on SSH climatology.**

In the eastern equatorial Indian Ocean a positive SSH is established by November and associated with the Equatorial Jet. However, the magnitude is much smaller compared to May – June probably because the Jet is much weaker during the autumn transition compared to the spring transition in the annual cycle.

In the southern tropical Indian Ocean a large anti – cyclonic gyre continues to dominate. The negative SSH south of Java moves south and a well marked positive SSH dominates in this region by December thus changing the direction of currents.

A close examination of the circulation shows a clear seasonal pattern observed in all the regions of the tropical Indian Ocean. The current reverses once in six months in most parts of the Indian Ocean north of the equator. The regional variability is dealt separately in the following sections.

The analysis also clearly indicates two prominent eddies in the Bay of Bengal which have profound influence on the formation and evolution of the EICC. They are clockwise/anti-clockwise eddy associated with positive/negative SSH off Visakhapatnam and another similar eddy off Sri Lanka with its consequent meridional movement. In the following discussion these are denoted as the Visakhapatnam High/ Visakhapatnam Low and the Sri Lanka High/ Sri Lanka Low respectively. Vinayachandran and Yamagata (1998) named the Sri Lanka Low as the Sri Lanka dome, which appears during the summer monsoon, However it may be more appropriate to term it as the Sri Lanka Low as an equally prominent +SSH dominate in the other season. Similarly the WICC is governed by LH and LL which show westward propagation.

## 2.4.5 Currents and circulation in the Bay of Bengal

The seasonal reversal of currents in the Bay of Bengal was understood from the ship drift data (KNMI, 1952). More details of the currents and circulation emerged from hydrographic observations (Murty and Varadachari; 1968, Rao et al 1986; Murty et al 1992; Shetye et al., 1993; Shetye et al., 1996; Sanilkumar et al., 1997) and modeling studies (McCreary et al., 1996; Shankar et al., 1996). Satellite tracked drifting buoys also provide information on the Bay of Bengal circulation (Molinari *et al.*, 1990, Shenoi et al 1999a).
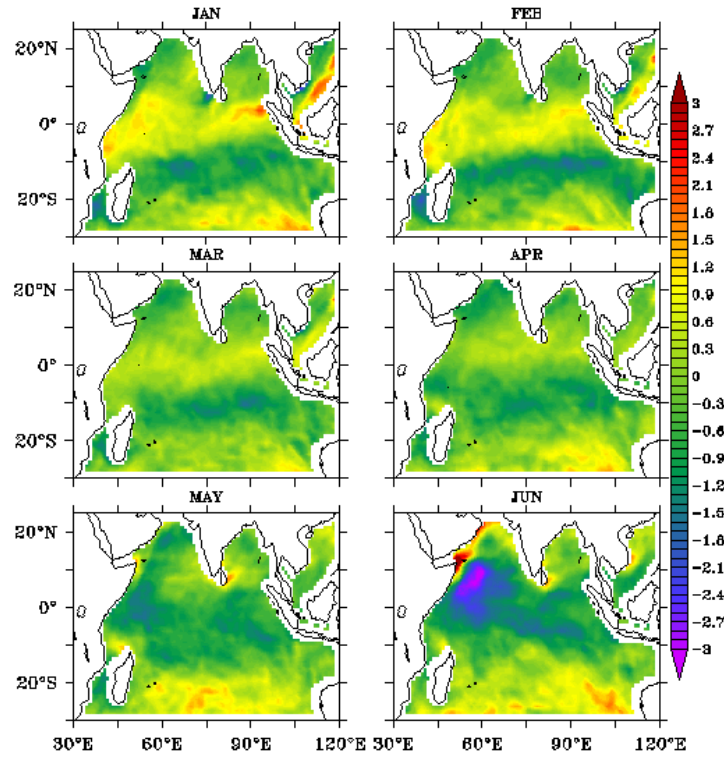
Fig. 2.13 Wind stress curl for Jan to June over the Indian Ocean
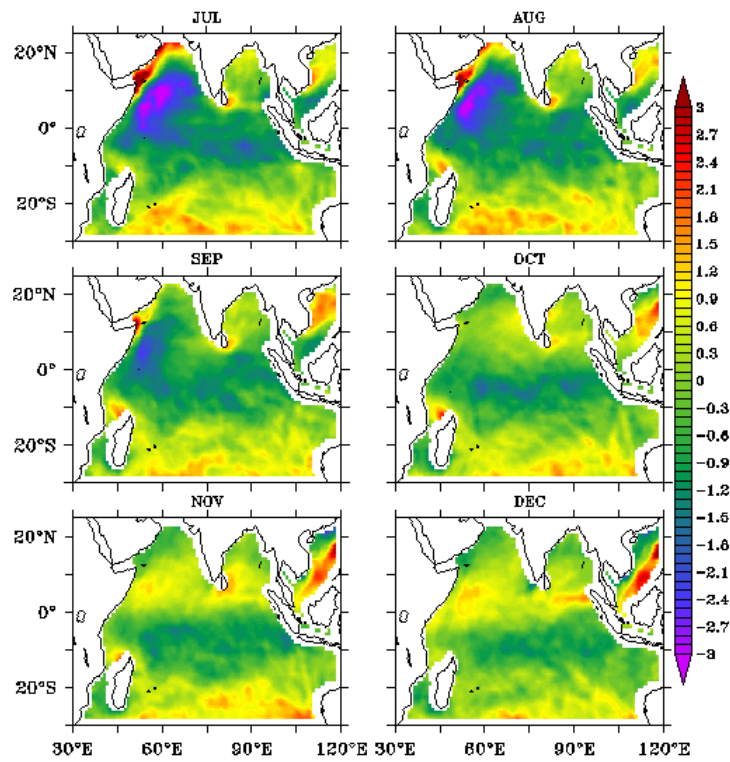


Fig. 2.14 Wind stress curl for July to August over the Indian Ocean

Very strong currents were observed off Visakhapatnam in February – March (La Fond, 1957) but it was Legeckis (1987) who reported the occurrence of a western boundary current along the east coast of India. Subsequent observational programmes (Shetye et al., 1993; Shetye et al., 1996; Sanilkumar et al., 1997) further confirmed the occurrence of the western boundary current i.e., the northward flowing EICC during the pre-monsoon period.

The present study reveals many unique aspects on the evolution of the EICC in the Bay of Bengal. Two eddies due to Visakhapatnam High/Low sustain and modulate the northward /southward flowing EICC. In fact the EICC turns northward north of Visakhapatnam with the formation of Visakhapatnam High in January and at the same time the Sri Lanka High forces northward currents east of Sri Lanka, while the EICC flows southward along the rest of east coast of India. From February onwards both the Visakhapatnam High and Sri Lanka High gradually moves towards each other, coalesces by April – May thus producing the continuously flowing southward flowing EICC along the east coast of India. The wind stress curl becomes negative from January (Fig. 2.13) forcing the Visakhapatnam High which is consistent with the Shetye et al (1993).

**2.4.5.1 The East India Coastal Current**

In May, the Visakhapatnam Low forms and the associated cyclonic eddy forces EICC to reverse direction north of Visakhapatnam (Fig.2.5). The Visakhapatnam Low strengthens along with the formation of Sri Lanka Low. These are the two cyclonic eddies in the western Bay of Bengal. In fact the northward flowing EICC is limited to about 10°N - 17°N and becomes weak by June. Both the Visakhapatnam Low and Sri Lanka Low strengthen and move closer during July – September and entire EICC flows southward by September. The two eddies coalesce by October – November and the EICC flows southward up to December. Thus it is very clear that the Visakhapatnam High/Low and Sri Lanka High/Low modulate the EICC. The northward flowing EICC is well established during March – May and southward flowing EICC very prominent during September – December. The transition occurs in January – February and June – August. However the northward flowing EICC is strong off Visakhapatnam especially in February – April and off Sri Lanka during January – February.

With the onset of the summer monsoon, the northward flowing EICC does not strengthen as might be expected (Schott et al 2001), but it weakens and reverses direction in the northern Bay of Bengal. The ship drift and surface geostrophic flows derived from T/P (Eigeneheer and Quadfasel (2000)) has shown that there is a western boundary confluence at 10°N, with the EICC flowing northwards to north of 10°N and southwards to the south of 10°N at the height of summer monsoon. The hydrographic observations (Shetye et al 1993; Shetye et al 1996) found that the transport of southward flowing EICC relative to 1000 db is about 2Sv in the northern Bay of Bengal which increases southward to about 8Sv. The northward flowing EICC showed a transport of 10Sv during March – May (Shetye et al 1993).

Since observations show a weak relationship with the local wind field in the Bay of Bengal, other processes such as basin-scale interior Ekman pumping, local along shore winds adjacent to northern and southern boundaries of the basin, and remotely forced signals that propagate into the Bay from the equator are possible mechanisms regulating the EICC (Schott et al 2001). The modeling studies of Yu et al (1991) and Potemra et al (1991) have brought out the importance of remote forcing from the equator on the Bay of Bengal circulation. A Kelvin wave formed at the equator propagates along boundary of the Bay, and partly radiating westward propagating Rossby wave into the interior thus affecting the currents. McCreary et al (1993) and Shetye et al (1993) have suggested that Ekman pumping forces the EICC from February to May.

Modeling studies of Shankar et al (2002) and Kantha et al (2008) suggest a variety of factors such as local winds and remote forcing play an important role in the evolution of the EICC which vary in the spatial and time domain. Shankar et al (1996) have shown that the superposition of forcing by local winds and Ekman pumping yielded good estimation of the EICC from June – December.

McCreary et al (1996), Vinayachandran and Yamagata (1998) modeled the Sri Lanka Low (Sri Lanka Dome). They argued that the Sri Lanka Low is associated with positive wind stress curl and it moves northward as the season progresses and the Sri Lanka Low appear to follow this. In January, an anticyclonic cell appears around 10°N which was called the Bay of Bengal Dome (Vinayachandran and Yamagata 1998). However our study shows that the Sri Lanka High (in January) forms almost at the same location where the Sri Lanka Low

forms in June. The Sri Lanka High moves northward by February – March and Sri Lanka High appears to move northward around 10°N by March. However the wind stress curl (Fig. 2.14) doesn't show any one to one correspondence with Sri Lanka High unlike in the case of Sri Lanka Low in during the summer monsoon season.

**2.4.5.2 The Eastern Bay of Bengal Current (EBBC)**

Compared to EICC the EBBC is much less studied. The EBBC is rather weak compared to EICC during most part of the year. The EBBC turns northward by May, probably associated with convergence and positive SSH in the eastern equatorial Indian Ocean associated with the Equatorial Jet. The EBBC changes its direction again southward by December again seems to be associated with Kelvin waves generated at the equator during the transition periods and its propagation along the eastern coasts of the Bay of Bengal (Clarke and Liu, 1994). The reversal of EBBC is remotely forced and occurs about 4.5 months before the wind reversal. The southward flowing EBBC during the summer monsoon is expected to produce upwelling during January – April. This aspect will be discussed in Chapter-4.

**2.4.5.3 The Central Bay of Bengal Currents (CBBC)**

The CBBC is greatly influenced by the Visakhapatnam High/Low and Sri Lanka High/Low and its evolution is similar to that of the EICC. When the EICC flows northward the currents in the central Bay of Bengal (CBBC) flows southward, it is strongest during April – May (Fig. 2.4 and Fig. 2.5). In fact the EICC feeds both the CBBC and EBBC. The northward flowing CBBC is strongest during July –October (Fig. 2.7 to Fig. 2.10). During this time the CBBC is fed by the SMC and southward flowing EICC. The intrusion of the SMC into the Bay of Bengal is discussed by Vinayachandran et al. (1999). In fact within the Bay of Bengal most of the water re-circulates under the influence of Visakhapatnam High/Low and Sri Lanka High/Low. In addition other eddies at the confluence of the Visakhapatnam High/Low and Sri Lanka High/Low by makes the CBBC more complex. This could be the reason for the complex nature of salinity distribution within the Bay of Bengal (Murthy et al 1992, Sanilkumar et al 1997, Varkey, 1996). The CBBC moves more

westward with the progress of the season both during February – May (Fig. 2.2 to Fig. 2.5) and June – September (Fig. 2.6 to Fig. 2.9).

### 2.4.6 Currents and circulation in the Arabian Sea

The major currents in the Arabian Sea are the Somali Current in the western Arabian Sea, the WICC along the west coast of India and the WMC in the southern Arabian Sea. As in the Bay of Bengal, these currents also show considerable seasonal variability and change direction twice a year.

### 2.4.6.1 The West India Coastal Current (WICC)

A close examination of the WICC indicates that the seasonal changes are intrinsically related to the formation and evolution of the Laccadive High (LH) and Laccadive Low (LL). The LH forms in November – December (Fig. 2.11 to Fig. 2.12) when the WICC is northerly and the LL forms in the June – July (Fig. 2.6 and Fig. 2.7) when the WICC is southerly. The currents off the southern tip of India start reversing its direction in January and July when the LH and LL respectively gets detached from the coast. The currents south of 10°N turns southerly/northerly, as the LH/LL moves away from the coast, by March/September respectively. However, the WICC becomes southerly along the entire west coast of India by April and continues up to July. On the other hand, the northerly WICC covers the entire west coast of India by October and continues up to January - February.

Observations have shown that strong upwelling takes place along the southwest coast of India during the summer monsoon when the currents are southerly (Ramasatry and Myrland, 1959; Banse, 1968). In general an upwelling favorable wind blows near the coastal regions (SW coast of India) during May – September and Shetye et al (1990) suggested that the WICC is driven by wind; However model results suggested that flowing WICC is remotely forced from the Bay of Bengal. The observations by Shetye et al (1991) showed that the northward WICC during winter is about 400 km wide off the southwest coast of India and about 100 km wide at 22°N, during December – January 1988. The EICC is strongest during this period when the coastal winds are weak suggesting the importance of remote forcing (Schott et al. 1991).

The present analysis indicates that the WICC is strongest (>40cm/s) off the southwest coast of India in December (Fig. 2.12) and it has a width of about 400 km as reported by Shetye et al (1991). As the LH propagate westward and dissipates into multiple eddies, the WICC shifts westward by February – March. The WICC weakens considerably by March. On the other hand the southerly WICC is strongest off the southwest coast of India in July – August and the core of strong currents is about 100 -200 km away from the coast.

Models studies (McCreary et al 1993) have shown that the WICC is linked to forcing in the Bay of Bengal via coastally trapped Kelvin waves traveling around the Indian sub-continent. Both the LH and LL are closely linked to remote forcing (Bruce et al 1998; Shetye et al 1996) and the WICC variations are related to the formation of LH and LL especially off the southwest coast of India. It should be noted that the WICC is strongest in the southeastern Arabian Sea and much weaker in the northeastern Arabian Sea in both winter and summer monsoon seasons.

### 2.4.6.2. The Somali Current System

Among the current systems in the Indian Ocean, the Somali Current during the summer monsoon is the most studied and documented. The summer Somali Current is one of the strongest western boundary currents with current speeds exceeding 300 cm/s at its peak (Swallow et al 1983). The strong currents and exceptionally strong southwesterly winds produce intense upwelling off Somalia resulting in SST below 20°C. The drop is as below as 14°C near the coastal region (Swallow and Bruce, 1966). These cold upwelled waters are transported into the central Arabian Sea and it is one of the major factors of the summer cooling in the Arabian Sea (Duing and Leetma 1980; Hareesh Kumar and Mathew, 1997).

The geostrophic currents from SSH data clearly indicate that northward flowing Somali Current has its origin at 5°S associated with a cyclonic eddy centered around 4°S, 42°E in April and it intensifies by May (Fig. 2.4 and Fig. 2.5). Direct current measurements also showed a strong northward current near the east African coast in May 1979 (Swallow et al; 1983). Meridional currents can not cross the equator freely because the potential vorticity of flow has to reverse the sign when changing hemispheres. As a result, subsurface cross equatorial exchange must take place largely via western boundary current, where frictional effects can compensate the vorticity change (Schott et al 1990). After crossing the equator,

western boundary currents typically turn offshore to join near equatorial flows in the interior ocean (as the Brazil current and New Guinea Coastal Current (Schott et al. 1990). Earlier studies (Swallow et al 1996; Schott, 1983; Schott et al 1997, Fischer et al 1996) indicated two major anticyclonic gyres in the Somali Current during the summer monsoon. A small anticyclonic gyre is centered around 2°N; 48°N (southern gyre) and bigger gyre is centered around 7°N, 52°E known as Great Whirl (GW). The Southern Gyre (SG) is weaker and less dominant as seen in the present study especially in June. The SG becomes more prominent in July – August (Fig. 2.7 and Fig. 2.8). The GW has a diameter of 300-400 km and situated more than 100 km away from the coast. The GW is almost a closed circular cell with very little exchange of water between its offshore circulation branch and the interior Arabian Sea (Schott et al 2001). The GW extends even down to 1000m with speeds of 10cm and the gyre structure remains visible even at greater depths as determined from moored observations (Schott et al 2001). Transport in late summer monsoon phase can exceed 70Sv (Fischer et al 1996; Schott et al 1997). Strong upwelling occurs all along the Somali Coast and SST becomes cooler than even 17°C where the GW turns offshore. The low sea level (negative SSH) all along the Somali coast also indicates this. It is interesting to note the regions of maximum negative SSH shifts northward with the progress of the monsoon; and towards the end of monsoon (September) maximum upwelling occurs off the Arabia coast. The Somali Current and the GW weaken considerably by October (Fig 2.9), Schott and Quadfasel (1982) discussed observations from moorings in the GW in 1979. They reported a distinct westward propagating signal after the onset of the summer monsoon. They interpreted them as first mode Rossby waves, and concluded that the wind stress curl offshore from the Somali coast by the long Rossby waves which reflected into short Rossby waves at the boundary accumulating energy there, which is further supported by modeling studies (McCreary and Kundu 1988; Luther and  O'Brien (1989). It should be noted that the GW occurs in the region where there is strong wind stress curl during summer monsoon (Fig. 2.22). There is also strong interannual variability in the Somali Current which is a challenge to modelers (Schott, 1983; Schott et al 2001). The interannual variability is discussed in the next Chapter.

The Somali Current during the winter monsoon is much less studied compared to the Somali Current during the summer monsoon. The present study suggests that during the winter monsoon southward flowing Somali Current is well established by November and

strengthens by December. A well defined anti-clockwise eddy found almost at the location of GW forces the winter Somali Current as a closed gyre, though a part of it flows into southern hemisphere. The winter Somali eddy weakens by February-March and hence the winter Somali Current also weakens. The southward flowing Somali Current continues till April even after the cyclonic eddy disappears.

There are only few observations in the Somali Current region during winter. Bruce et al (1981) reported that the GW can preserve summer monsoon conditions underneath the winter monsoon surface circulation for some time into the latter period. The mean vertical structure of the winter Somali Current is presented by Quadfasel and Schott (1983) from historical hydrographic data. The northern winter Somali Current is characterized by an inflow from the east which causes a divergence between 6-8°N near the coast with northward flow north of these latitudes and equator flow south of these latitudes (Schott and Fischer, 2000). The southward Somali Current is quite shallow, at the equator with a transport of 5Sv in the upper 150m (Swallow et al. 1983).

The model simulations of McCreary et al (1993) clearly show the winter Somali Current which is consistent with our observations, a strong southward coastal current develops along much of the Somali coast from 7°N-8°N across equator to 2.5°S and north of 8°N there is a weak northward current.

However, the present study shows that the winter Somali Current is also closely related to LL. The LL completely gets detached from the west coast of India and rapidly moves westward and reaches the western Arabian Sea by November as a strong cyclonic eddy which forces the winter Somali Current. Unlike the LH, the LL doesn't disintegrate rapidly, though two distinct cyclonic eddies can be seen within a larger cyclonic eddy. These two cyclonic eddies coalesce by January thus forcing strong southerly current along the western side of the eddy i.e., along the Somali Coast and northward flow on the eastern side of the eddy i.e., east of 52° E; between 3° and 8°N both westward and southward currents are found which are contrary to model results of McCreary et al (1993), but consistent with ship observations. The current vectors suggest currents as strong as 50cm/s during December-January. The formation and propagation of LL appears to be closely related to the region of positive wind stress curl from July to January as evident from Fig.2.14

**2.4.6.3 Currents along the Arabian coast**

The currents along the Arabian coast are much less understood compared to the Somali Current. The LH sheds into multiple eddies and reaches Somali coast by March. The Somali Current flows southward in April and same is the current along the Arabian coast. However the SSH indicates that the LH often after reaching the Somali coast propagates northward and by May the current along the Arabia coast turns northerly with multiple anticyclonic eddies north of Socotra and along Arabia coast forcing a northward current. There are at least three clockwise eddies of 200 – 300 km across within a large clockwise eddy off Arabia coast in June, which weakens and turns further off shore with the progress of the monsoon. The significantly negative SSH during August – September and October indicates intense upwelling extending 400 km offshore, which is unusually large for any upwelling region (Smith and Bottero, 1977). In the large upwelling zone there are a number of cyclonic eddies which cause the water to re-circulate around these eddies and carry the upwelled water away from the coast along the northern boundaries. The presence of these eddies may be one of the reasons for the unusually large extent of upwelling off the Arabia coast. The large number of cyclonic eddies moves away from the coast by October – November and the coastal currents turns southward by October and strengthen by November. Hence in general the currents off Arabia are northerly (northeasterly) from May – September and southerly (southwesterly) from October – April.

During JGOFS (1994 – 1996) extensive repeated ship observations were made normal to the Arabia coast. They have shown the presence of a northeastward coastal Jet along the south coast of Oman in May which persisted during the summer monsoon, which is called the Ras Al Hadd Jet (Bohm et al; 1999). This jet is associated with an anticyclonic gyre just south of its offshore turning point and a cyclonic eddy to its north (Flagg and Kim 1998; Bohm et al 1999). Its velocity may reach over 1 m/s and has largest transport in September varying between 2- 8Sv. The alongshore northward flow during monsoon is caused by an onshore pressure gradient due to intense upwelling which reduces sea level near the coast by about 30 cm (Shi et al 1999).

There are other circulation cells existing elsewhere along the Oman Coast, their location seems to be linked to protruding capes of Arabian Peninsula (Schott et al 2001).

Between these cells (gyres), upwelled waters can be transported offshore in filaments or squirts, where offshore currents exceed 50 cm/s (Brink et al 1999), with transports of 1 – 2Sv.

The JGOFS investigations showed four persistent filaments off Arabia during summer monsoon, with offshore transport of 4 -8Sv which is larger than the estimated offshore Ekman transport (Schott et al 2001). The offshore Jets are deflections of alongshore flow that carry upwelled waters offshore and this transport is partially balanced by on shore currents at the other periphery in the re-circulating gyres.

The present study also confirms a large number of mesoscale gyres offshore off the Arabia coast not only during the summer monsoon, but also during October – December and April, where recirculation of waters takes place. These gyres are mostly anticyclonic during May – June, but cyclonic during latter part of the monsoon and October /December.

**2.4.6.4 The Coastal Arabian Sea Current (CASC).**

Like the WICC the westward movement of CASC is also dependent on the LH and LL. The CASC is northerly from December (Fig. 2.12) and occurs at the confluence of anticyclonic LH and cyclonic LL. As the LH and LL move westward the core of the northward CASC also move westward. During this time the CASC is fed by the westward moving WMC which carries low salinity water from the Bay of Bengal and also the re-circulating waters of the LL which with its core near the Somali coast. In January (Fig. 2.1) the WMC is seen as far west as 60°E where an eastward flow due to the recirculation from the Somali Current also joins the CASC, which continues in February as well. By March the WMC extends up to the western side of the Arabian Sea but an anticyclonic eddy off Somalia causes the recirculation of WMC as an eastward flow between 5° and 10°N and moves northeastward, which continues via April, May and June. The model simulations of McCreary et al (1993) shows the WMC flowing westward far into the Arabian Sea with some of its flow turning northward along an elongated LH and some continuing towards Somalia coast.

Schott et al (2001) points out that the CASC is due to remote forcing by Rossby waves originating in, or propagating across, the central Arabian Sea and also confirmed by observations (Brandt et al 2002).

The CASC flows southward and southeastward during July – October, between the large anticyclonic gyre in the central Arabian Sea and the LL. However, these CASC during this period is weaker (<10cm/s) compared to northward CASC. During this period part of CASC re-circulates within LL and the anticyclonic eddy west of it and another part joins the SMC and flows into the interior Bay of Bengal through the CBBC. Similarly the northward flowing CASC during April – May the CABC is mostly fed by the WMC retro flexion from the western Arabian Sea, and part of flow from the northern Arabian Sea.

### 2.4.7 Equatorial current system

The conventional surface equatorial current system in the Pacific and Atlantic Oceans consists of the North Equatorial Current (NEC) driven by the northeasterly trade winds, the South Equatorial Current (SEC) driven by the southeasterly trade winds and the Equatorial Counter Current (ECC), sandwiched between the WMC and SEC. In the Indian Ocean the WMC and SEC flow westward while the ECC flows eastward.

### 2.4.7.1 The Winter Monsoon Current (WMC)

The wind system in the equatorial Indian Ocean is similar to those in Atlantic and Pacific Oceans only during the northeast monsoon. Hence similar current systems as in the Pacific and Atlantic are expected in the Indian Ocean. The WMC develops in the eastern and central Indian Ocean (south of India) in December and extends as far west as 55°E in January and up to 48°E in February. The WMC is observed throughout the north Indian Ocean in March with speeds 60 -80cm/s. Though diffused the WMC is seen in April also. At its peak (January – March) the WMC is mostly fed by the waters from the Bay of Bengal which are low saline. Observations have shown that WMC had a transport of 11Sv in 1991 (Schott et al 1994). The WMC was supplied by re-circulating water brought eastward north of equator (Hacker et al 1998). The WMC carrying fresher water from the Bay of Bengal into the Arabian Sea through EICC (Stramma et al 1996) and possibly into coastal and western Arabian Sea through CASC as inferred from the current direction.

**2.4.7.2 The Summer Monsoon Current (SMC)**

With the onset of summer monsoon the WMC completely disappears and the eastward SMC is driven by southwesterly winds that appear between the equator and 5 – 7°N, which become well established from July to October. These currents are particularly strong centered around 5°N and south of India and Sri Lanka with speeds in the range of 60 – 80cm/s. However, observations south of Sri Lanka have shown that the SMC decayed rapidly with depth (Schott et al 1994). The eastward SMC transport between 4° - 6° N was estimated to be 8.4Sv between 4 – 6°N, in the top 100m. The source of water for SMC is mostly from the Arabian Sea, two inflowing branches are supplied by the near equatorial flow of the Somali SG and the northward outflow of the Somali Current (Schott et al 2001), though their relative contributions are unknown. Most of the SMC after crossing Sri Lanka flows into the Bay of Bengal with an estimated transport of about 10Sv across 6°N. Thus considerable amount of high salinity Arabian Sea water is transported into the Bay of Bengal through SMC which are re-circulated by the Visakhapatnam Low(VL) and Sri Lanka Low(SL) and into the EICC. The present study doesn't indicate any significant flow of SMC east of Sri Lanka near the equatorial belt; though a portion of the SMC waters are seen to re-circulate through an anticyclonic gyre southeast of Sri Lanka.

**2.4.7.3 The Equatorial Jet**

The westerly winds produce strong currents along the equator towards east known as Equatorial Jets (EJ) (Wyrtki, 1971). The Equatorial Jet is confined to 2°N to 2°S of the equator and is strongest in the central Indian Ocean. The EJ is clearly seen in the present study also, but the speeds are to be viewed with caution as geostrophic approximation has limitation close to the equator.

The two EJs have roughly the same strength of about 100 cm/s, being somewhat stronger in the Fall than in the Spring (Schott et al 2001). The observations at Gan Island also showed similar results (Knox, 1976) and also in 1993 – 1994 (Reppin et al 1999), but 1993 – 1994 were two contrasting years for the equatorial wind forcing.

The EJ transports waters from west to east decreasing mixed layer thickness and sea level in the west and increasing them in the east (Wyrtki, 1973). At the eastern boundary EJ

is reflected as Rossby waves and part propagating along eastern boundary poleward. These eastern boundary waves generate slowly propagating Rossby waves into the Bay of Bengal and the eastern Arabian Sea (Perigoud and Delecluse, 1992; Basu et al, 2000). Models suggest that the equatorial variability is carried around the boundaries of the Bay of Bengal and even around Sri Lanka though supporting observations are lacking. Similarly southward traveling EJ signals may produce variations in the Indonesian through flow (Sprintel et al 2000). Solution by Han et al (1999) has shown that direct forcing by the semiannual component of the wind is the dominant forcing mechanism and it accounts for 81% of the maximum amplitude. Some models driven by realistic winds show weaker Fall EJ than the Spring one (Anderson et al 1993, Han et al 1999). The present study also shows similar results from SSH data. Larger positive SSH in the eastern Indian Ocean in May compared to November and the resulting northeastward and southeastward currents are also stronger in May – June. It should be noted that there are at least two years when Fall EJ was totally absent in the Indian Ocean. Hence the averaged SSH (1993 – 2004) is also effected by these unusual events.

**2.4.7.4 The Equatorial Counter Current (ECC)**

The ECC is very clear south of the equator, though with varying magnitude and width from December – March (Fig. 2.1.1 to 2.1.3). The wind system over the tropical Indian Ocean resembles the classical trade winds as in the Atlantic and Pacific during December – March i.e., northeast monsoon. The Inter Tropical Convergence Zone moves slightly south of equator during this period. The equatorial currents are also expected to follow the wind system with the WMC, the SEC and the ECC. The ECC flows eastward. The ECC is very clear in the ship drift data (KNMI, 1952; Cutler and Swallow, 1984; Rao et al. 1991). Duing and Schott (1978) and Swallow et al (1991) termed this current as South Equatorial Counter Current (SECC). However, ECC would be more appropriate name it is consistent with the case of Atlantic and Pacific Oceans. The SECC is classified as countercurrents within the westward flowing SEC. The ECC disappears with the formation of EJ by April. Monthly drifter data showed continuous eastward flow across the basin in February (Shenoi et al 1999a), causing high sea level in the eastern Indian Ocean (Murrow and Briol, 1998).

**2.4.7.5 South Equatorial Current (SEC)**

The SEC flows westward throughout the Indian Ocean in the annual cycle, mostly between 10° - 20°S (Fig. 2.1 to 2.12). This is consistent with ship drift currents. The SEC is more organized at the western boundary during winter than in summer (Schott et al 2001). Estimates based on hydrographic data (using geostrophy) shows that the SEC has a transport of about 39Sv across 54°E (Schott et al 1997) while the SEC south of northern end of Madagascar was only 25Sv (Stramma and Lutjeharms 1997). But in any case the transport of SEC is much higher than that of the WMC or the SMC.

The present study indicates the presence of westward propagating cyclonic and anticyclonic gyres within the SEC, which probably originates in the eastern Indian Ocean. A large cyclonic gyre in the eastern Indian Ocean formed in February propagates westward as far as 70°E by June and dissipates, at the same time in the western Indian Ocean a similar cyclonic eddy forms centered around 60°E which also grows and propagate westward up to the African coast. Similarly an anticyclonic eddy forms in the eastern Indian Ocean by May propagates as far west as 70°E and dissipate by February. Both the cyclonic and anticyclonic eddies formed in the eastern Indian Ocean do not propagate west of 70°E. The reason for this is not clear. Under the influence of the anticyclonic eddy strong eastward currents form around 13 - 15°S in the eastern Indian Ocean.

**Interannual Variability of Surface Geostrophic Circulation (1993 -2004)**

**3.1 Introduction**

As seen in the last chapter, most of the mesoscale features of the Indian Ocean circulation are transient, but recurring. The year-to-year variability in their strength, location and timing are largely unknown due to lack of adequate observational data.

Superimposed on the mean circulation there is strong variability of currents and hence circulation of various time scales ranging from synoptic to interannual (Kantha et al 2008). At times the variability may be moderate and can also be very large as in 1994 and also 1997 – 98, when anomalous winds appeared in the equatorial Indian Ocean (Webster et al 1999, Saji et al 1999, Murtugudde et al 2000). Oceanic and atmospheric variability of very large scale was reported in the year 1961 (Kapala et al 1994). No systematic monitoring system as in the equatorial Pacific exists in the Indian Ocean. In this context the satellite observations provide the best tool to understand the interannual variability of currents and circulation in the Indian Ocean. Unlike the SST observations, the SSH data contains the signals of subsurface also.

There are few observations of currents in the Indian Ocean covering few seasonal cycles. The first of its kind was collected near the Gan Islands in the equatorial Indian Ocean (Knox, 1976). Observations using current meter moorings provided more information on the Somali Current system during INDEX-79 (Schott and Quadfasel, 1982; Swallow et al 1983; Schott, 1983). Current meter array mooring south of Sri Lanka during WOCE (1993 -94) brought out many aspects of winter and summer monsoon current variability (Reppin et al 1999). Large variability in the equatorial currents was also noted from earlier measurements in different years (Luyten et al 1980; Luyten and Roemmich 1982). Spatial observations over an eight year period (1971 – 1978) during the pelagic fisheries programme showed large interannual variability in upwelling off the southwest coast of India (Pillai et al 1980). Similar variability was observed in the surface salinity field in the winter off the southwest coast of India during these years indicating probable variations in current field which transport low salinity water into the southeastern Arabian Sea.

All these studies are limited to either short time or spatial scales and hence inadequate to provide basin scale variability of these features. Hence monthly mean SSH is utilized to compute the surface geostrophic flow over the tropical Indian Ocean for each month for the entire period 1993 – 2004. The data sets used for estimation of geostrophic currents are the same as in Chapter II.

## 3.2 Interannual variability of geostrophic currents and circulation in the Indian Ocean.

In the absence of direct measurements of currents the geostrophic currents from SSH provide the best tool to understand the interannual variability of currents and circulation in the Indian Ocean. For this purpose monthly averages of each year of SSH was calculated from weakly SSH data for the period 1993-2004. The computed geostrophic currents are superimposed on monthly weekly SSH field. Maps of alternate months from January (January – March – May – July – September – November) are only presented in the following discussion for brevity. These are presented in Fig 3.2.1 – 3.2.18. For easier comparison the evolution of flow field on the interannual time scale is brought out for the Arabian Sea, the Bay of Bengal and the equatorial Indian Ocean as in Chapter II. For easy referencing of figures a tabular form also made. From this table figure number is known for a given area and month. Each figure has 12 panels corresponds to 1993 to 2004 with year label.

| | January | March | May | July | September | November |
|---|---|---|---|---|---|---|
| Arabian Sea | Fig. 3.1 | Fig. 3.2 | Fig. 3.3 | Fig. 3.4 | Fig. 3.5 | Fig. 3.6 |
| Bay of Bengal | Fig. 3.7 | Fig. 3.8 | Fig. 3.9 | Fig. 3.10 | Fig. 3.11 | Fig. 3.12 |
| Equatorial | Fig. 3.13 | Fig. 3.14 | Fig. 3.15 | Fig. 3.16 | Fig. 3.17 | Fig. 3.18 |

Table: 3.1 Showing figure numbers for given area and month for easy reference

In the discussion, the term summer and winter corresponds to the northern hemisphere. Since the scale of interannual variability is too complex in the tropical Indian Ocean the discussion is limited to only salient features and as brief as possible. It may also be noted that the limited discussion is also due to lack of direct observations for comparison purposes.
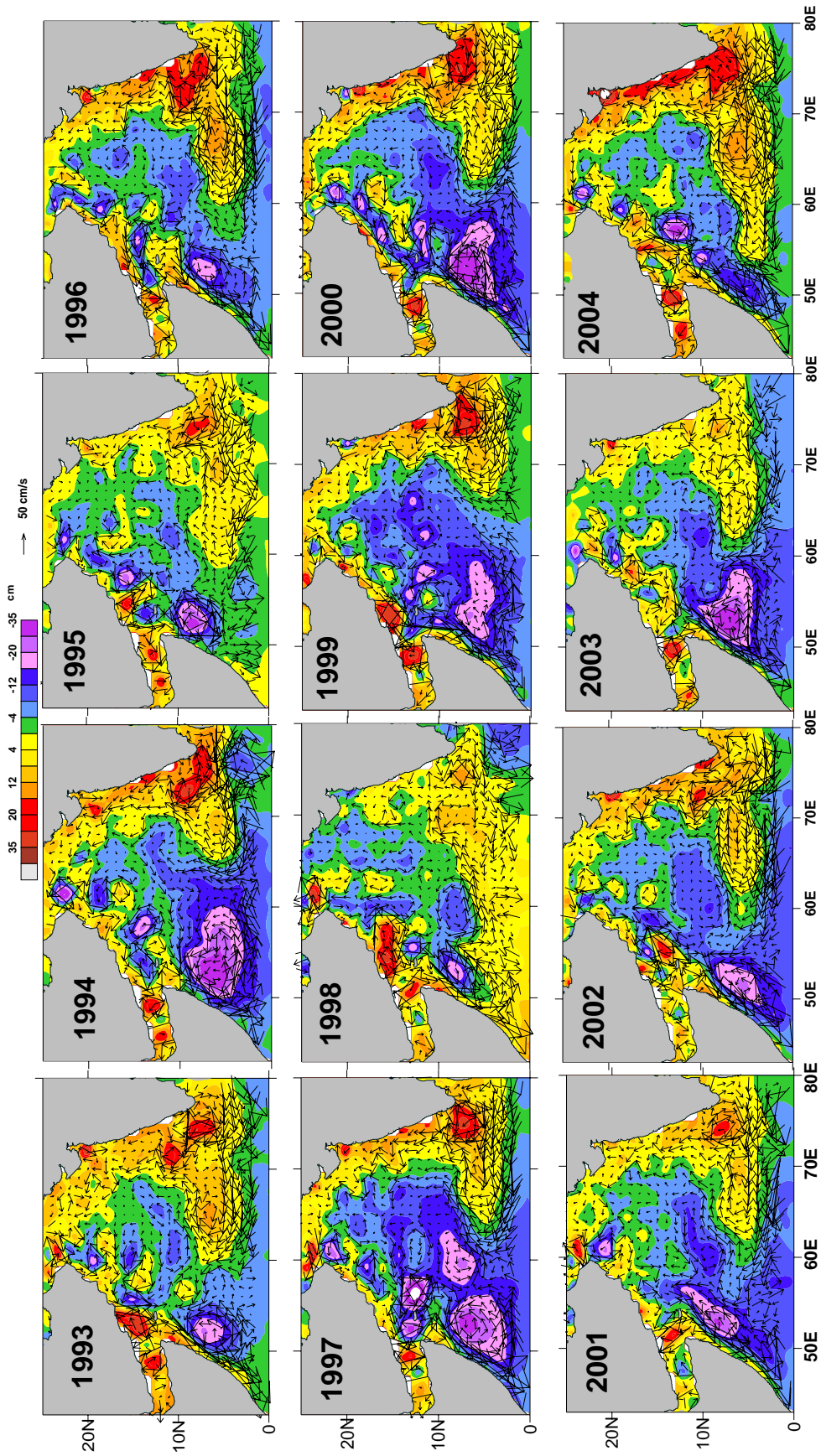
Fig. 3.1 January mean geostrphic currents overlaid on SSH in the Arabian Sea

52
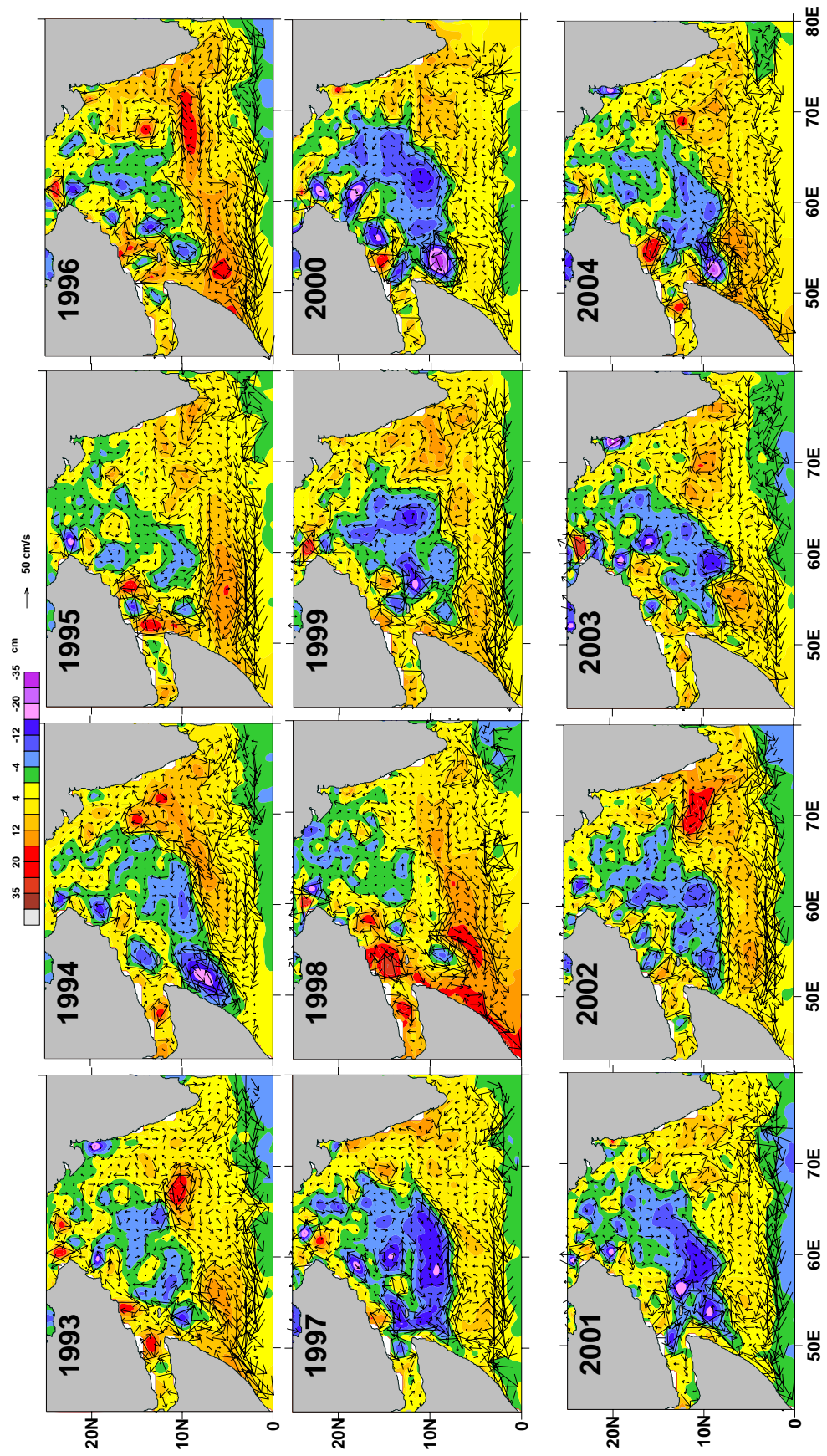
Fig. 3.2 March mean geostrphic currents overlaid on SSH in the Arabian Sea
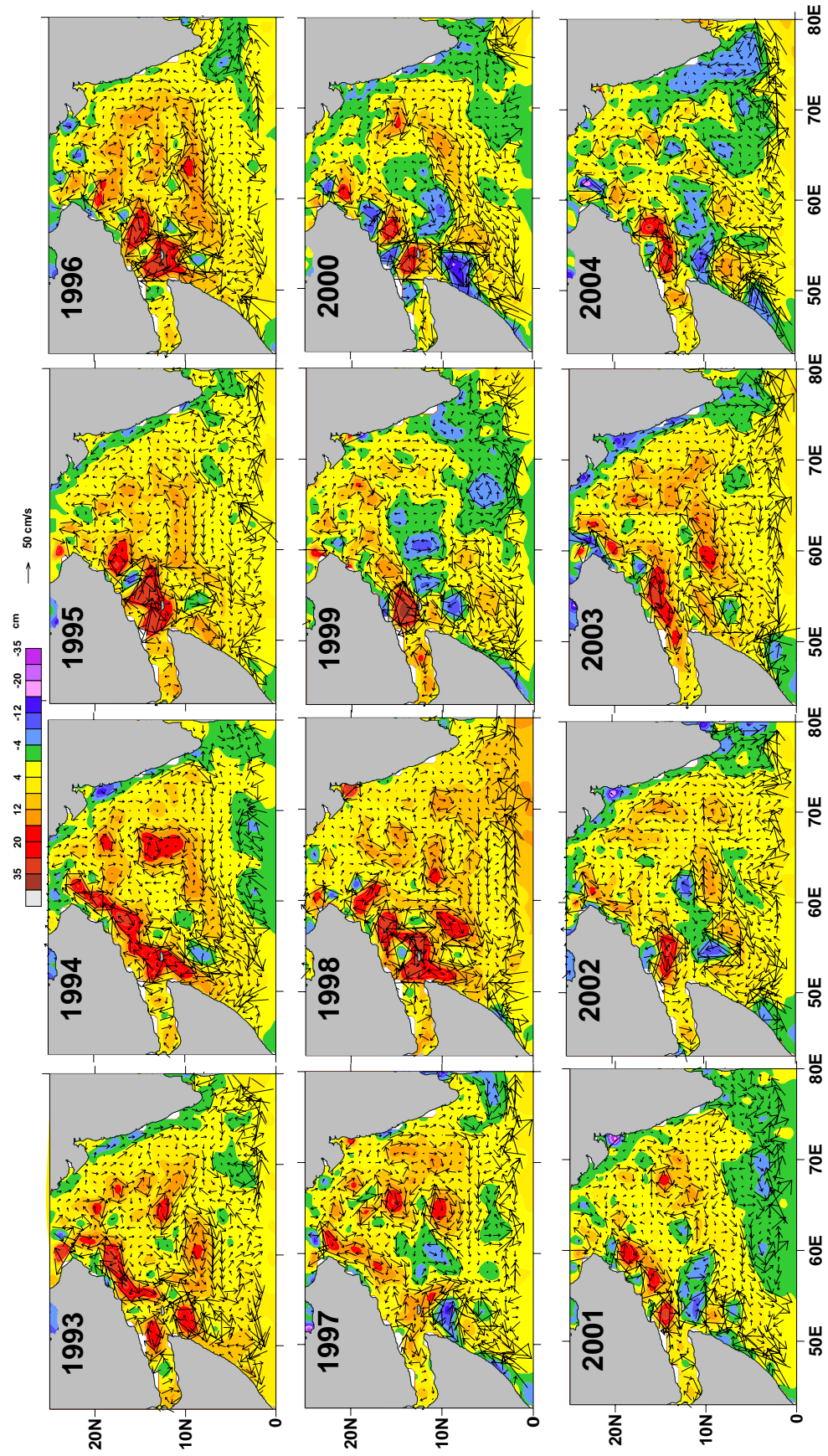
Fig. 3.3 May mean geostrphic currents overlaid on SSH in the Arabian Sea

54

**3.3 Interannual variability in the Arabian Sea.**

Though the large-scale features of circulation in the Arabian Sea are repetitive from year to year, there are considerable interannual variations in the mesoscale and synoptic scale circulation pattern. The major features of interannual variability in the current and circulation are discussed below.

**3.3.1 The West India Coastal Current (WICC)**

In general the WICC turns southward off the southwest coast of India in January itself as the LH detaches from the coast, which sometimes occur, as early as in December (1994, 1995, 2002) and as late as in February (2000,2004) (Figure not presented). The WICC becomes southerly along the entire west coast of India by April as a weak current (< 20 cm/s) in most years, which strengthens, with the onset of the summer monsoon. The LL was particularly strong during July/August. The LL was weak in both the anomalous years (1994 and 1997) with weaker WICC and lesser extent of LL, which is also indicative of weaker upwelling off the southwest coast of India. The LL was very strong in 1993, 1995, 2001 and 2002 especially in August September. Within the LL there are large number of cyclonic eddies especially close to southwest coast of India which also indicates closed gyres within the large LL and also upwelling wedge at many locations of the southwest coast of India which vary within the season and also on the interannual time scale (Fig. 3.4 and 3.5). Similar conditions must be the reason for the large scale interannual variability in upwelling between 1971 -78 observed off the southwest coast of India (Pillai et al 1980).

Though the WICC turns northerly all along the west coast of India by October (Figure not presented), the negative SSH remains. However, these are replaced by positive SSH and stronger northward WICC occurs during both 1994 and 1997. This suggests that stronger northward WICC during the Fall when strong positive IOD occurs. Further the LH formed at least one month ahead (October) in both the years. In fact the LH formed in October, propagated westwards in October 1997 itself, and by November in 1994(Fig. 3.6). This could be related to earlier onset of WMC during these years.

Signal from LH propagate not only westward but northward as well. The positive SSH engulf the eastern Arabian Sea close to the coast by November (by October in 1994 and 1997) with the exception of 1998 and 1999. Within the northward WICC there are

indications of number of anticyclonic eddies which modifies the northward WICC into several cells where at its boundaries they transport waters zonally (Fig. 3.5 and 3.6). The relative positions and number of these cells vary within the EICC during all seasons could be relative to coastally trapped waves (Kelvin waves) which may also radiate Rossby waves which propagate westwards. The dynamics and its considerable interannual variability of the cells remain unclear.

### 3.3.2 The Somali Current System

There are few observations within the Somali Current during summer monsoon to study the interannual variability during WOCE (Fischer et al 1996). These observations are made during the summer monsoon of 1993, 1995 and 1996.

The present study clearly shows the Great Whirl (GW) occurs in June although in some years it is evident in May itself (1993, 1995, 2001, and 2004) (Fig 3.3). The GW formed in the region of strong negative wind stress curl (Schott and Quadfasel 1982), and by July the GW is seen as a strong anticyclonic gyre with varying diameter (300 -500 km) in different years (Fig. 3.4). The GW was much smaller in dimension in 1994, 2000, 2001 and 2002 in July. The shape of GW also varies from year to year though it appears as a circular gyre in most years (Fig. 3.4) and elliptical gyre in other years. The northern limit of GW extends up to 10°N in many years (1994, 1995, 1996, 1998, 2003 and 2004) but it was at about 8°N in 1993, 1999, 2000, 2001 and 2002.

The Southern Gyre (SG) moves offshore between 2° -4°N in all the years during June – July. But the SG seems to be maintained by different mechanisms in different years. In 1993, 1997, 1999, 2000, 2001 and 2002 the SG appeared as an anticyclonic eddy with offshore transport at its northern periphery around 4°N (Fig. 3.4). On the other hand the SG appeared with strong offshore flow at the southern boundary of strong upwelling wedge in some years (1994, 1995, 1996, 1998, 2003 and 2004). It is not clear why such large changes occur in SG during different years. Both local and remote forcing may play an important role in sustaining the SG which differs from year to year.
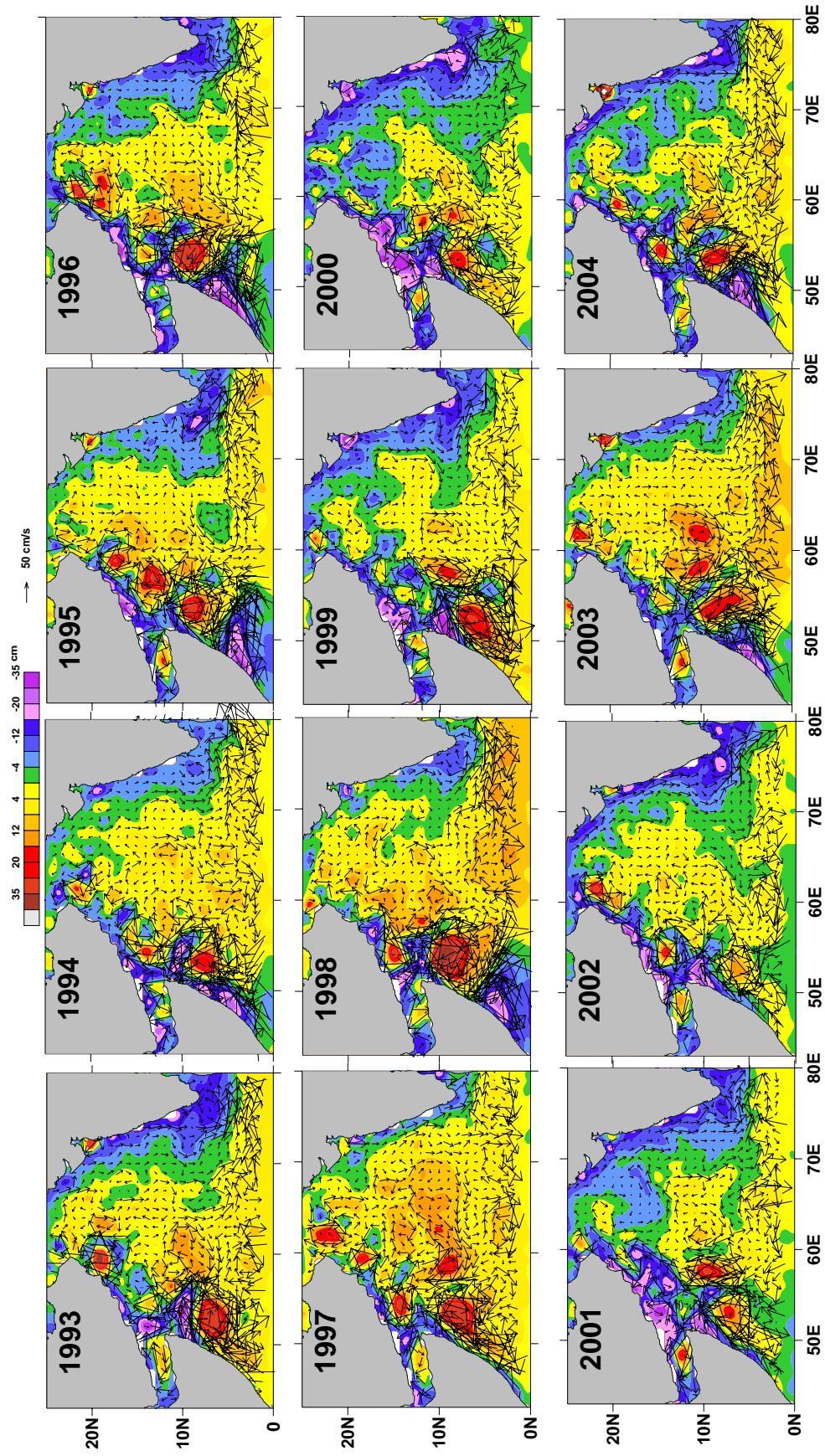
Fig. 3.4 July mean geostrphic currents overlaid on SSHA in the Arabian Sea

57
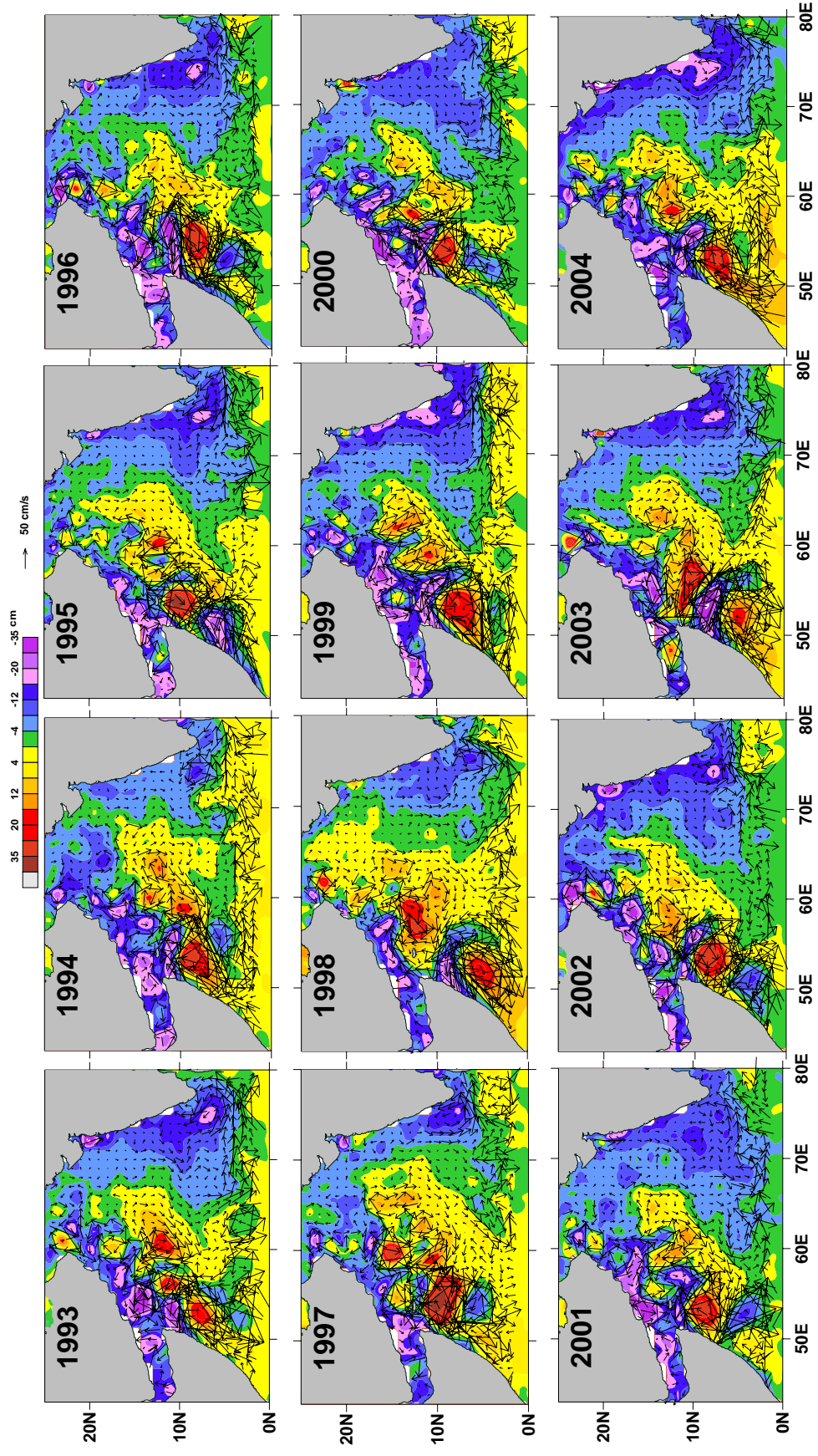
**Fig. 3.5 September mean geostrphic currents overlaid on SSH in the  Arabian Sea**

58
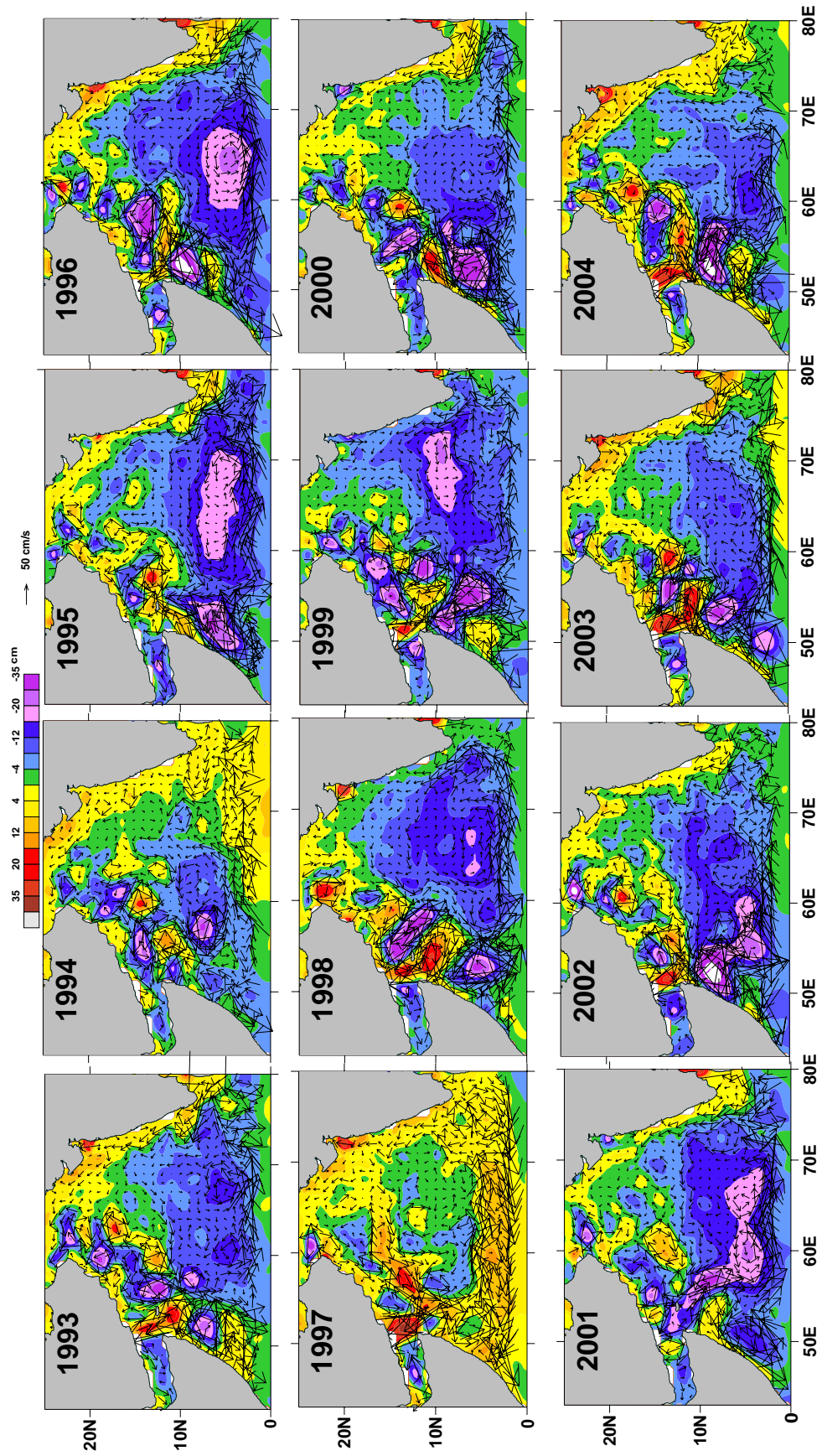
Fig. 3.6  November  mean geostrphic currents overlaid on SSH in the  Arabian Sea

59

Some observations have suggested that the SG and GW coalesce to form a single gyre as in 1979 (Evans and Brown, 1981; Schott 1983; Swallow et al 1983) as the southern cold wedge propagate at a speed of about 1m/s northward with the progress of the summer monsoon. However such coalescence was not observed during the WOCE observations in 1995 – 96 (Schott et al 1997). The breakdown of the two gyre system may be a rare occurrence (Schott et al 2001). Both the SG and GW could be observed in the present study till September (Fig 3.5) with the exception of few years (1993, 1994, 2003 and 2004). This suggest that during most of the years the two gyre system prevails within the summer Somali Current and merging of both SG and GW occur only on rare occasions as suggested by Schott et al (2001).

Moored and ship board observations during WOCE (1993-1996) showed that the northern boundary of GW at about 200 Km south of Socotra in 1993 while in 1995 it was close to Socotra and continued till mid October as a well organized gyre as in 1993, and the gyre transports were weaker than 1995 and the GW became disorganized by August 1996 (Fisher et al 1996). The present study also supports the observations for 1993 and 1995 but not in 1996. A strong upwelling wedge off the northern Somalia coast appears to have pushed the GW at least 400 Km offshore (Fig 3.4) by August 1996 and hence the observations of Fisher et al (1996) missed the GW.

The present study shows intra-seasonal variability in the SG, GW and upwelling wedges. In 1997 both SG and GW were vary strong as anticyclonic eddies by August. The upwelling wedges off the Somalia coast were particularly weak both during 1994 and 1997 (August onwards) indicative of weak upwelling off Somalia. The weaker upwelling off Somalia and consequent SST changes are related to strong positive IOD events.

Models forced by interannual varying winds (Luther 1999) could not simulate the Somali Current variability. High resolution modeling (Wirth et al 2002) showed that the interannual GW variability is stochastic and predominantly determined by internal processes and not by interannual variability in the wind field. Hence comparisons with observations would not be meaningful for individual realizations, only for ensembles of output fields (Schott et al 2001).

Overall, the interannual and intra-seasonal variability in each year within the summer Somali Current is so complex that it is extremely difficult to model. There is large variability

in the characteristics and locations of both SG and GW and accordingly the currents at any place within the Somali Current are not repeatable. This also causes large variations in the distribution of mass and momentum in the Arabian Sea.

The Socotra Gyre is prominent as another anticyclonic gyre during the earlier half of the monsoon (June – July) (Fig. 3.4). The location and characteristics of the Socotra gyre also show considerable interannual variability as the SG and GW.

In general, the winter monsoon Somali Current is established by November due to the westward movement of LL with variable currents in October. Till now there are few direct observations on the interannual variability of the winter Somali Current. The winter Somali Current flows southward by November in most years (Fig. 3.6) but there are exceptions as well, the notable being in 1997 (Fig 3.6), when the southward flow was weak and variable and also in 1999 where a weak GW continued till November (Fig 3.6).

The winter LL occurs almost at the same location as the GW near the Somali coast. However as in the case of GW, the winter Somali eddy has varying characteristics from year to year. The winter Somali Current occurs in a region of strong positive wind stress curl. The winter Somali Current was particularly strong (~ 50 cm/s) except in both 1994 and 1997 the years of strong IOD events. Strong positive IOD events seem to weaken the winter Somali Current. Observations during WOCE (Schott and Fischer 2000) showed that the winter Somali Current is caused by divergence developed at the coast near 6 – 8°N, with northward surface flow passes through Socotra passage, but also veers eastward along the southern banks of Socotra.

There are not much modeling studies on the interannual variability of winter Somali Current. It appears that both the local and the remote forcing could play an important role in the interannual variability of winter Somali Current. The relative importance of these factors on the variability of winter Somali Current is yet to be understood.

**3.3.3 Interannual variability of currents off the Arabia coast**

One of the most important aspects the currents of the Arabia coast is the presence of large number of cells (small eddies) or filaments. The northward current of Arabia starts in March itself in 1998 (Fig. 3.2) following strong IOD event. In other years the northward current is well established by May with the exceptions of 1993, 2000, 2001 and 2004. During

November to April both cyclonic and anticyclonic cells could be observed off the Arabia coast where the exact location and number of cells vary from year to year. However during May – June mostly anticyclonic cells are observed. In most of the years these cells are spaced 200 – 300 km apart but in few years (1993, 1994, 1998 and 2003) few cells coalesce (Fig 3.2) to form continuous northward current. In later part of the monsoon mostly cyclonic cells prevail off the Arabia coast, with varying dimensions and numbers in different years. These cells or filaments carry water offshore/near shore at its boundaries.

These cells or filaments could not be observed in the ship drift observations. The ship drift can be affected by Ekman drift and also 'windage' which adds artificial current in the direction of wind (Schott et al 2001).

Observations during JGOFS (1994 – 1996) confirmed the existence of filaments off the Arabia coast during the summer monsoon, with large offshore transport. Earlier ADCP observations also showed similar results (Elliot and Savidge 1990). The offshore transport of these filaments are much larger than excepted. These filaments are apparently linked to protruding capes of Arabian Peninsula (Schott et al 2001). However the interannual variability of these filaments could be due to the many factors as well such as monsoon variability and remote forcing as in other parts of the tropical Indian Ocean.

The extremely low sea level (negative SSH) off the Arabia coast during late summer monsoon is evident in all years, with stronger upwelling in 1993, 1994, 1999, 2000, 2001 and 2003 (Fig. 3.5). The location of strong upwelling wedge of the Arabia coast has also varied from year to year. So far no detailed model study addresses the interannual variability of current off the Arabia coast.

### 3.3.4 Interannual variability of the CASC

In the Arabian Sea the northward CASC is observed during December – April (Fig. 3.1, 3.2 and 3.5) with its core progressively shifting westward with the progress of time. Within the CASC a large number of both cyclonic and anticyclonic eddies modify the flow as many closed gyres which vary seasonally and interannually. The strength of these eddies and the resulting currents and also its locations vary from year to year. Similar large scale variability was observed in the southward CASC as well in different years.

The existence of several eddies in the central Arabian Sea was observed in ADCP surveys (Flagg and Kim 1998) and further confirmed by Kim et al (2001). The eddy scales are several hundred km near the Arabia coast but only 100 – 200 km in the central Arabian Sea (Kim et al., 2001). They also observed that intra-seasonal variability is less south off 15°N. However, the present analysis suggests considerable inter-seasonal and interannual variability south of 15°N as well. Recently Shenoi et al (2007) have shown that a number of eddies in the Arabian Sea propagate westward and reaches the Red Sea. They argued that these eddies are related to Rossby waves generated in the eastern and coastal Arabian Sea which propagate westward.

## 3.4 Interannual variability in the Bay of Bengal

Till now, very little is known about the interannual variability of currents in the Bay of Bengal.

## 3.4.1 The EICC

As in climatology, each year the evolution of EICC is closely limited to the VH/VL and SH/SL (Fig. 2.1 to 2.12 in Chapter-II). However, there is considerable interannual variability in the geographical location of VH/VL and SH/SL and also in the relative strength of currents. For example in January the VH is located off Visakhapatnam as a strong anticyclonic eddy (panels of 1993,1996,1997,1999, 2001 and 2002 in Fig. 3.7) thus producing strong western boundary currents), on the other hand in some other years VH appears as a weak anticyclonic eddy (panels of 1994, 1995, 1998, 2000, 2003 and 2004 in Fig 3.7) with weaker currents. The SH (Fig 3.7) appears as strong anticyclonic eddy in few years (1993, 1999, 2001 and 2002) where as it was much weaker in other years. Both the VH and SH (Fig 3.7)  are also not observed at the same location in all years i.e. they appeared with a shift of 100 -200 km, thus the region of strong currents may be located at different locations in different years.

The EICC off Visakhapatnam is strongest during March – May (Fig 3.8 to 3.9). The currents around VH (~75 cm/s) ae stronger (Fig. 3.8) compared to that around SH (~50 cm/s) in March (Fig 3.8), although in some years the SH is also strong (1993, 1997, and 2002). Within the EICC a number of smaller anticyclonic and cyclonic eddies are seen (1996, 1997,

1998, 2000, 2001, 2003 and 2004 in Fig 3.8) whereas strong cyclonic eddy separate the VH and SH in few years (2002, 2003 and 2004 in Fig 3.8). These eddies originated in the eastern Bay and propagate westward. Under the influence these eddies there are closed cells of circulation within the EICC, where the location and strength of currents vary considerably from year to year. This could result in large interannual differences in current speed and direction at any location within the EICC.

Though the climatological cycle shows the coalescence of VH and SH by May (Fig 2.5 in Ch-II), it need not be the case in all years. In most years both VH and SH keep their identity within the northward flowing EICC, as strong anticyclonic gyres. The presence of a cyclonic eddy centered around 15°N, 83°E often forces strong offshore currents at its southern boundary (1993, 1997, and 2002). Moreover in some year the EICC flows northeastward and feed the CBBC (1996, 1998, 2000, 2001, 2004) while in other year there are indications of EICC abruptly turning eastward at its northern boundary (1993, 1994, 1995, 1997, 1999, 2002, 2003). The reasons for this are unclear. Probably a number of factors such as remote forcing, wind stress and wind stress curl must be contributing to this.

Similar large scale interannual variability could be observed in the southward EICC also (Fig 3.11). The VL could be observed from May and SL from May/June. As in the case of VH and SH the VL and SL also show differences in its geographic locations and strength from year to year (Fig. 3.11 and 3.12). The SL shows more spatial variability than the VL. Though the VL and SL merge to form continuous southward EICC by October – November they keep their identity as multiple cyclonic eddies within a large cyclonic eddy. In fact more than two cyclonic eddies could be identified in most years within the southward flowing EICC with average speed of ~50 cm/s along the east coast of India.

One notable observation is the formation of an clockwise eddy east of Sri Lanka during the summer monsoon of 1997 which has pushed the SL further northwest. This eddy could be observed in 1994 as well by September – October (Fig 3.11-3.12). It should be noted that anomalous atmospheric and oceanographic conditions prevailed in the Indian Ocean associated with Indian Ocean Dipole (IOD) event, during 1994 and 1997 – 98 (Saji et al 1999; Webster et al 1999). Due to presence of this anticyclonic eddy the EICC could not flow southward east off Sri Lanka and join the WMC as a continuous coastal current, but flowed eastward along 10°N and then joined WMC as a re-circulating gyre.
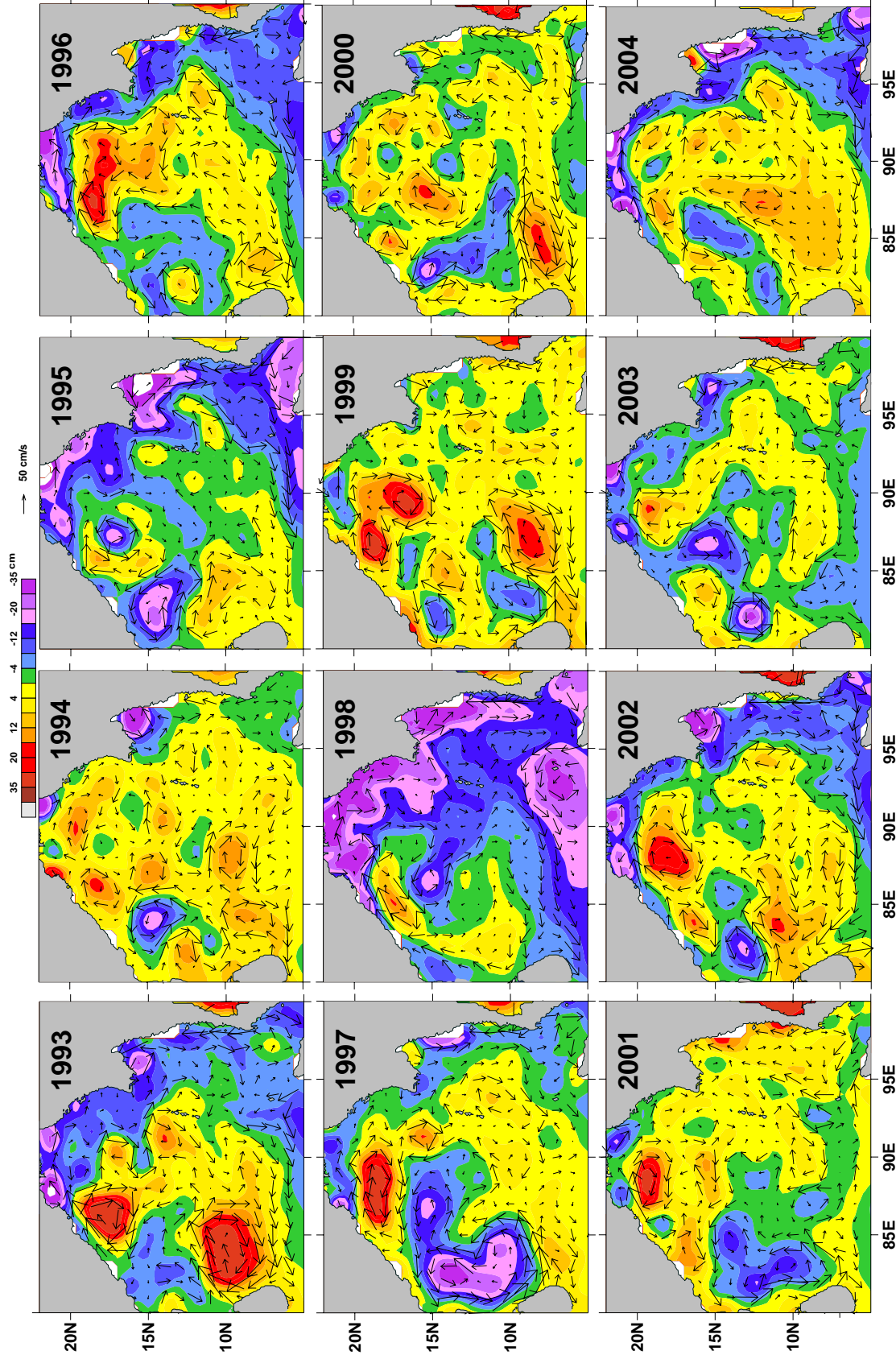
Fig. 3.7 Jnauary monthly mean geostrphic currents overlaid on SSH in the Bay of Bengal
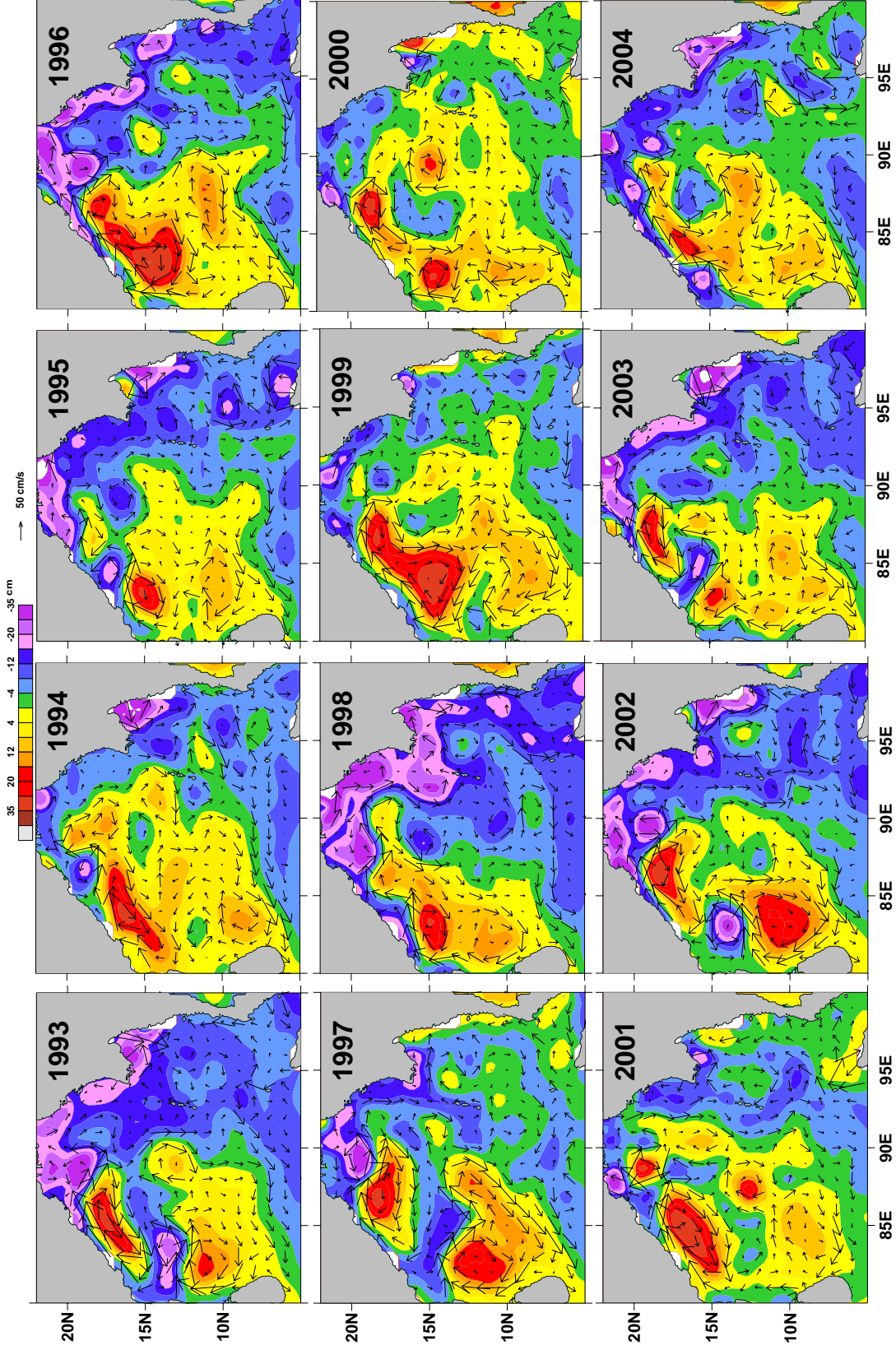
65

**Fig. 3.8 March monthly mean geostrphic currents overlaid on SSH in the Bay of Bengal**

66
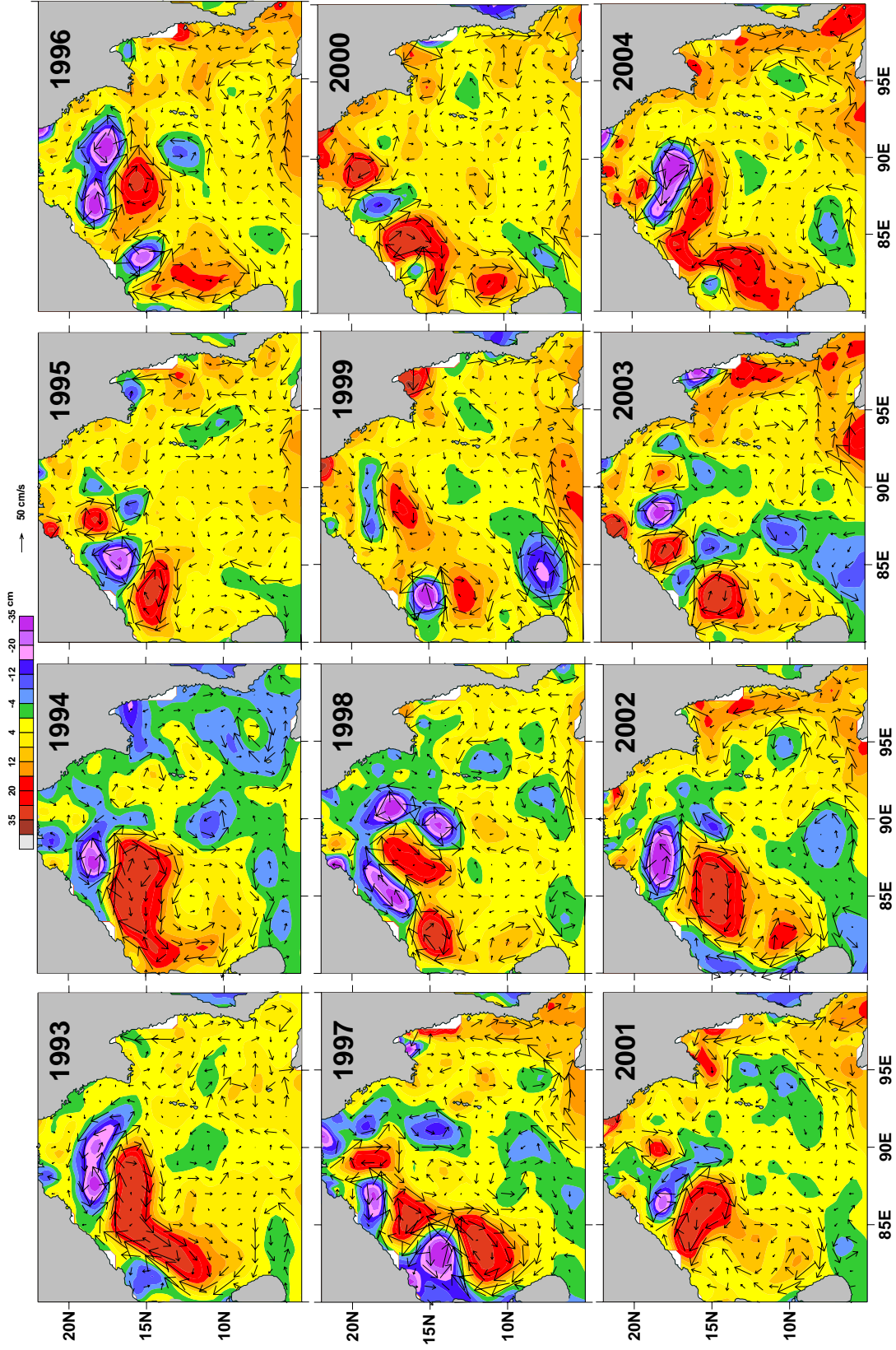
**Fig. 3.9 May monthly mean geostrphic currents overlaid on SSH in the Arabian Sea**

67
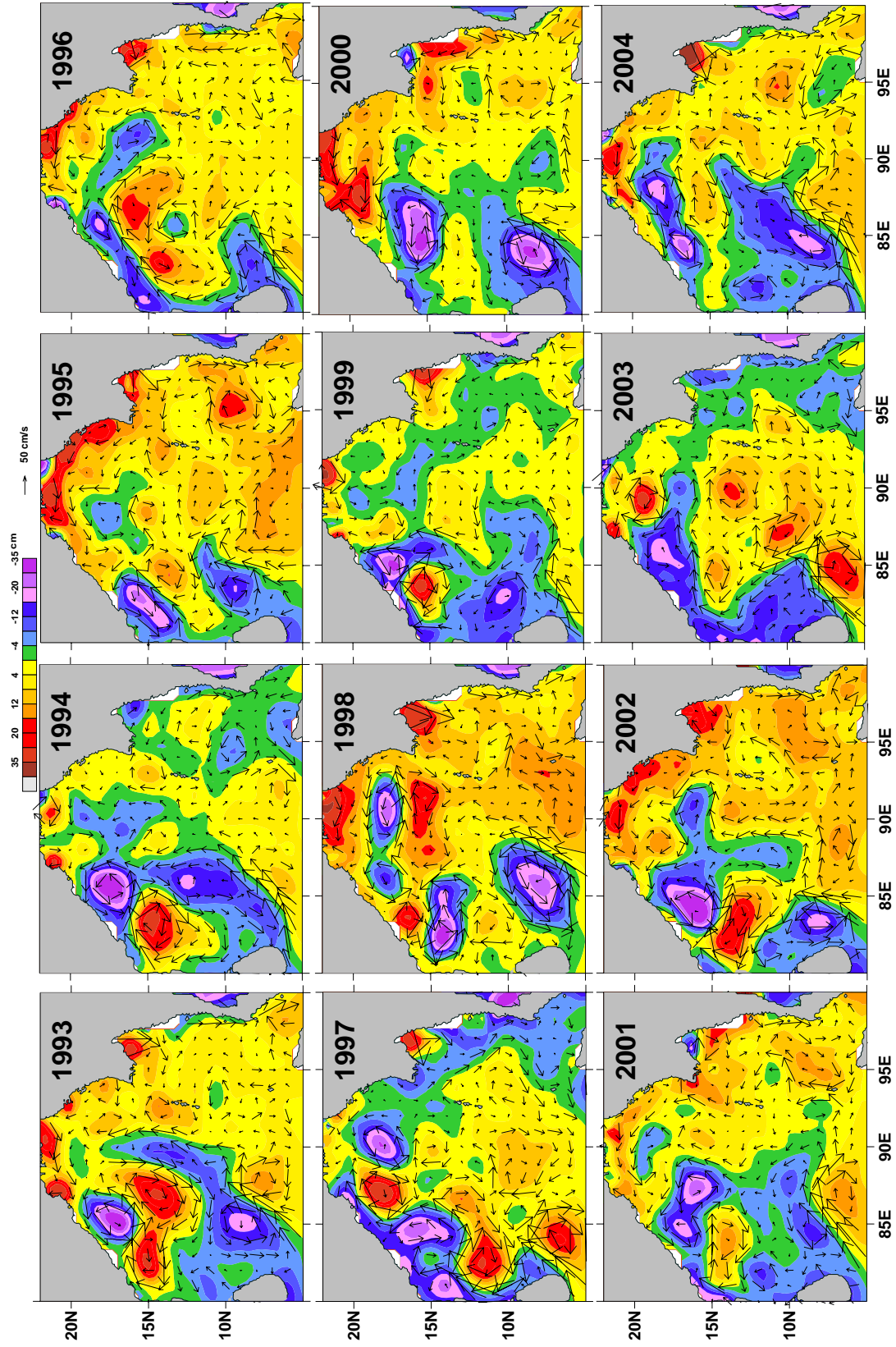
**Fig. 3.10 July monthly mean geostrphic currents overlaid on SSH in the Bay of Bengal**

68
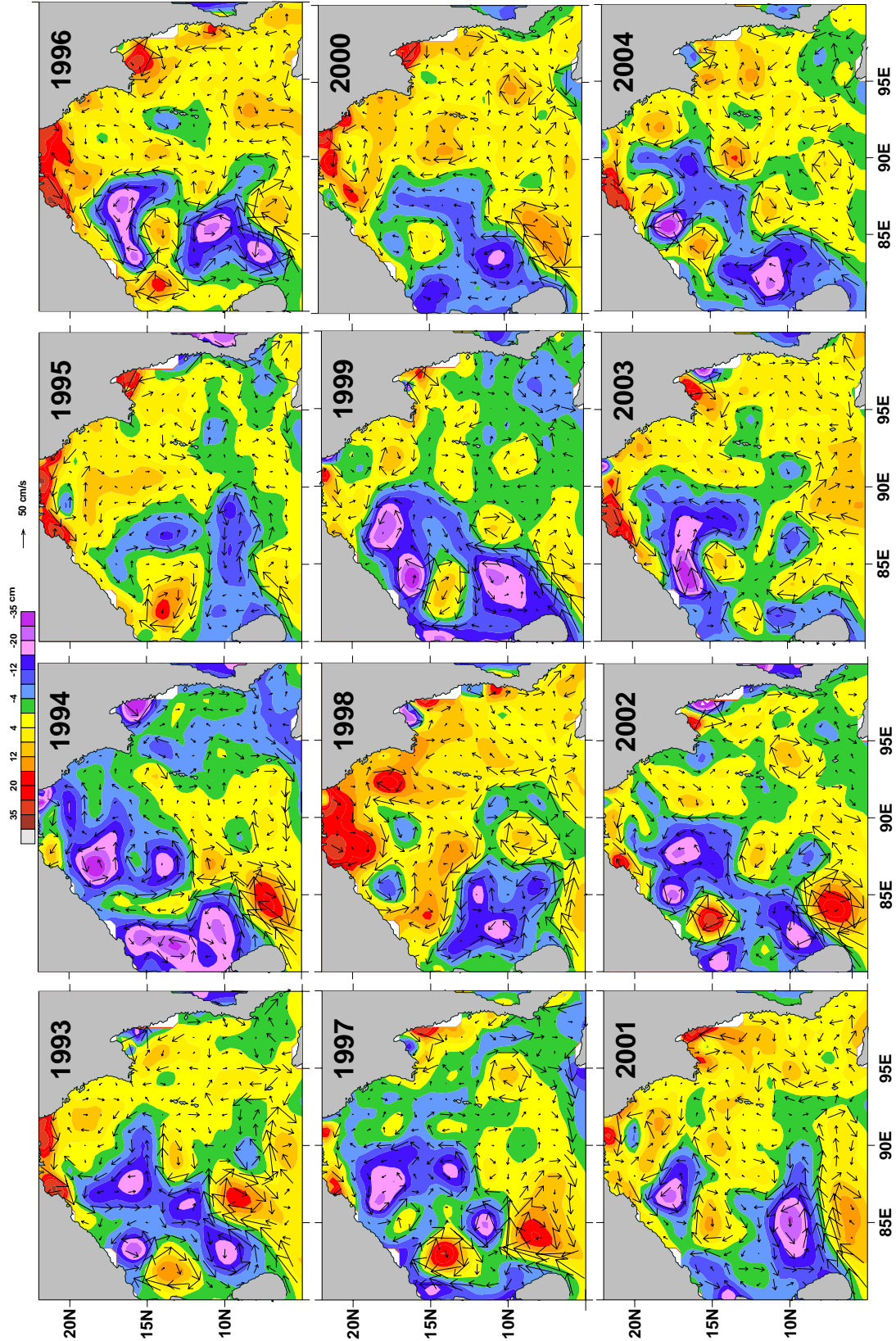
Fig. 3.11 September monthly mean geostrphic currents overlaid on SSH in the Bay of Bengal

69
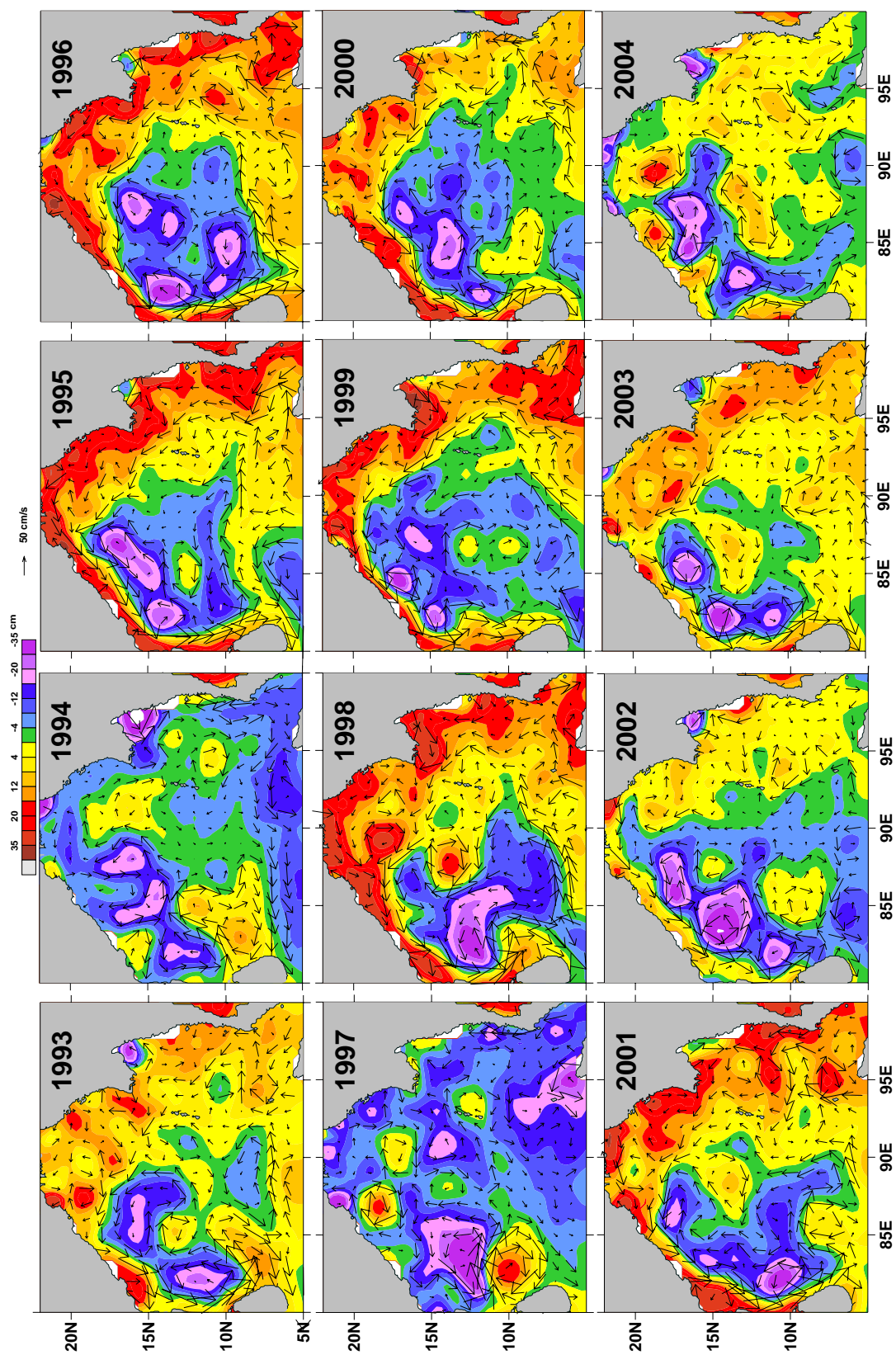
Fig. 3.12 November monthly mean geostrphic currents overlaid on SSH anaomaly from 1993 to 2004

70

### 3.4.2 The CBBC

As seen from Chapter II, the CBBC is mostly fed by the re-circulating waters of northward flowing EICC from January to May (Fig. 2.1 to 2.5 in Ch-II). The CBBC becomes continuous flow from February (Fig. not presented) in few years (1994, 1997, 1998) but in some years by March (2001, 2002, 2004 in Fig. 3.8) and in other years by April (Fig. not presented). The CBBC is also partly fed by the re-circulating waters of EBBC especially in January – February. It is interesting to note that the contribution of CBBC to WMC is particularly strong in some years (1995, 1996, 1998, 2002 and 2004 in Fig. 3.8)). The strongest CBBC (~30 -40 cm/s) occurred in the following years of strongest IOD in January – February (Fig. 3.7). The northward flowing CBBC during summer monsoon is fed by the re-circulating waters of the EICC and the SMC. The relative contribution of the EICC and the SMC to the CBBC also varies from year to year. The CBBC during the summer monsoon was found to be particularly strong and organized during 1994; 1999 and 2004 (Fig 3.10). Even small changes in the wind field or remote forcing may trigger large changes in the structure of the CBBC. The simulations by Kantha et al (2008) have shown that the currents in the Indian Ocean are underestimated by 20 – 30% with model results using ECMWF winds compared to scatterometer wind fields in all seasons. The CBBC is modulated by large number of cyclonic and anticyclonic eddies of 100 – 200 km diameter in the central Bay of Bengal. The relative positions and propagation characteristics of eddies vary from year to year. Unless a clear relation between its causes and life span are understood, modeling of the details of CBBC could remain as a challenging task.

### 3.4.3 The EBBC

As in the case of the EICC and the CBBC the EBBC also shows considerable interannual variability. The EBBC (southward) was particularly strong (25 – 50cm/s) in the year following strong positive IOD events (1994 and 1997) and also in 2002 and 2004 (Fig 3.9 to Fig. 3.11). During the years of strong EBBC the northern and the eastern Bay of Bengal were characterized by unusually low sea level indicative of strong upwelling from October to March in 1994/95 and 1997/98 and January to March in other years. The northward EBBC is in general weaker (~ 25 cm/s) compared to southward EBBC (Fig. 3.7, 3.8 and 3.12).

One of the most notable features is the change in direction of EBBC (towards south) during the Fall of 1994 and 1997. During both the years the southward EBBC is fed by the re-circulating water from several eddies in the eastern Bay of Bengal and also due to currents due to abnormally low sea level in the eastern Bay of Bengal. The abnormal equatorial winds would have triggered the anomalies in the southward EBBC in the eastern Bay during the Fall of 1994 and 1997. A number of anticyclonic eddies are found to modulate the EBBC during June to December (except in 1994 and 1997 when cyclonic eddies modulate the EBBC) while cyclonic eddies modulate the southward EBBC between January and May. These eddies could be related Kelvin waves originating in the equatorial Indian Ocean propagating along the eastern rim of the Bay also shed Rossby waves westward (Shankar et al 2002; Kantha et al 2008). The regional differences in the EBBC is greatly manifested by these eddies.

## 3.5 The Equatorial Currents

Among the Equatorial Currents in the Indian, the Equatorial Jet always receives maximum attention as it is unique to the Indian Ocean. The Ship drift data have shown that both the Spring and Fall EJs have similar speeds. However, recent studies suggested that there can be considerable interannual variability in the characteristics of the EJ (Reppin et al 1999; Kantha et al 2008).

As the geostrophic approximation has considerable limitation, the EJ is not well depicted in the present study. However, lot of inferences can be obtained about the strength of EJ from the SSH in the eastern equatorial Indian Ocean. As the EJ piles up lot of water in eastern equatorial Indian Ocean, the magnitude of SSH is directly linked to the strength of EJ. The Spring EJ was particularly strong in 1995, 1996, 1998, 2000, 2001, 2002 and 2004 and very weak in 1994 and 1997 (Fig. 3.14 -3.15). Therefore there is considerable decrease in the strength of Spring EJ during the year of strong positive IOD events, which is consistent with the winds in those years. Stronger EJ indicates strong northeasterly / southeasterly flows in the eastern Indian Ocean north/south of equator whereas weak EJ or its absence may even force reversing currents in the same location. The direct current measurements in 1994 showed very weak EJ in the Spring transition in the region south of Sri Lanka (Reppin et al 1999).

On the other hand strong Fall EJ could be observed in 1995, 1996, 1998, 1999, 2002 and 2003 (Fig 3.13 & Fig. 3.18). The Fall EJ was absent in 1994 and 1997 due to absence of westerly winds and in the presence of easterly wind along the equator during these years. In fact westward current prevailed along the equatorial belt which was stronger in 1997 compared to 1994. In the Fall of 1997 westerly currents persisted on either side of equator in the entire equatorial Indian Ocean, with varying magnitude. This could have produced considerable equatorial upwelling and significant changes in the oceanic circulation and properties. During the period of EJ there is strong pressure gradient from east to west along the equator (Eriksen, 1979). However, this situation reverses in the years of strong positive IOD events.
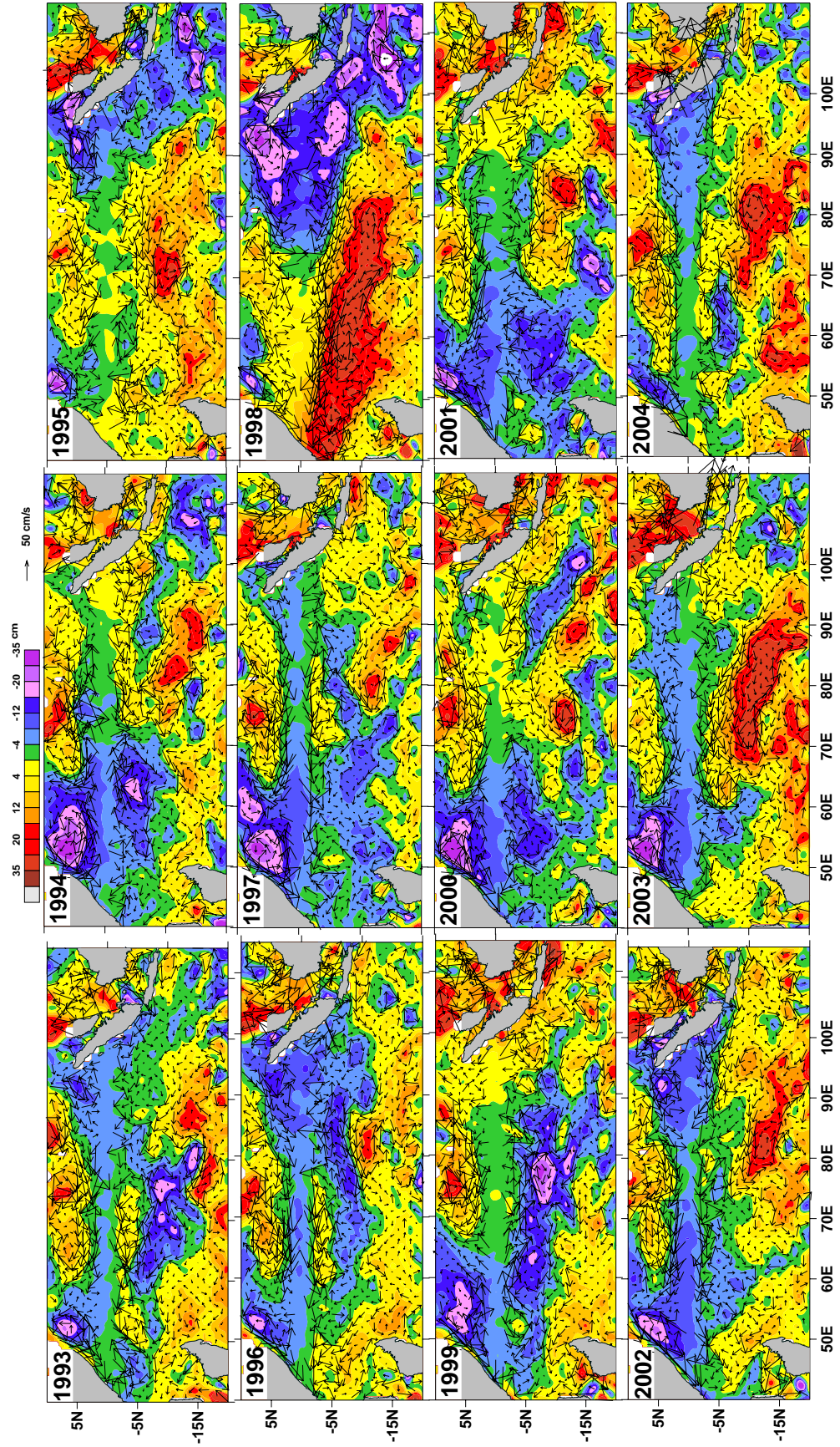
Fig. 3.13 Jnauary monthly mean geostrphic currents overlaid on SSH in the equatorial region
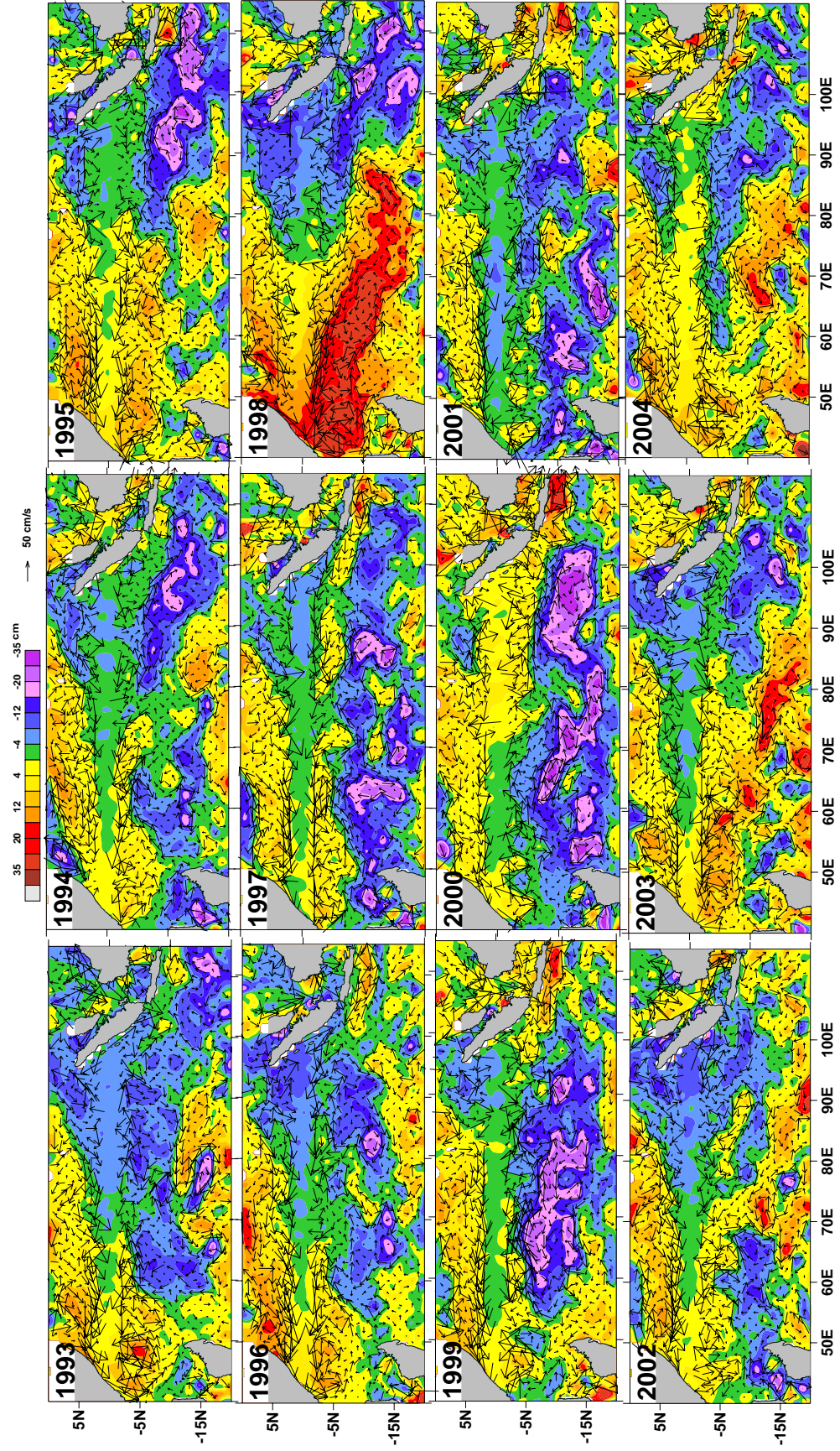
**Fig. 3.14 March monthly mean geostrphic currents overlaid on SSH in the equatorial region**

75
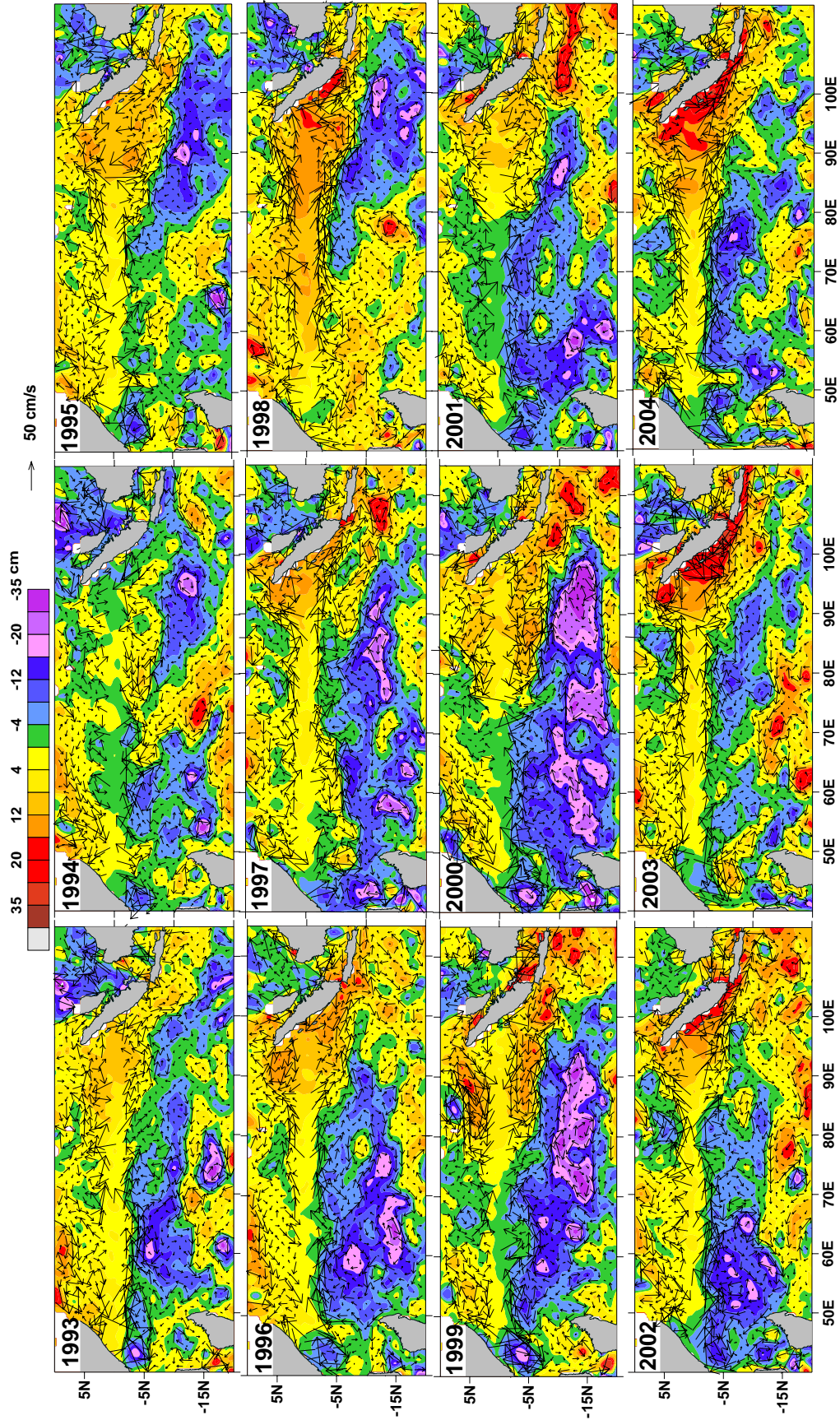
**Fig. 3.15 May monthly mean geostrphic currents overlaid on SSH in the equatorial region**
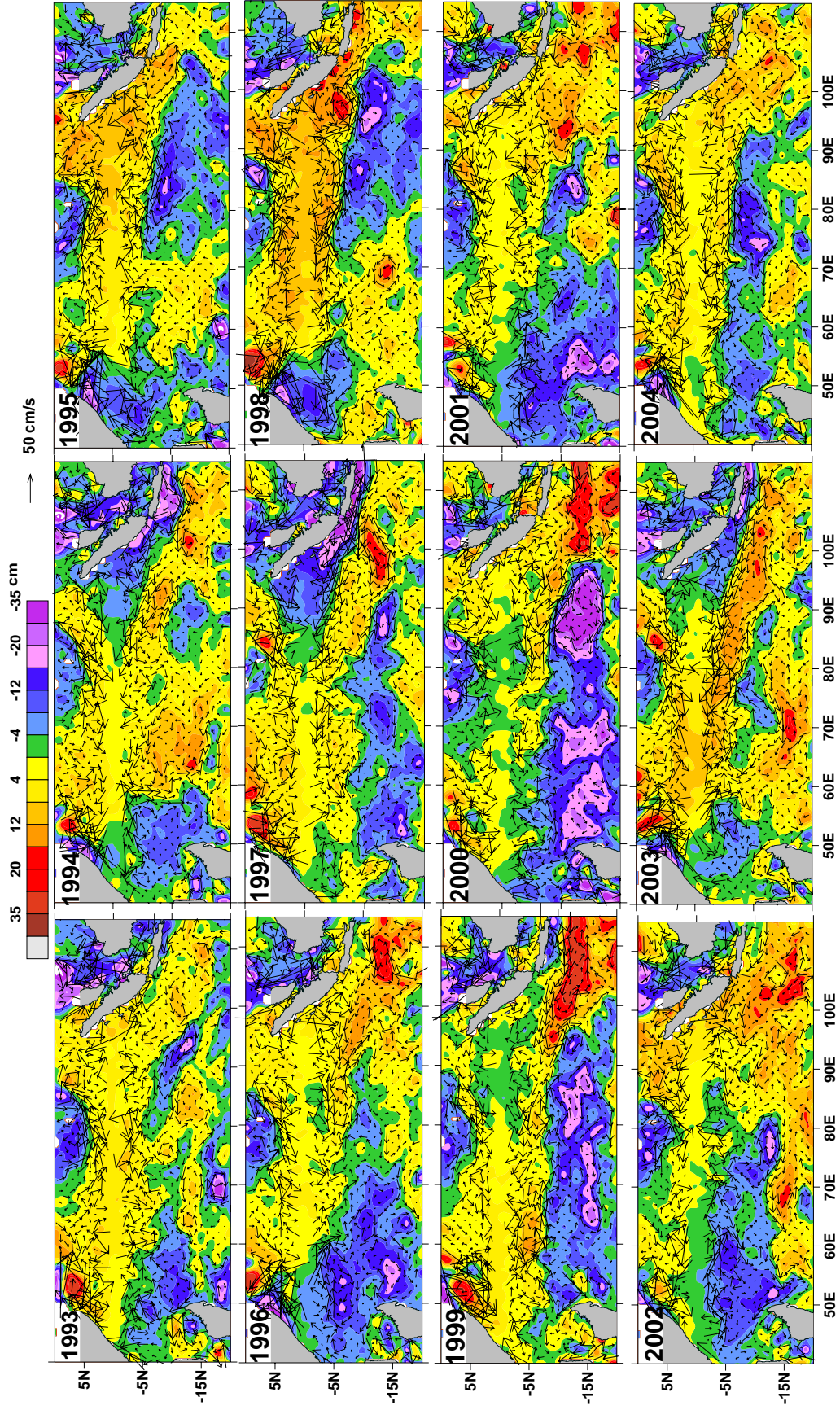
**Fig. 3.16 July monthly mean geostrphic currents overlaid on SSH in the equatorial region**

77
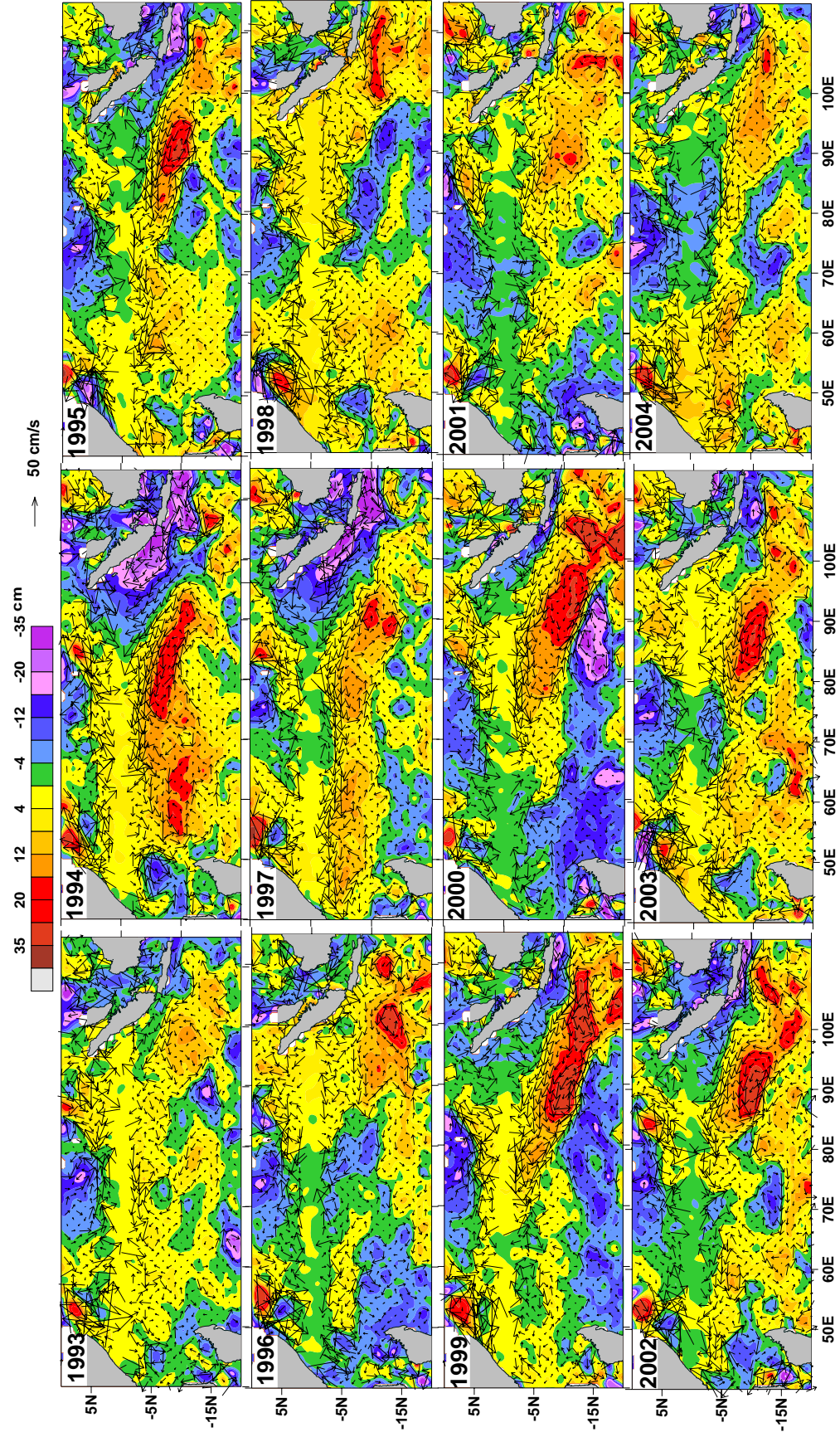
Fig. 3.17 September monthly mean geostrphic currents overlaid on SSH in the equatorial region
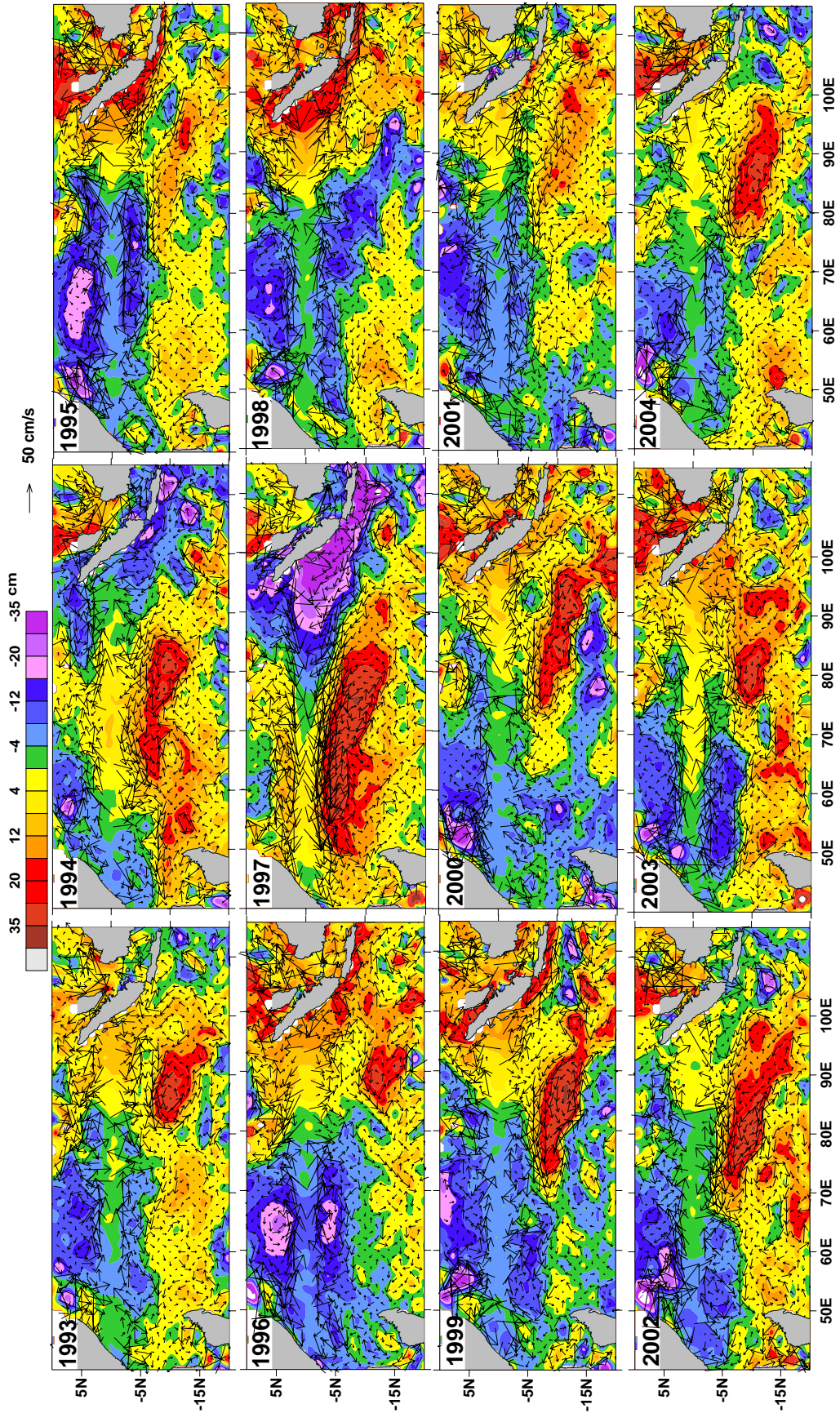
Fig. 3.18 November monthly mean geostrphic currents overlaid on SSH in the equatorial region

79

Current records at Gan Island (Knox, 1976; McPhaden, 1982) confirmed the importance of wind forcing near the equator. Knox(1976) also confirmed further that the pressure gradient term was also a significant part of zonal momentum balance at Gan indicating the importance of remote forcing by propagating equatorially trapped waves (Schott et al 2001).

Modeling studies have shown confusing results regarding the relative strengths of Spring and Fall EJ. Some models have shown stronger Spring EJ. Schott et al (2001) attributes these discrepancies to inaccuracies in the wind field used for modeling. Anderson and Carrington (1993) obtained weaker Fall EJ using HR wind stress, but a stronger Fall EJ using UKMO winds. The sensitivity of model solution to different wind products is also discussed by Han et al (1999).

The present study indicates that there were some years when the Spring EJ was stronger (1995, 1998, 2000, 2001, 2002 and 2004) while in some years the Fall EJ was stronger (1993, 1994 and 1999) and some years both Spring and Fall EJ were weak or absent (1994 and 1997) and both jets were of more or less same strength (1993 and 2003). Hence it is difficult to conclude whether the Spring or Fall EJ is stronger and the EJ has different characteristics in different years. These variations could be mainly due to difference in wind forcing, but internal ocean dynamics also may be crucial, though much less understood.

### 3.5.1 The South Equatorial Current

The interannual variability of SEC is substantial in all seasons. During the winter monsoon the SEC is in general south of 10°S. However, significant changes are observed in the SEC following strong IOD positive years i.e., the winter of 1994 and 1995 (1994 and 1995 panels in Fig. 3.13 and Fig. 3.18). In these years the winter SEC is pushed northward very close to the equator with substantial increase in strength i.e., over 30 cm/s in 1995 and over 50 cm/s in 1997. The northward limit of SEC extends up to 5°S in some other years (2003 and 2004 panels in Fig. 3.13) as well at least in the central and the eastern Indian Ocean. Most of the SEC waters during 1995 and 1996 winter re-circulated through a strong anticyclonic eddy causing very strong (~30/s) eastward current at around 10° -12 °S during these years i.e., the SECC is stronger and moves northward during strong IOD events and also the SECC extends as far as in the western Indian Ocean. In all other years the winter

SEC is found south of 10°S extending up to around 20°S with several eddies within the SEC modulating the SEC regionally.

In general the SEC during the summer monsoon is stronger as observed from ship drift data. The SEC during this period also shows considerable north – south shift in different years. In many years the SEC extended up to 5°S (1994, 1997, 2003 and 2004 panels in Fig. 3.16) but in most other years the SEC was significant only south of 10°S. As during summer monsoon, several eddies modulate the SEC in the regional scale during winter monsoon. A series of wave fronts (possibly Rossby) could be the reason for this. The most interesting aspect of this feature is large number of cyclonic/anticyclonic mesoscale eddies embedded in large cyclonic/anticyclonic gyres.

The presence of annual Rossby waves in the southern tropical Indian Ocean was first reported by Perigaoud and Delecluse (1992) from geosat altimetry. The waves have large amplitudes at about 10 -15°S and 90° – 100°E. This occurs at a region of weak wind stress curl (Perigaoud and Delecluse (1992) which was further confirmed by Morrow and Birol (1998).

The variability of 20°C isotherm from time series of XBT tracks revealed annual Rossby waves in the eastern Indian Ocean between 0° and 20°S (Masumoto and Meyers, 1998). Modeling with OGCM (Masumoto and Meyers, 1998) have shown that these waves originating in the eastern boundary are strongly modified by Ekman pumping along their propagation path indicating that these waves are generated from a southeasterly propagating signal originating in the transition period, but this requires further confirmation through observations and modeling. The interannual variation of winds and remote forcing and its influence on SEC are not clearly understood.

### 3.5.2 The Winter Monsoon Current (WMC)

The WMC originates in eastern Indian Ocean north of the equator in October and gradually extends westward and engulfs the entire width of the north Indian Ocean by February (Fig. 3.13 for January and Fig. 3.18 for November). In general the WMC is confined to south of the Bay of Bengal in October. Notable differences occurred during both the strong positive IOD events 1994 and 1997. Anomalous winds over the equatorial Indian Ocean forced westerly currents near the equatorial Indian Ocean from July onwards which

peaked by October – November. Consequently the WMC in the eastern Indian Ocean became prominent from July (Fig. 3.16) itself and became strong by October – November (Fig. 3.18) the WMC extends in the entire Indian Ocean even by October in 1997 in response to a strong positive IOD event. In all other years the WMC extended up to the entire north Indian Ocean with varying magnitude by February, and continued till April – May (Fig. 3.16).

Very little is known about the interannual variability of WMC. In 1991, the WMC was confined to upper layers and was marked by low salinities (<33 PSU) in the central Indian Ocean (Hacker et al 1998). The upper layer ADCP measurements (Hacker et al 1998) and ship surveys in 1995 have shown that WMC was supplied by circulating water brought eastward north of the equator. Schott et al (1994) estimated the transport of WMC to be 11Sv for 1991. However, very little is known about the interannual variability of transport of the WMC in the Indian Ocean.

### 3.5.3 The Summer Monsoon Current (SMC)

The SMC was considerably weak and mostly confined to a narrow strip centered on 5°N in both the IOD events (1994 and 1997). The SMC was strong especially south of Sri Lanka in most of the other years with speeds in the range of 25 – 50 cm/s, where it is also fed by the southward WICC. A major portion of these waters carried by the SMC flows into the Bay of Bengal (Vinayachandran et al 1999). During most of the years SMC turns northward/northeastward around 83 – 85°E. However, in same years this occurs first east of Sri Lanka as a strong boundary current during August – September (1994, 1997, 2000 and 2002) and even in October (1994, 1997). A large anticyclonic eddy with boundary current, east of Sri Lanka, also inhibits the flow of southward flowing EICC into the equatorial Indian Ocean.

The SMC is also observed as a shallow current with a transport of 8.4Sv (Schott et al 1994). There are also sometimes narrow countercurrents in the SMC which causes low saline waters of eastern Indian Ocean to the western Indian Ocean (Schott et al 2001).

The numerical models (McCreary et al 1993; Vinayachandran et al 1999) attribute two driving mechanisms for the SMC – south of Sri Lanka. These are 1) The local wind stress curl 2) Reflection of equatorial Kelvin waves associated with the Spring EJ as a packet

of downwelling favorable Rossby waves. So far there are very little observations available on the interannual variability of the SMC in the Indian Ocean.

**3.5.4 The Equatorial Counter Current (ECC)**

The ECC occurs as a weak eastward current between the WMC and the SEC between December and April (Fig. 3.13 and Fig. 3.14). The ECC is observed between 3°S – 8°S during most years. The notable exceptions are following the two positive IOD events 1994 – 1995 and 1997 – 1998.

The ECC was practically absent from November 1994 to April 1995 and November 1997 to April 1998 (when it is expected). The strengthening of WMC and northward shifting of SEC during this period might have the reason for the absence of ECC during this period. In all other years ECC was observed though with varying spatial and temporal variability.

Another noteworthy observation is the late formation of the cyclonic eddy near the African coast covered around 3°S in 1998 (June) and early occurrence in 1999 (April). This cyclonic eddy forces a strong boundary current in the southern hemisphere before the onset of monsoon which crosses the equator and joins the Somali Current. The late occurrence of this boundary current by June in 1998 is caused by the unusual atmospheric and oceanic conditions due to strong positive IOD event. The dimensions and characteristics of this eddy varied from year to year during the observational period, but occurrence in all years from 1993 – 2004.

**3.6 Scales of seasonal and interannual variability in SSH**

The scales of seasonal and interannual variability of SSH and related circulation over the Indian Ocean are dealt in this Chapter.

**3.6.1 Interannual variability of SSH during 1993 -2004**

The occurrence of semiannual and annual processes in the Indian Ocean is well known (Clarke and Liu, 1994), but the processes occurring in the interannual scale received lot of attention in the last decade following large scale variability in the tropical Indian Ocean (Saji et al 1999; Webster et al 1999, Murtugudde et al 2000, Sakova et al 2006)

Some of the studies indicated that the IOD is an independent mode in the Indian Ocean (Saji et al 1999; Webster et al 1999) but Murtugudde et al (2000) indicated some link to ENSO cycle. Other theories suggested IOD is a part of ENSO cycle (Baquaro-Bernal et al 2002) or related to tropical biennial circulation (Meehl and Arablaster 2002). Previous studies also indicated several scales of interannual variability of periodicities around 2.7 year (Quasi biennial) and 5.5 years (quasi-pentadal) and peaks of about 18 -20 months (McClean et al 2005) while Tourre and white (2003) based on EOF of SST anomalies argued that interannual variability of SST over Indian Ocean represents global climate signal that includes quasi biennial signal (2.1 to 2.8 years), the ENSO signal (3-7 years) and quasi-decadal oscillation. Altimeter data analysis over 1995 – 1999 and models have shown that the first mode of interannual variability of tropical Indian Ocean corresponds to IOD, but the second mode shows quasi biennial tendency (Rao et al 2002). They also pointed out that the quasi biennial signals in the tropical Indian Ocean are related to Rossby wave propagation and at some locations it appears as quasi- pentadal oscillations. Recently Sakova et al (2006) have shown that there are several dominant scales of variability in the Indian Ocean such as semi-annual, annual, 18-20 months, 2-3 year and 4-6 periods, where the 18-20 months signals were particularly strong between 1994 -2000. In the following part the dominant scales of variability of SSH in the Indian Ocean is investigated utilizing 12 year (1993 -2004) altimeter data.

**3.6.2 Data and methods**

The weekly SSH data with spatial resolution of 1/3° is utilized for this analysis (1993-January to 2004-December). Data very near to the coast (<30m depth) are excluded. Monthly mean fields were computed by averaging the grids and the seasonal cycle signal was removed for the interannual EOF analysis by dealing only with the residual time series. For the seasonal variability of EOF analysis the climatological monthly means (discussed in Chapter II) from January to December is subjected to EOF analysis.

**3.6.3 Seasonal Variability of SSH**

Fig. 3.19 shows first EOF mode for the seasonal variability of SSH (and also circulation) in the Indian Ocean. It accounts for 41% of the total variance. This corresponds

to the annual cycle due to the winter and summer monsoons. Maximum variability is noticed along the coasts of India, the Somali Current region and western and central equatorial Indian Ocean (region of WMC and SMC) and also in the southern tropical Indian Ocean (region of SEC). These regions correspond to maximum seasonal variability in the annual cycle with peaks during winter and summer.

Mode 2 (Fig. 3.19) also has an annual cycle but not in phase with Mode 1. This mode as peaks during February –April (positive) and August – November (negative) which accounts for 28% of the total variance. Maximum variability is noticed in the western Bay of Bengal, in the regions of propagation of LH and LL, the western equatorial Indian Ocean south of equator and southeastern Indian Ocean. The evolving EICC, WICC, westward propagating LH/LL large eddies in the SEC and the region of strong boundary currents contribute to large variability in the Indian Ocean which is not in phase with the monsoons.

Mode 3 (Fig 3.19) accounts for 19% of the total variance and has semiannual periodicity. Maximum variance is observed in the central and eastern tropical Indian Ocean, region of ECC (south of equator) and northern Arabian Sea. The semiannual Equatorial Jets and large variations in the currents between  0° and 10°S in the western Indian Ocean also substantially contribute to the Indian Ocean variability in the annual cycle. The positive peaks occur in May – June and November – December and negative peaks in February – March and August – September.

Mode 4 (Fig. 3.19 ) accounted for only 5% variability in the eastern and western Indian Ocean, in the southeastern Bay of Bengal and central Indian Ocean north of equator.

Mode 3 and mode 4 have semiannual periodicities which are not in phase. Mode 4 has positive peaks in April and October and negative peaks in Jan and July.

Hence the annual variability of SSH in the Indian Ocean is governed by two annual cycles (41% and 28%) and two semiannual cycles (19% and 5%) which are not in phase, with each other.
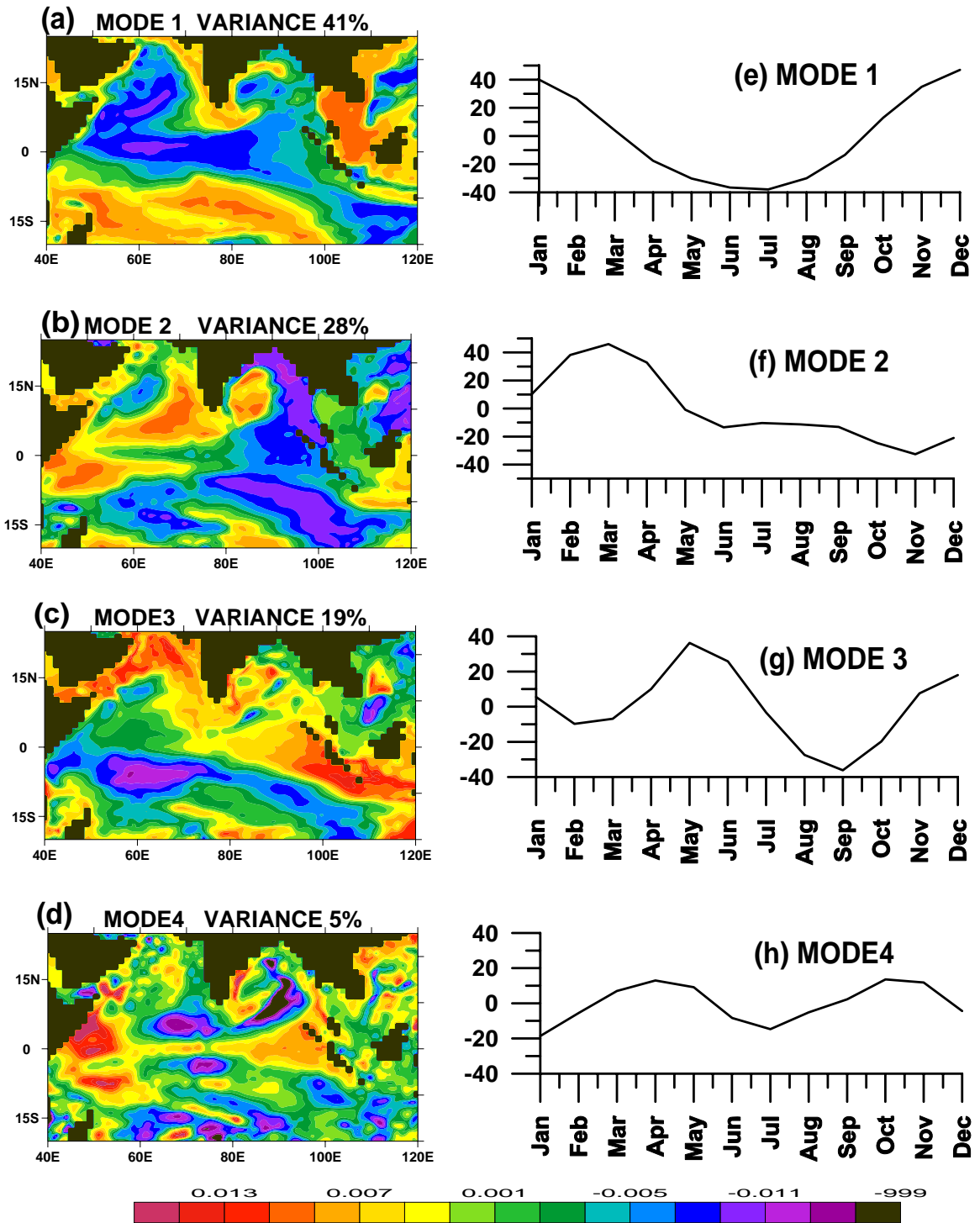
Fig. 3.19 First four dominant modes of annual cycle. First column contains spatial distribution of modes (plates a, b, c and d) and second column contains times series (plates e, f, g and h).

**3.6.4 Interannual variability of surface circulation in the tropical Indian Ocean**

The low frequency SSH variability in the tropical Indian Ocean is connected to the signals represented in the first four EOF modes (Fig. 3.20). The first EOF mode represents 37% of total variance and its spatial pattern and time series are shown in Fig. 3.20. Maximum variance is observed in the eastern and western tropical equatorial Indian Ocean with opposite signs and also in the eastern Bay of Bengal. This mode obviously belongs to the IOD. The time-series of the first EOF mode indicate strong signals in 1994 – 1995, 1997 – 1998  where the positive IOD events were very strong (Saji et al 1999, Vinayachandran et al 2007) and also in 1998 – 1999 when the negative IOD signal was strong. The time-series of the first EOF mode also indicate decadal variability as in the South China Sea (Fang et al 2006).
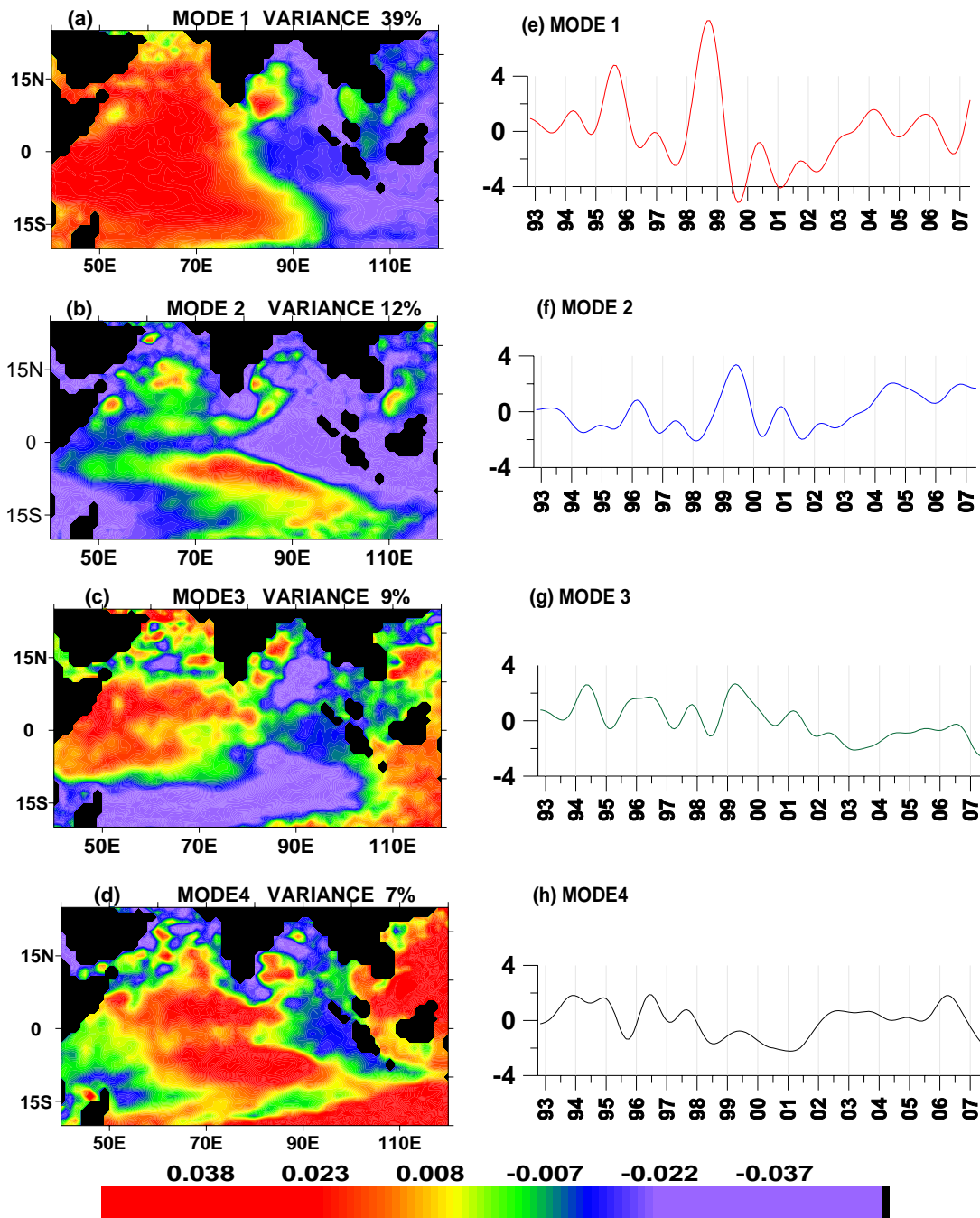
Fig 3.20 First four dominant EOF spatial and time-series modes in the Indian Ocean obtained from low pass (> annual) filtered SSH data in the Indian Ocean region. First column is spatial distribution of four modes (plates a, b, c and d) and second column shows the time series (plates e, f, g and h).

Sakova et al (2006) indicated 18-20 month signal in the tropical Indian Ocean based on the analysis of SSH and XBT data. They also suggested that the extreme IOD events are possibly related to an intensification of this signal in some years (eg : 1994 – 1995, 1997 – 1998). The time series of the first EOF mode also suggest an 18-20 month signal (Fig 3.20) which were strong during extreme IOD events, but otherwise weak which is embedded in the decadal variability. This 18-20 month signal was particularly strong during 1994 to 2001 which become weak during 2002-2005 and again strong in 2006, the reasons for which remain unclear.

The second EOF mode (Fig.3.20) accounts for over 19% of total variance. Maximum positive signals are in the equatorial current system especially in the region of EJ and in the central Arabian Sea while strong negative variance is observed along the west and south coasts of India. This implies that the interannual variability of currents in the equatorial Indian Ocean and in the Arabian Sea is very significant. The time series of the second interannual EOF mode also has about 18-20 month periodicity which is not in phase with the first mode. It appears that in the tropical Indian Ocean much of the interannual variability (56% for the first two modes) is caused by 18-20 months signals which are not in phase with each other (Fig. 3.20). Perhaps the IOD signals with 18-20 month periodicity induces signals in other parts of Indian Ocean with a time lag, which appears as the second mode.

The third EOF represents 13.5% of the total interannual variability (Fig 3.20). Maximum variance is noticed in the Arabian Sea particularly in the region of LH/LL, the Bay of Bengal and in the central and eastern south Indian Ocean (region of SEC). The time series of the third mode indicate quasi biennial periodicity (2 – 3 year) and were significant only from 1993-2001 which is a surprising result.

Perhaps strong IOD event occur when the different scales of the variability in the Indian Ocean are in resonance. However, this has to be verified from observations.

## 3.6.5 Wavelet analysis

Wavelet analysis programs developed by C. Torrence and available at http://paos.colorado.edu/research/wavelets/ are used to study the interannual variability. The interannual variability of SSH is also examined using wavelet analysis. For this, 5 locations

in the Indian Ocean are selected (Fig. 3.21) based on the regions of maximum variance in the first two interannual EOF modes.

### 3.6.5.1. Wavelet analysis on SSH time series

The wavelet analysis clearly indicate an 18 month signal in all locations in the Indian Ocean as a dominant signal in the interannual scale except in the western equatorial Indian Ocean, where the 2-3 year signal is dominant (Fig. 3.22). In all other locations the 18 month signal and the 3 year signal (Fig. 3.22) are prominent in the interannual scale.
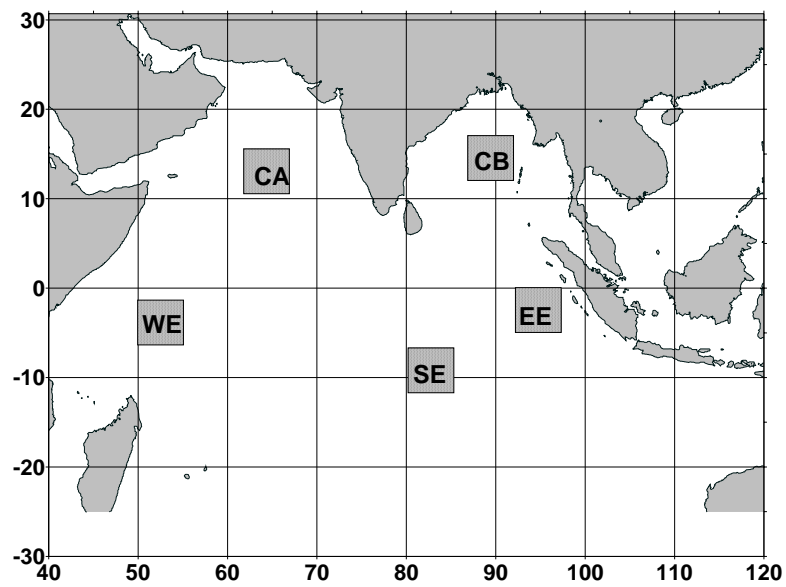


Figure 3.21 Location map of time-series points selected for SSH wavelet analysis. (WA-western Equatorial, CA – Central Arabian Sea, CB – Central Bay, EE – Eastern Equatorial, SE – Southern Equatorial).
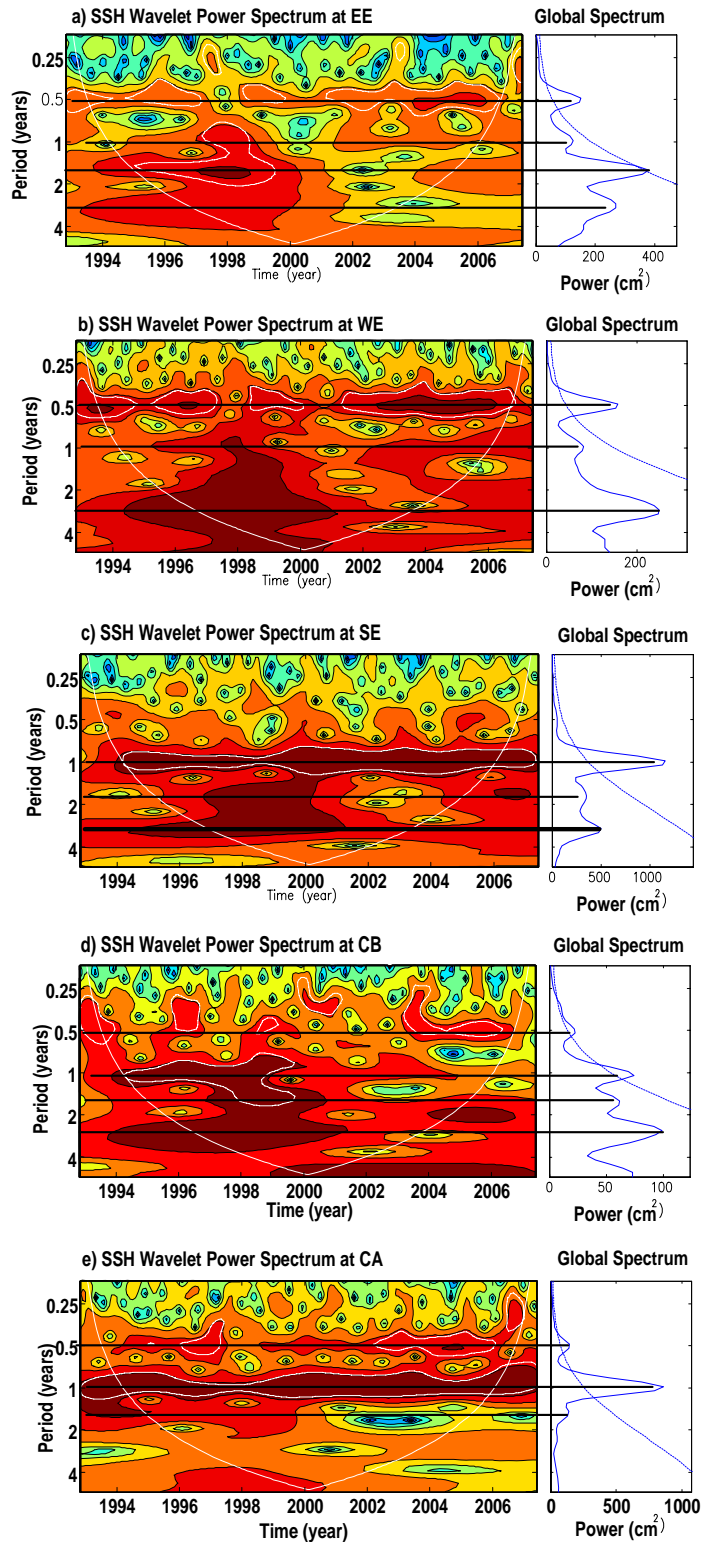
Figure 3.22 Wavelet power spectrum of equatorial Indian Ocean 5 locations (a, b, c, d and e corresponds to EE, WE, SE, CA and CB in Fig. 3.21

From the analysis of SSH and XBT data in the eastern equatorial Indian Ocean Sokova et al (2006) identified five bands of low frequency signals in the tropical Indian Ocean i.e., semi-annual, annual, 18-20 months, 3 years and 4-6 years. They could not identify a quasi-biennial signal though it was observed in the SST field (Tourre and White 2003). As of now little is known about the interaction of the 18-20 month signal and the 3 year signal. Sakova et al (2006) concluded that the spatial/temporal dynamics of the 18-20 month signal indicate the primary internal mode of Indian Ocean. They further argued that the extreme IOD events may be caused by the constructive interference of the 18-20 months signal and 3 year signal.

The present analysis also conclusively prove the existence of the 18 months signal which was stronger during 1994-2001 and became weak during 2002- 2005 and again became strong by 2006. On the other hand the 3 year signal became more dominant signal when the 18 month signal became weak. The qualitative interaction of various signals in the Indian Ocean is crucial in understanding the complex physical processes in the Indian Ocean leading to extreme events.

**3.6.5.2 Wavelet analysis on wind field**

In order to verify whether the 18 – 20 months and 36 months are related to wind field, wavelet analysis is carried out for the surface wind field over an area 0° - 5°S; 85° - 90°E. This is the region where the interannual variability of surface winds are maximum (Da Silva et al 1994). Monthly mean wind data from 1970 to 2004 prepared by Florida State University (FSU) is used (Jones et al 1995).

Wavelet analysis is carried out for the scalar wind speed and also u and v components of the wind (Fig. 3.33). The wavelet analysis clearly indicates signal of about 20 months, 3 years, 4 years and also 12 years in the interannual scale in the scalar wind speed (Fig. 3.33a). On the other hand, dominant periodicities of about 20 -22 months, 4 year and decadal scales are prominent in the zonal wind (Fig. 3.33b) in the interannual scale. The periodicities of 4 year and 12 year are only prominent in the meridional winds (Fig. 3.33c).
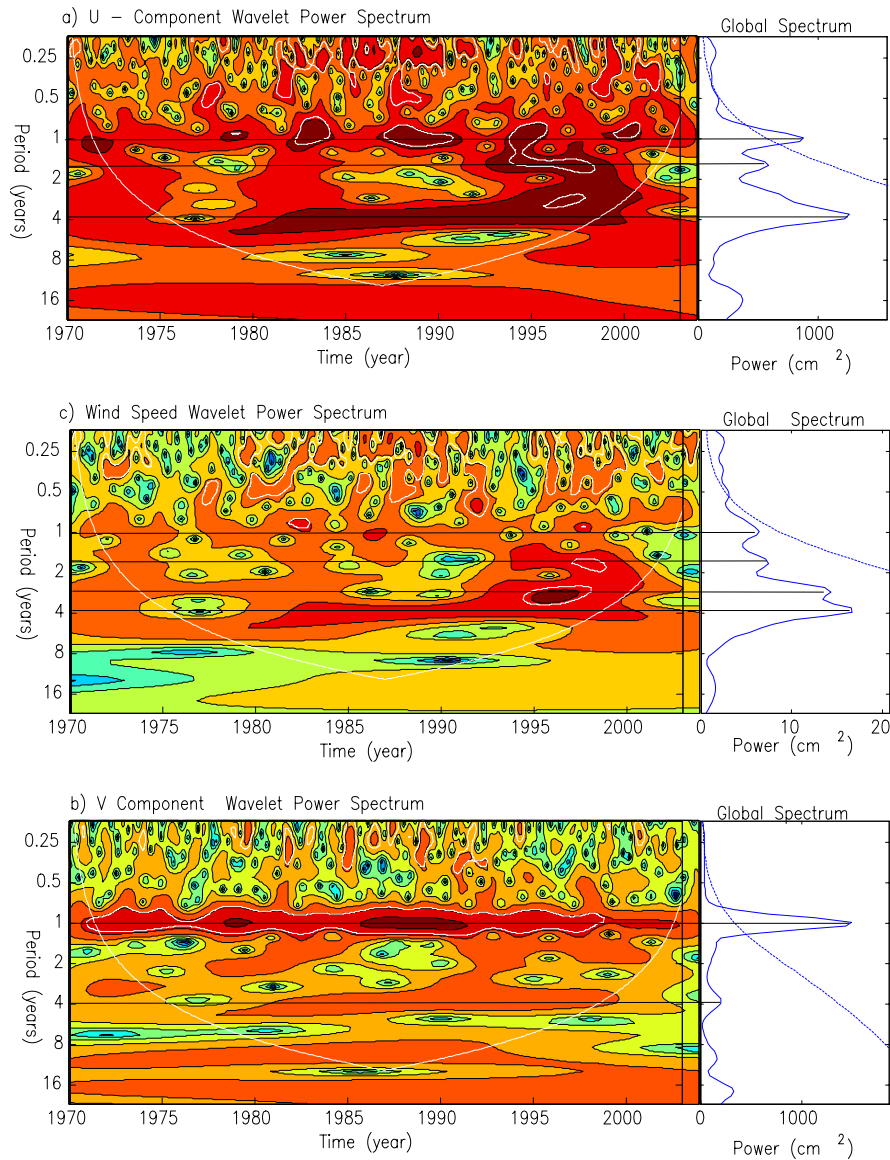
Fig. 3.33 Wavelet analysis of Florida State University monthly mean wind data. A) u – component, b) v – component and c) wind speed

The wavelet analysis of winds indicates the 18 – 20 months and 3 year signals are significant in the scalar wind speed. It may have a bearing on the similar periodicities in the SSH as well. Conspicuously the 3 year signal is absent in the zonal and meridional winds, but it is a dominant signal in the SSH field. More observational studies with modeling are required to conclusively prove one to one relationship between major signals in the wind and SSH fields.

## Influence of Propagating Waves on the Circulation

### 4.1 Introduction

In the previous chapter we have seen that there is large scale interannual variability in the currents and circulation in the tropical Indian Ocean. Most of this interannual variability is caused by the eddies generated by propagating waves either as large scale features (LH/LL) or as mesoscale feature embedded in the mean flow. Planetary waves are long period waves where Coriolis force is also important. Most common in the oceans are Rossby and Kelvin waves. Planetary waves consists of fast moving barotropic and slow moving baroclinic waves. This study is limited to baroclinic waves which can be resolved with the available altimeter data.

In middle and high latitudes, the effect of change in wind stress propagates mainly westwards by Rossby waves and hence western boundaries of the ocean are more affected than the eastern boundaries of the oceans. However, in the low latitudes signals can travel westward by Rossby waves and eastward by Kelvin waves (equatorial wave guide) LeBlond and Mysak (1978), Pedlosky (1979), and Gill (1982).

The tropical Indian Ocean, due to its proximity to the equator can support fast traveling planetary waves. The seasonally varying monsoon winds provide the mechanism for generating these low frequency waves (Shetye et al 1996).

### 4.1.1 Planetary waves in the Indian Ocean

The abrupt change in the wind direction along the equatorial region during April – May causes change in the upper ocean, depressions in the thermocline along with a rise in the ocean surface, which propagates eastward along the equator as a downwelling Kelvin wave (McCreary et al., 1993). This downwelling Kelvin wave is mainly triggered by the equatorial westerlies during monsoon transition. The first mode baroclinic Kelvin wave has a moderate speed of 250 cm/s (McCreary et al., 1993), and takes about 30 days to travel from the western boundary to the eastern boundary (40°-100° E) in the Indian Ocean. The numerical results showed that the first three baroclinic Kelvin wave speeds are 280 cm/s, 173 cm/s, and 111 cm/s (Gent et al., 1983). Similar conditions again occur during October – November.

The equatorial Kelvin wave hits the eastern boundary (Sumatra coast) and splits into two coastal Kelvin waves, one northward and the other southward. The northward Kelvin wave propagates along the rim of the Bay of Bengal and the Andaman Sea (Potemra et al., 1991), leading to remotely driven coastal currents and it is also thought that it may also radiate long Rossby waves with the same frequency. These Rossby waves propagate westward leading to currents in the interior of the ocean and in the western boundary region of the Bay of Bengal (McCreary et al., 1996; Shetye et al., 1996).

Recent modeling results (Potemra et al., 1991; Yu et al., 1991; McCreary et al., 1993) showed that the coastally trapped Kelvin waves travel along the rim of the Bay of Bengal and along the entire east coast of Sri Lanka and finally reach the southwest coast of India. There these coastally trapped Kelvin waves move poleward along the west coast of India and also radiate westward propagating Rossby waves (McCreary et al., 1993), which strongly influence the velocity fields in the eastern part of the Arabian Sea. The numerical experiments raise the possibility that the coastal circulation along the west coast of India and the annual cycle of currents over the Arabian Sea are mainly influenced by the events in the Bay of Bengal.

Studies (Shankar et al 1998) show that existence of the Laccadive eddy (Bruce et al 1994), off the southwest coast of India, is a consequence of the westward propagating Rossby waves. On the other hand this study also states that the annual cycle of the Laccadive eddy is the consequence of the semi-annual Kelvin waves off the southwest coast of India; these being forced primarily by the alongshore winds in the Bay of Bengal and by the winds in the equatorial Indian Ocean. This energy also transfers to the Arabian Sea by the way of coastally trapped Kelvin waves (McCreary et al 1993; Perigaud and Delecluse, 1992).

**4.1.2 Generating mechanisms**

Some of the studies show that the existence of semi-annual periodicities is due to semi-annual reversals of wind (Gent et al., 1983; Clarke and Liu, 1994; Unnikrishnan et al., 1997). In the Bay of Bengal wind stress curl is thought to generate Rossby waves in the interior (Shetye et al., 1993; 1996), which then propagate westward generating western boundary currents (McCreary et al., 1996; Shankar et al., 1996).

Shankar et al. (1996) showed that in response to interior Ekman pumping, baroclinic Rossby waves are excited in the interior of the Bay when the interior circulation is anti-clockwise;

they propagate to the western boundary where they generate a northward coastal current and if the interior circulation is clockwise, it generates a southward coastal current. On the otherhand cyclonic and anticyclonic Ekman pumping off the southern tip of India has also a profound effect on the Laccadive eddy (Bruce et al., 1994) and in the Somali Current generation (Schott, 1983).

## 4.2 Spatial Variability of Planetary waves in the Indian Ocean

In the previous section concepts of planetary waves are discussed. Theoretically the variability of Rossby waves is latitude dependent. With increasing latitude they move at slower rates. To highlight some the characteristics of Rossby waves time-latitude sections of SSH along 8°N, 4°N, equator, 4°S and 8°S  is presented (Fig. 4.1) from 1993 to 2006.
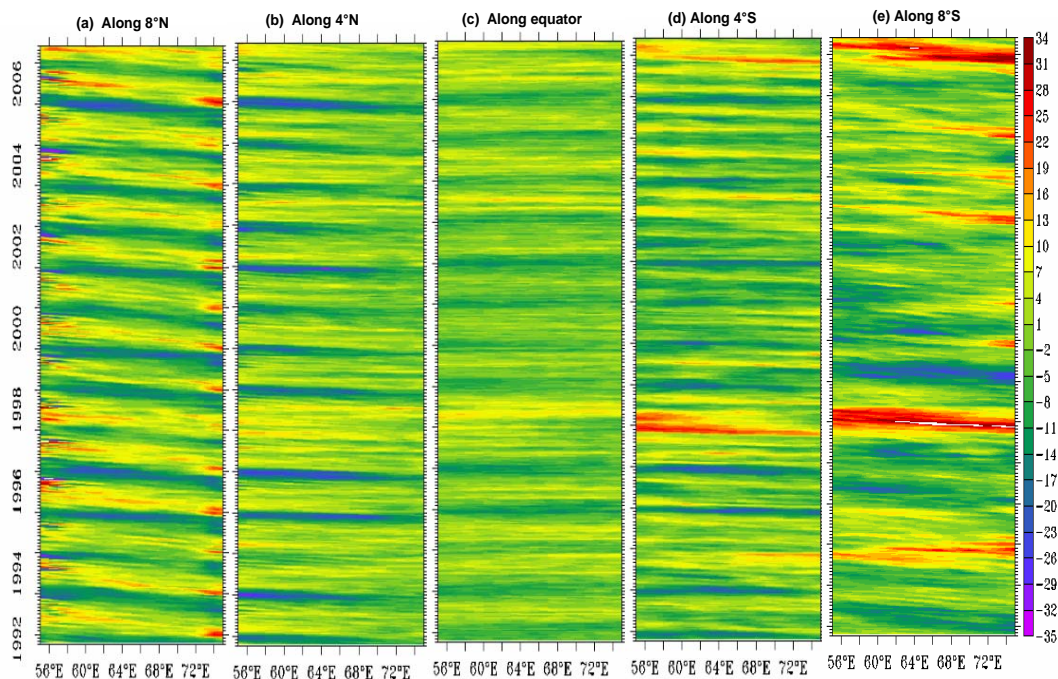


Fig. 4.1 Latitudinal variability of propagating waves in the Indian Ocean (a) along 8°N, (b) along 4°N, (c) along equator, (d) along 4°S and (e) along 8°S.

The westward propagating waves are interpreted from east to west diagonally moving highs and lows. It is observed that the speed of the wave gradually decreases from lower latitudes to higher latitudes(Fig. 4.1). The time of origin from west coast of India is almost same on all latitudes, but the arrival timings vary for obvious reasons already discussed. Both the transition periods i.e. April/May and October/November happened to be the time of

origin for the high and low phases of Rossby wave. The continuity and intensity of the sea level variation varies from year to year. Over 8°N time-latitude the high sea level because of the presence of Laccadive high didn't propagate along with the Rossby wave instead it dissipated after certain distance (~west of 70°E)(Fig. 4.1a). This dissipation was varies from year to year. During extreme events (1994, 1997-98) the dissipation appears less.

## 4.3 Planetary waves and the thermal structure in the Indian Ocean

### 4.3.1. Introduction

Both numerical and observational studies have strongly suggested that the equatorial Kelvin wave plays a major role in oceanic events. Linear equatorial wave theory (Moore and Philander 1977) in the past has assumed that the waves propagate in a quiescent ocean with a horizontally uniform stratification, which is clearly not a realistic approximation of the real ocean. Hydrographic observations indicate the density field at low latitude varies not only in the vertical direction, but also in the horizontal plane. The most prominent feature of this is the east-west tilt of the thermocline along the equator. From Sverdrup's classical theory this tilted thermocline can be thought as a result of a simple balance between the zonal wind forcing and the zonal pressure gradient.
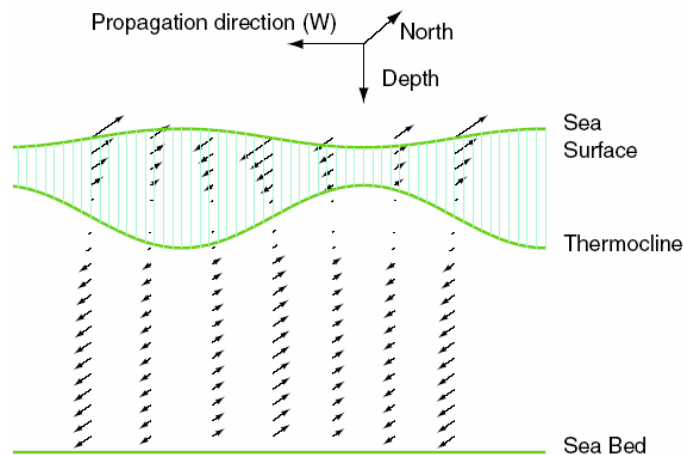


Fig. 4.2 Schematic diagram showing the influence of Rossby wave on thermocline and currents.

Hughes et al. (1981) has derived a simple relationship between the amplitude of a Kelvin wave and the depth of the thermocline. Gill and King (1985) have investigated the

question concerning whether the modal decomposition of a Kelvin wave with a given frequency can undergo significant changes as a result of propagation through a region of shoaling thermocline. Busalacchi and Cane (1988) concluded that the zonally varying stratification does not produce substantial changes in the energy flux of propagating equatorial waves, but can cause significant change in wave amplitudes.

The studies of Gill and King (1985) and Busalacchi and Cane (1988) have assumed that the Kelvin wave is periodic in time. In the real ocean, however, the observed Kelvin waves are closely correlated with impulsive changes in the wind forcing, and thus propagate in the form of wave fronts (Ripa and Hayes 1981; Knox and Halpern 1982; Eriksen et al. 1983; Lukas et al. 1984). There are fundamental differences between a periodic wave and a wave front in the sense that the latter carries mass (i.e., volume) whereas the former does not. In this study an attempt is made to understand whether the Kelvin wave front on propagation causes any variations in the vertical stratification. For this we have taken both Kelvin and Rossby wave cases to study whether any changes in the depth of thermocline over and above the natural tilt of thermocline (due to wind).

### 4.3.2. Data

**T**hree data sets used in this study are (i) altimeter-derived SSH data (ii) hydrographic data from Levitus climatology on 0.25° x 0.25° grid resolutions and (iii) wind data from COADS climatology interpolated to 0.25° x 0.25° resolution.

### 4.3.3. Results and discussion

It is well known that the transition of wind pattern triggers the Kelvin waves along the equator. This type of planetary waves is aperiodic in nature and they move fast towards east. In this study we address the changes taking place in the thermocline during the passage of Kelvin(Rossby) wave along the equator (9°N).

### 4.3.3.1 Along the equator

Time-longitude plots of mixed layer depth (MLD –depth of temperature drop of 1°C from surface temperature) and depth of 20°C isotherm (Fig.4.3) have been presented. Deeper

thermocline (~125m) on the western side compared to eastern side (90m). In the equatorial region, the transition period of wind regime, i.e. March-April, is characterized by shallow mixed layer(~10m) on the eastern side and deep mixed layer (>30m) around 85°E.
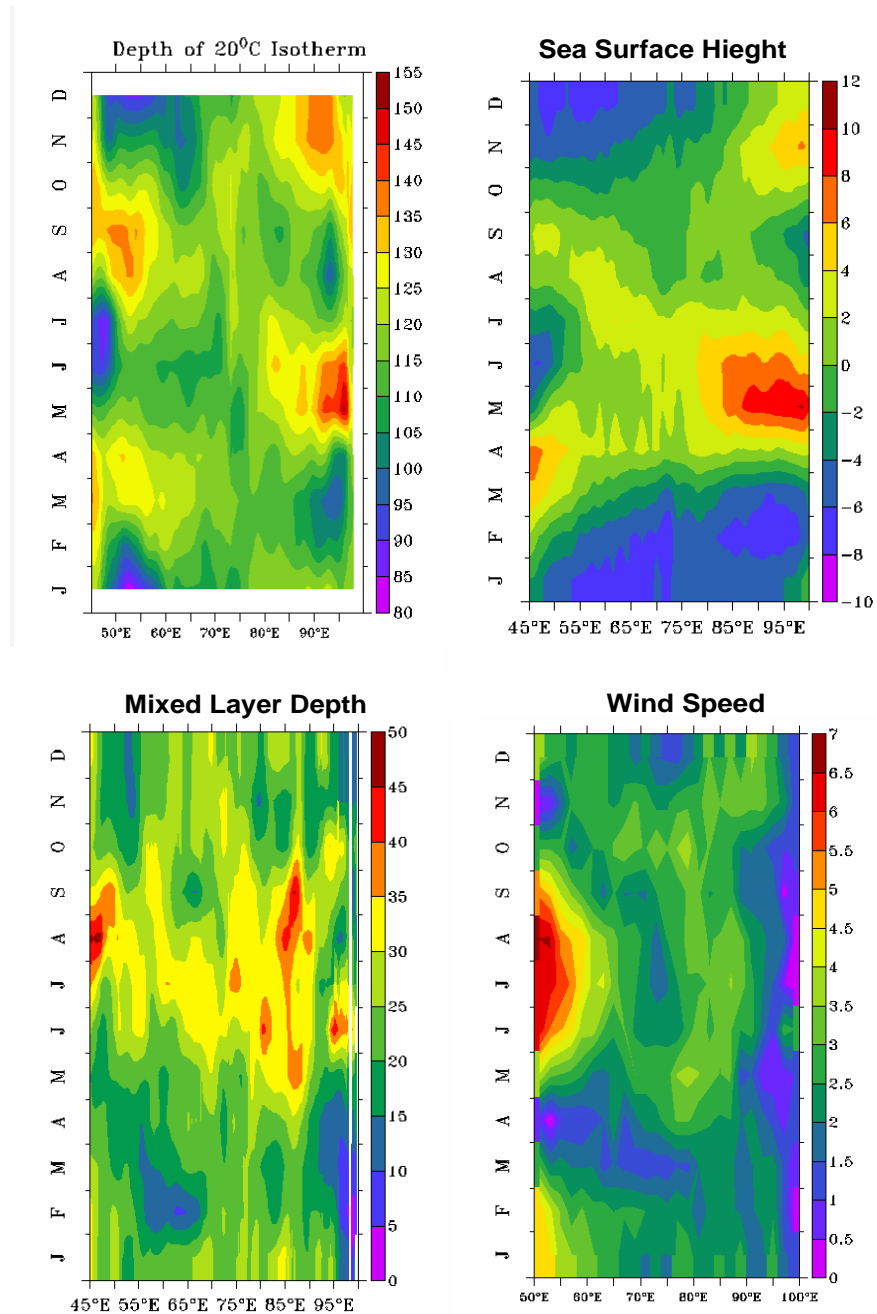


Fig. 4.3: Time latitude plots of 20°C isotherm depth in meters (left), Monthly mean SSH in centimeters (top-right), monthly mean Mixed Layer depth (right) in meters and scatterometer monthly mean wind speed along the equator

Analysis of the wind data for the corresponding periods (Fig.4.3) indicated that shallow mixed layer in the western Arabian Sea coincided with low wind speeds. On the other hand, the deeper mixed layer noticed around 90E, corresponding to stronger winds. Similar variations are noticed in the depth of 20°C isotherm which is not found to be related to the local wind. This suggests the influence of remote forcing on the upper ocean thermal structure in this region.

To study the characteristics of Kelvin wave along the equator, the time- latitude plot of the monthly mean SSH has been analyzed (Fig.4.3). The figure clearly indicated the generation of Kelvin waves at the equator around 60°E during April, as evident from the appearance of high sea level in this region. This high, associated with the Kelvin wave, reaches the eastern boundary (100°E) with in one month, i.e. in May, suggesting a speed of 2.35 m/s. Speed of this wave agrees with the speed of equatorial Kelvin waves (Subrahmaniam et al., 2001). The propagation speed of 2.1 m/s in the 20°C isotherm is slightly less than the speed of baroclinic Kelvin wave computed from the SSH data (2.35 m/s).

The arrival of the Kelvin wave on the eastern boundary is characterized by the deepening of mixed layer by more than 15m (10m in March to 35m in May), and the depth of $20^o$C isotherm by more than 50m (90 m in March to 240m in April) even though the winds were very weak. This suggests the influence of this Kelvin wave on the variability of thermal structure and its effect was more pronounced in the thermocline region than at the surface layer. The observed displacement of the order of 50m in the $20^o$C isotherm is much less than that reported by Kessler et al. (1995) for the Atlantic Ocean (90m).

Another notable feature along the equator is that the Kelvin wave get reflected on hitting the Sumatra coast and gets modified into a westward propagating Rossby wave, as evident from the westward propagation of sea surface high (Fig.4.3). These Rossby waves are found to travel at much slower speed (0.39 m/s) compared to the equatorial Kelvin waves (2.35 m/s).

**4.3.3.2 Along the 9°N**

Time-latitude plots of the sea-level anomalies show westward propagation at all latitudes, the speed of propagation decreasing with increasing latitude. Similar westward

propagation has been noted in earlier hydrographic (Kumar & Unnikrishnan, 1995; Unnikrishnan, Kumar, & Navelkar, 1997; Rao, 1998) and altimetry studies (Perigaud & Delecluse, 1992), and has been attributed to westward propagating Rossby waves. In the Bay, however, westward propagation is seen at all depths throughout the entire year, indicating geostrophy is dominant there (Vinayachandran and Yamagata, 1998).
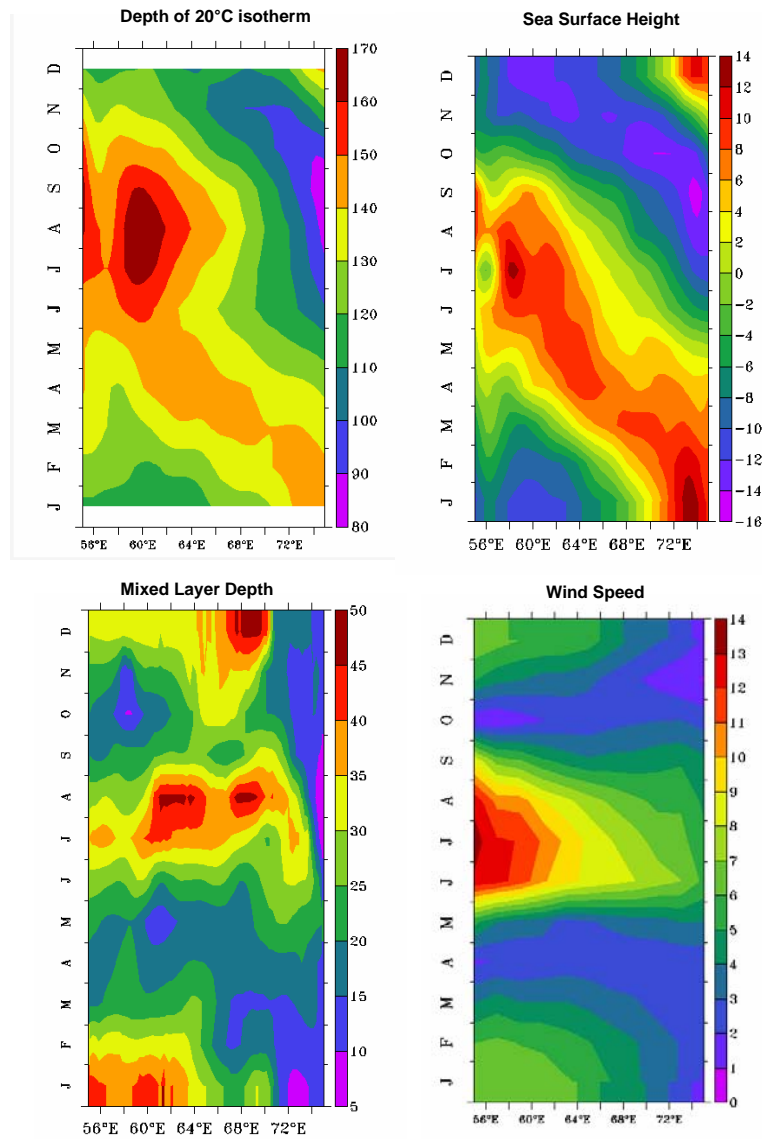


Fig. 4.4: Time-latitude plots of 20°C isotherm depth in meters (top-left), Monthly mean SSH in cm (top-right), monthly mean MLD (left-bottom) in meters and monthly mean wind speed along the 9°N in the Arabian Sea.

To study the influence of propagating waves north of the equator, time latitude plots of sea level anomaly, depth of 20°, MLD and wind along 9°N is presented (Fig. 4.4). The figure clearly indicated the formation of a high sea level around 75°E during December. This high is found to propagate westward and reaches 60°E by May suggests a speed of 12 cm/s. The westward propagation of this high and the speed of the order 12 cm/s suggest that this can be a Rossby wave. Earlier studies attributed similar features to a propagating Rossby wave (Subrahmanyam et al 2001). After reaching 60°E this high merges with another high which is stationary. The eddy lay about 300 km offshore of the Somali coast and between 4°N to 12°N; large parts of the Somali Current were re-circulated around this eddy, known as the 'Great Whirl' (Bruce, 1968). After encounter with Great Whirl this became a standing eddy and continued till September.

The influence of westward propagating wave is clearly seen on the depth of 20°C. Deepening started during December and propagated to 65°E by May. This is very well in agreement with the propagation of high in the time latitude plot of SSH. However the time latitude plot of MLD is different. The MLD plot is more closely coincides with scatterometer wind maps on the same latitude.

## 4.4 Influence of planetary waves on circulation in the Laccadive High

The Laccadive High is a large anti-cyclonic eddy observed during winter. The Kelvin waves generated during the transitional periods over the western equatorial Indian Ocean travel fast along the equator and reach Sumatra coast (~30 days). After hitting the Sumatra coast they travel as coastally trapped waves. These waves radiate Rossby waves westward. In this study the coastal Hovmoller diagram is used for tracking coastally trapped waves. Satellite altimeter data for 1998 -99 and *insitu* observations made during February 1999 are utilized to study influence of the westward propagating Rossby waves on hydrography and currents in the Laccadive High. Coastal Hovmoller of filtered data shows only one signal during October with 30 day periodicity is reaching the southwest coast of India. Finally it is shown that the time of arrival of this wave is matching with formation of LH in the *insitu* observations.

### 4.4.1. Introduction

The Kelvin wave formed in the equatorial Indian Ocean during March-April; travel along the eastern perimeter of the Bay of Bengal (BOB) as coastally trapped Kelvin wave (Potemra et al., 91; Yu et al., 1991; McCreary et al., 1993; Hareesh Kumar and Sanilkumar, 2004). The spatial and temporal patterns of the complex EOF analysis (Subrahmanyam et al 2001) indicated a period of 40-60 days. Shankar and Shetye (1997) also reported same periodicity using tide gauge data. Although, the monthly maps of SSH showed a wave-like signal along the perimeter of the Bay (Fig 3.10 -3.11), it is difficult to prove conclusively these are coastal Kelvin Wave with the available data. The detection of such Kelvin wave from altimetry requires careful additional data processing as described in Jacobs et al. (1998).

This Kelvin wave radiates Rossby wave as it propagate poleward along the eastern boundary of ocean. Studies have attributed the formation of the LH and its subsequent westward propagation to the Rossby wave radiated from the downwelling Kelvin wave (Shankar and Shetye, 1997). Bruce et al (1994) reported the formation of a high sea level off the southwest coast of India during the early part of December 1993, suggesting a clockwise eddy circulation in this region. Afterwards many studies have confirmed this feature off the southwest coast of India during winter (Bruce et al, 1998). The numerical simulation by Shankar and Shetye (1997) also captured the sea level high during winter.

Studies on LH are mostly based on T/P altimetry (Bruce et al, 1994, 1998) and to a lesser extent by in situ measurements (Bruce et al, 1998). Hence, specific observations collected along transect in the LH during 1999 are utilized to study its characteristics.

### 4.4.2. Data and methodology

INS Sagardhwani conducted a spatial survey in the southeastern Arabian Sea (69°E to 76°E) across the LH during winter (22-26 February, 1999). Along this transect vertical profiles of temperature and salinity were collected at 15 stations (at 30 nautical mile intervals) using mini CTD system (accuracies: temperature +0.01°C, salinity +0.02 PSU, pressure +0.02% of 1000m). The altimeter sea surface height anomaly data in 1/3°X1/3° is utilized to map the variability of LH.

To study the propagating waves along the coast, SSH data within the coastal regions (mostly along 30m bathymetry) of the north Indian Ocean (Fig.4.5) is sorted out for the grids

of $1/3^o$ x $1/3^o$ (latitude by longitude) all along the coast. As the offshore length scale of the Rossby wave varies with latitude, a length scale of $1/3^o$ is chosen (Shankar, 2000). The grids start from off the southwest coast of India ($15^o$N, $74^o$ E) and end off Sumatra ($1^o$N, $97^o$E) and are numbered in serial order (Fig. 4.5.).
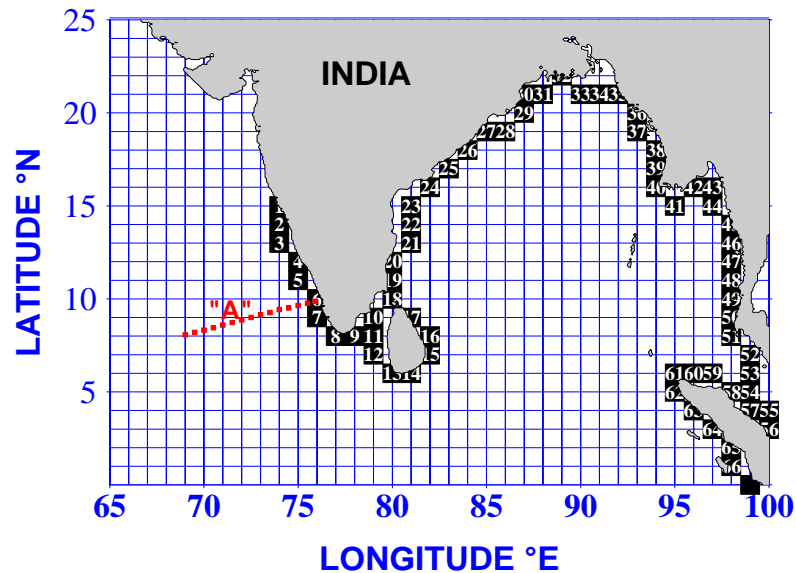


Fig.4.5 Area map: Numbers 1 to 66 points along the coast from off the southwest coast of India ($15^o$N, $74^o$E) to Sumatra ($1^o$N, $98^o$E). Dotted line perpendicular to west coast indicates the cruise track where *insitu* measurements made.

## 4.4.3. Results and discussion

### 4.4.3.1 Equatorial Kelvin wave in the Indian Ocean (Fig. 4.6)

To understand the generation and propagation of equatorial Kelvin waves during 1998-1999, the processed SSH data along the equator is presented a time-latitude section (Fig.4.6). In the western Arabian Sea, positive sea level anomaly is noticed during end March / early April and October/November 1998. Similar features are observed during 1999 also. The intensities were less comparative to the 1998. The high propagates eastward and hits Sumatra coast in May, suggesting an average speed of ~ 2.4 m/s. in agreement with earlier results;
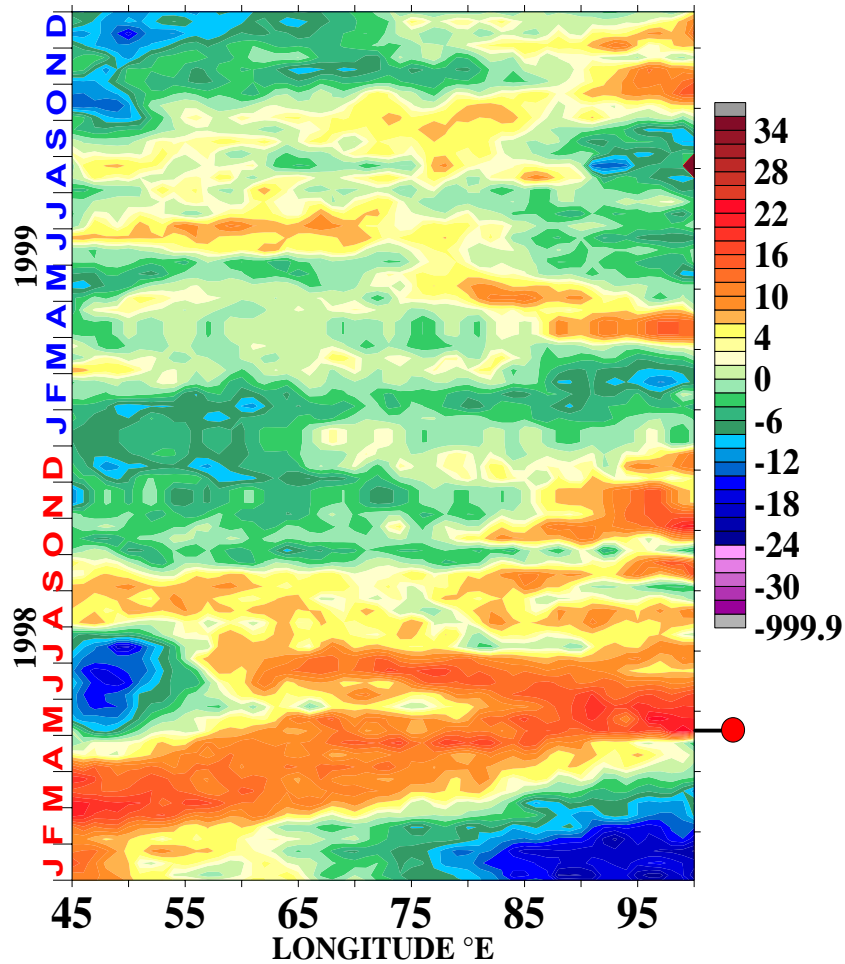
Fig.4.6 Hovmollor diagrams of SSH (in cm) for 1998-1999 along the equator. The red color indicates high sea level anomaly.

It is well known that the wind systems in the equatorial Indian Ocean reverses semi-annually. Equatorial westerlies during both the monsoon transitions generate equatorial Kelvin waves in the Indian Ocean and are found to propagate eastward (Schott, 2001) along with the Equatorial Jet. As a result, high sea level is noticed in the eastern equatorial Indian Ocean twice in a year, one during May – June and the other during October – November (Prasanna Kumar et al, 1998).

It is seen that the positive SSH traveled along the equator (Fig. 4.6) reached Sumatra Coast by May 1998. Now in the following section movement of the positive SSH along the perimeter of the BOB is discussed.

**4.4.3.2 Coastally trapped Kelvin wave propagation along the boundary of the Bay of Bengal**

It is understood that the equatorial Kelvin wave after reaching the eastern boundary of the ocean, propagate northward and southward as coastally trapped Kelvin waves. To understand the variation in the sea level associated with these waves, Hovmoller (time-coast) plots of SSH (1998-1999) along the coasts of the north Indian Ocean are generated (Fig.4.7).
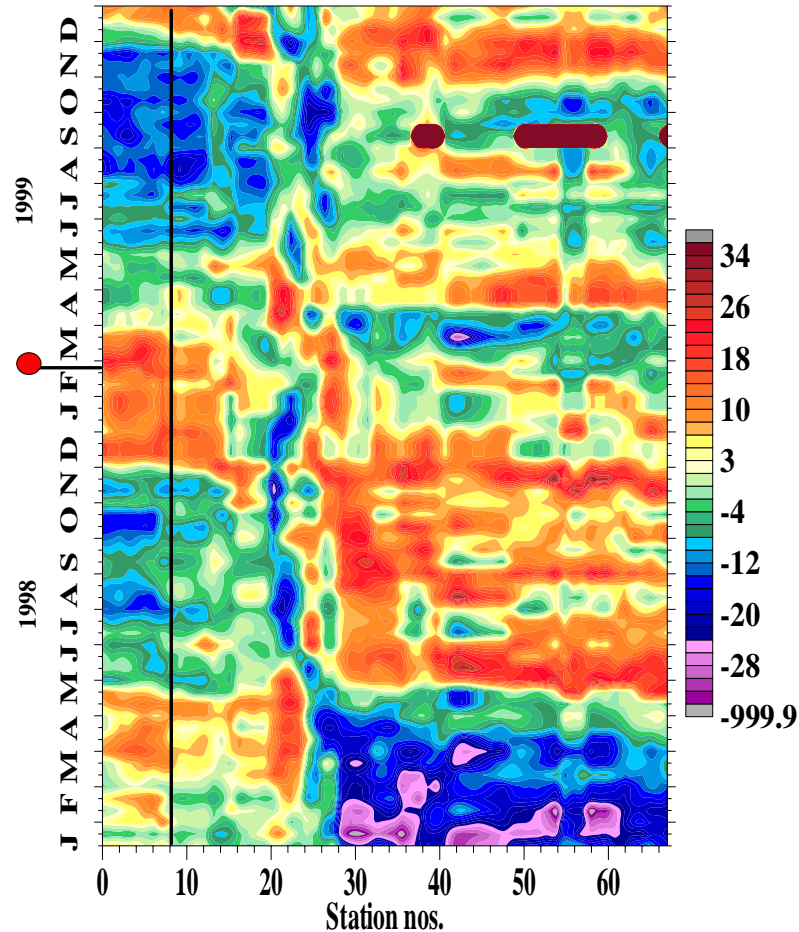


Fig. 4.7 Hovmoller diagrams of SSH (cm) for 1998-99 along the coastal belt. Vertical black line indicates the southern tip of India. Black line with red circle indicates the *insitu* measurement period. (Station 1-10 are along the southwest coast increasing towards south. Stations 9-31 are along the coast of Sri Lanka and along east coast of India increasing towards north. Stations 35- 55 correspond to eastern rim of the Bay. For location of station no's refer Fig4.5)

From the equatorial region of the eastern the Bay of Bengal, these highs and lows are found to propagate along the coast. The positive SSH noticed off Sumatra (station No.66 in Fig. 4.5) in May propagates along the coastal boundaries of BOB and reaches the southern tip of India (station no. 8) by end May / early June.

Bruce et al., (1994); Shankar and Shetye(1997); Hareesh Kumar and Sanilkuamr (2004) attributed the formation of LH off the southwest coast of India to the arrival of high sea level in this region by the coastal Kelvin waves. After reaching the southern tip of India, this high propagates further northward along the southwest coast of India. Shankar and Shetye (1997) and Subramanyam et al., (2001) have indicated that as this Kelvin wave propagates northward, it radiates Rossby waves offshore, resulting in the westward propagation of the LH. Off the southwest coast of India, this high is noticed up to March '99.
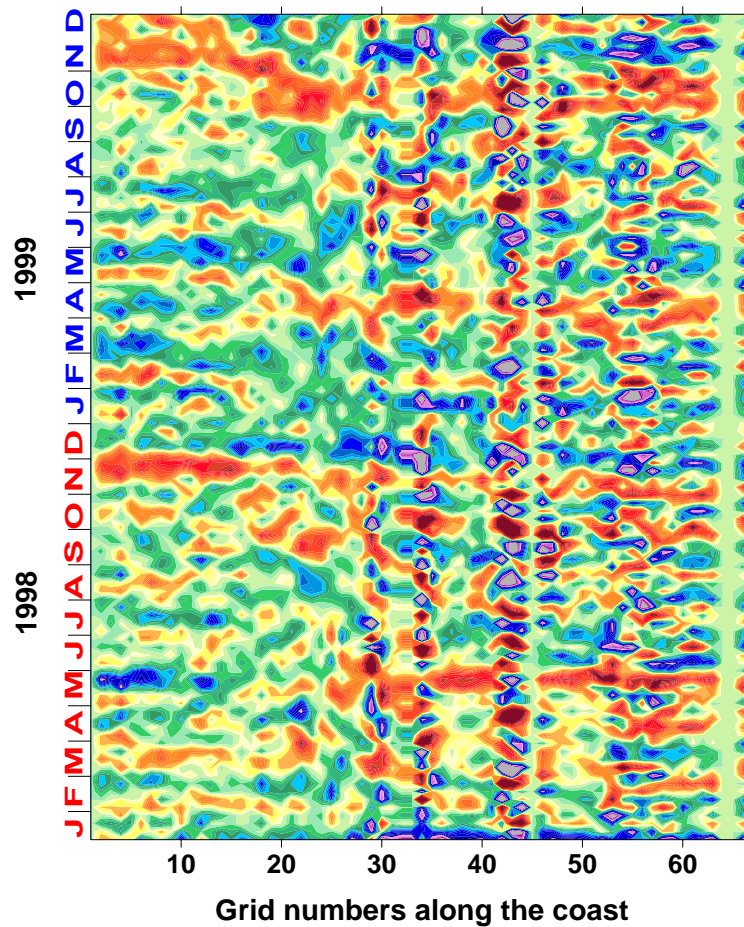


Fig. 4.8 Time-coast Hovemoller of filtered SSH (50 day high pass) anomaly along the coasts

The time-coast data generated for Fig 4.7 was subjected to 50 days high pass filter to see distinctly 30-40 day wave (Fig. 4.8). A high forms at the eastern boundary appears to vanish after reaching head Bay. It appears that the signals formed during November December only reaches the southwest coast of India. The periodicity of these signals is within the coastal Kelvin wave periodicity (30-40 day).

### 4.4.3.3 Westward propagating Rossby wave (Fig. 4.9)

Time latitude plot of SSH data along 9°N depicts a westward propagating wave (Fig 4.9). This wave appears to start from 75°E during December and reaches western Arabian Sea. This time space information suggests a westward propagating wave with an average speed of 11 cm/s.

Low frequency fluctuations of surface winds generate a broad spectrum of Rossby waves (i.e. over a range of frequencies) everywhere in the ocean. In the Arabian Sea in addition to wind forcing a coastal Kelvin wave can also radiate westward propagating Rossby waves. At all frequencies, both long and short Rossby waves will exist. The long Rossby waves will rapidly carry energy to the west. One would expect that the eastern region of the ocean will not have energetic flows (i.e. the kinetic energy associated with low frequency motions will be small). Further, the energy will eventually be carried to the western boundary region by long Rossby waves. In this study we restrict our discussion on low frequency westward propagating Rossby wave along 9°N latitude.
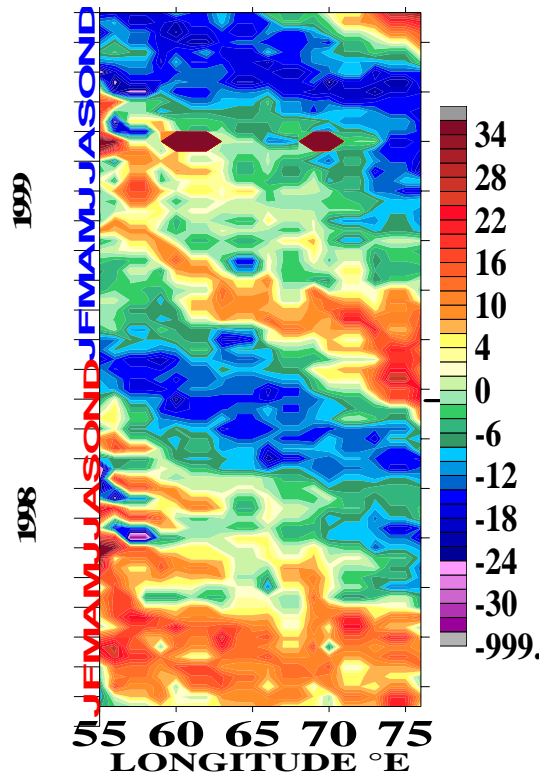
Fig. 4.9 Time-latitude plot along 9°N showing westward propagation during 1998-99.

In section 4.6.3.1, section 4.6.3.2 and section 4.6.3.3 the arrival of high sea level off the southwest coast of India during end November/early December '98 associated with the arrival of Kelvin waves is clearly indicated. In the next section detailed observational description of LH formation is discussed using both insitu and satellite observations.

**4.4.3.4 Evolution of Laccadive High during 1998-1999 from satellite altimetry**

To understand the evolution of the LH during 1998-99, the SSH data for the Arabian Sea from 25th November 1998 to 14th April 1999 is presented (Fig.4.10). Positive SSH is appeared off the southwest coast of India from 25th November onwards. However, the LH becomes prominent by the second week of December, i.e. by 9th December, as indicated by a region of positive SSH between 5° to 15°N and east of 74°E. The core of the LH centered at 7°N, 77.5°E on 9th December moves to 7°N, 75°E by end December and to 7°N, 74.5°E by 6th January. During this period, the LH is evident as a well defined clockwise eddy, with clockwise circulation around its centre. This suggests that the LH propagates westward from December onwards with an approximate speed of 12.7 cm/s. By end January, the LH extends

westward up to $60^o$E along $5^o$N. This high splits into two highs on $20^{th}$ January, one east of $66^o$E and another between $55^o$ and $60^o$E, with lateral dimension of $\sim$ 400km and 200 km respectively. By $24^{th}$ February, the dimension of the high increases and moves slightly westward towards the Somali basin. These multiple eddies can be clearly seen from the *insitu* measurements carried out along a track perpendicular to the LH for the same period (Fig.4.10).
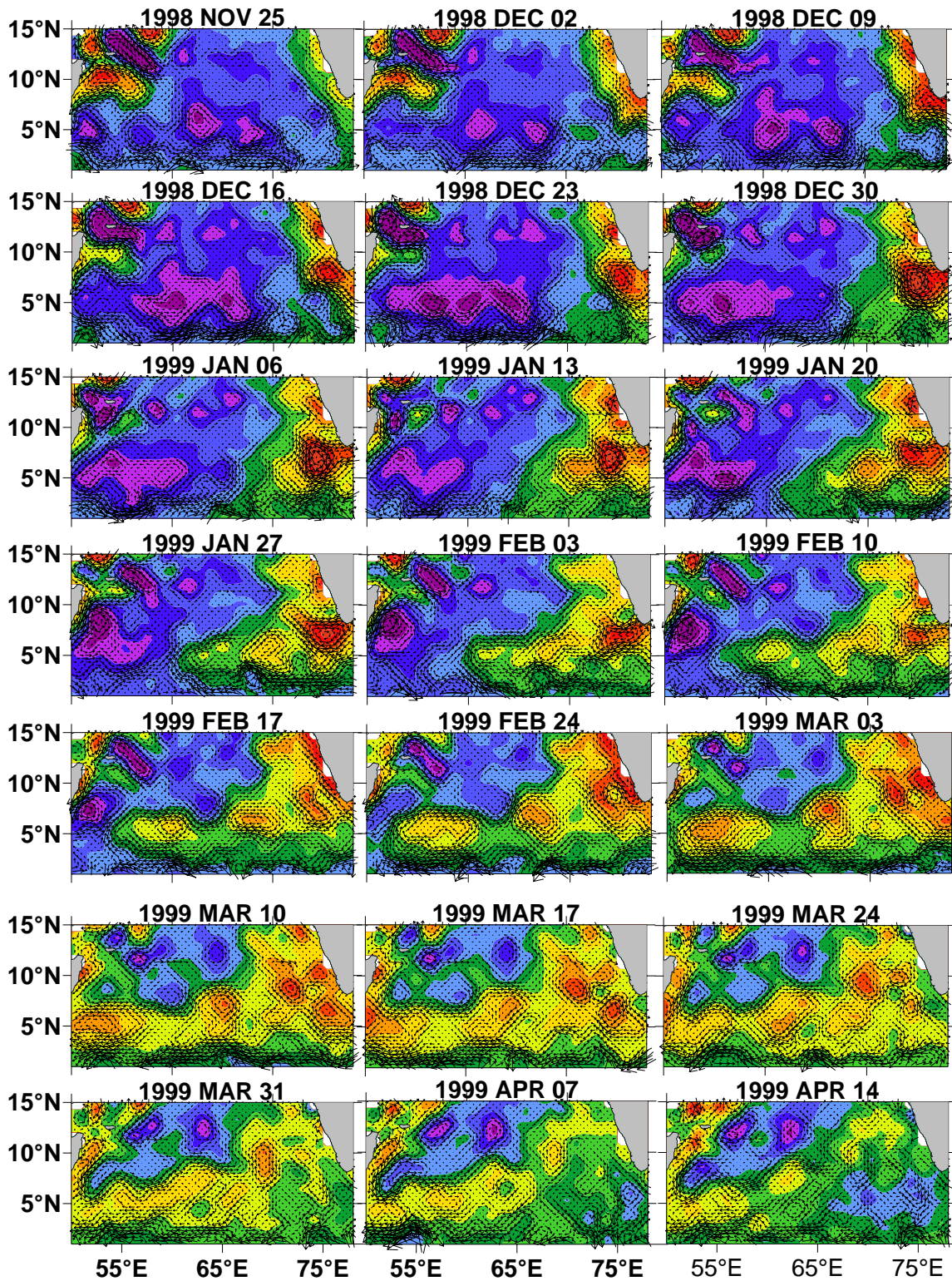
Fig. 4.10 Evolution of Laccadive High during 25$^{th}$ Nov '98 to 14$^{th}$ Apr '99

All these highs merge by the first week of March (1$^{st}$ March) and seen as a single high extending across the entire basin. From the figure, it can be seen that the eddy formed off the southwest coast of India on 11$^{th}$ December 1998 reaches the Somali coast by 11$^{th}$ March. This high started dissipating afterwards.

**4.4.3.5 Laccadive High from *insitu* observations**

Having obtained an idea about the LH from satellites altimetry, it is worthwhile to examine its presence utilizing the *insitu* measurements made across the LH during 22-26 February 1999 (Fig.5a to 5c). The depth-space section of the temperature, salinity and density across the LH clearly revealed multiple eddies, in this region, which is in conformity with the satellite data (Fig.4.10). Even though, the eddy structure is seen in all the fields, it is more prominent in the salinity and density fields. The anti-cyclonic eddy with an apparent centre near station 8 (9$^{o}$N, 72.5$^{o}$E) and extends vertically down through the thermocline to more than 300m. The depth-space section further suggests that this anti-cyclonic eddy is sandwiched between two weaker anti-cclockwise eddies.
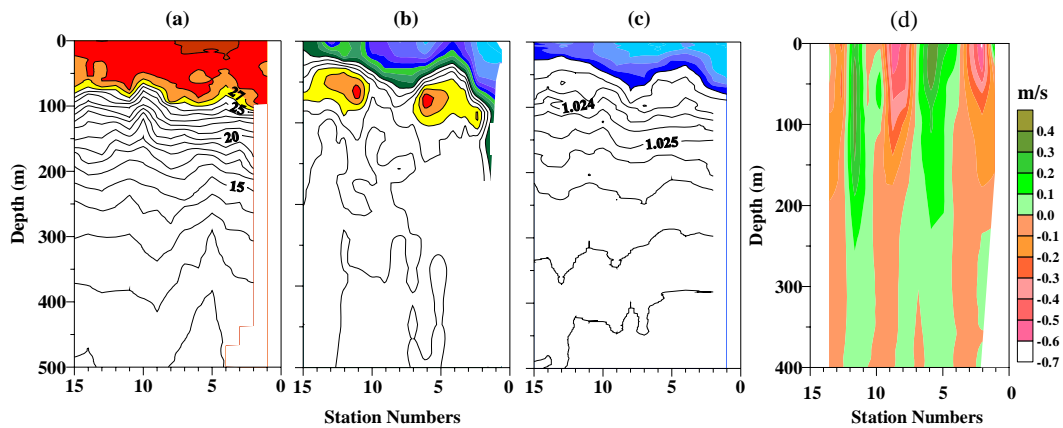


Fig.4.11 Depth-space sections of (a) temperature, (b) salinity and (c) density. d) Depth-space sections of geostrophic current across LH (22 -26 February 1999)

The geostrophic currents are derived from *insitu* measurements also indicated presence of eddy (Fig 4.11d). The figure indicated alternate bands of northward and southward flow, suggesting complex current pattern in the LH region. Bands of northward flow are noticed very close to the coast, between 200-425 km and 650-750 km, with maximum speed (>40 cm/s) centered at 350 km and 750 km. On the other hand, southward

flow bands are noticed between 100-200 km, 425-650 km and beyond 750 km, with speed exceeding 50 cm/s observed at 110 km and 500 km. The alternate bands of northward and southward flow also indicate the eddy type of circulation pattern in this region.

In the vertical, high salinity waters are noticed in the upper 60m near the coastal regions and in the regions of anti-cyclonic eddy. Characteristics of this low salinity water in the coastal regions agree with that of the Bay of Bengal water mass. This water was transported to the southeastern Arabian Sea by the prevailing northerly currents during winter (Darbyshire, 1967; Wyrtki, 1971; Pankajakshan and Ramaraju, 1987). In the offshore regions, the T-S characteristics of the surface waters also suggest that they are of the Bay of Bengal origin. Presence of this low salinity water in the offshore regions might have been due to the offshore movement of the LH, which was formed close to the coast, due to the westward propagating Rossby waves. Below this water, the Arabian Sea High Saline water mass, as evident from temperature in excess of $26^{o}$C and salinity in excess of 35.5 PSU can be clearly seen. The clockwise eddy splits the core of this water mass, noticed around 50-70m, in to two segments.

The coast-time Hovmoller diagram shows the movement of highs formed at the Sumatra coast along the perimeter of the Bay of Bengal. Band pass filtered SSH along the coast confirms that the signal formed during October of 1998 and 99 only traveling up to the southwest coast of India. Whereas the wave during April-May is appear to dissipate at the head Bay.

## 4.5 Influence planetary waves on circulation in the Bay of Bengal during the summer monsoon 1999

### 4.5.1. Introduction

The Bay of Bengal is one among the many regions where the ocean dynamics are complex due to seasonal reversal of circulation, massive fresh water discharges (Martin et al., 1981), eddies (Babu *et al.,* 1991; Sanilkumar *et al.,* 1997; Gopalan *et al.,* 2000) and prevailing planetary waves (Yu *et al.,* 1991; McCreary *et al.,* 1993). These waves are of major concern in problems of equatorial adjustment to unsteady wind forcing, monsoon dynamics, oceanic circulation etc. Simulations carried out by McCreary et al. (1993)

113

indicated that the circulation in the coastal Bay of Bengal appears to be predominantly forced by winds within the Bay throughout the year. Further, studies (Potemra et al 1991; Yu et al 1991; McCreary et al 1993; Sengupta et al 2001) have clearly demonstrated that planetary waves also play a dominant role in the dynamics of the Bay of Bengal.

As most of the studies confined to theoretical and satellite measurements, detailed observational evidences planetary waves in the Bay of Bengal are limited. This study describes the observed planetary waves and associated circulation pattern during summer monsoon of 1999.

The measured current and wind fields from a stationary location suggested that circulation in the Bay of Bengal during the monsoon season was not only driven by local winds, but also by the gyral circulation due to the presence of planetary waves.

Spectral analysis of the long-term measurements of wind, air temperature, sea surface temperature and wavelet decomposition of SSH indicated intra-seasonal oscillations. Variability in the 10-20 days is linked to local winds. The 2-D energy spectrum of zonal sea surface slopes along $13^o$N shows significant peaks at 0.01325 cycles/day (-0.11/degree) and 0.018 cycles/day (-0.09 /degree) and suggested these peaks correspond to the band of the Rossby waves. The phase speed and wavelength of these waves are 14.3 cm s$^{-1}$, 1000 km and 21.5 cm s$^-$1, 1200 km respectively.
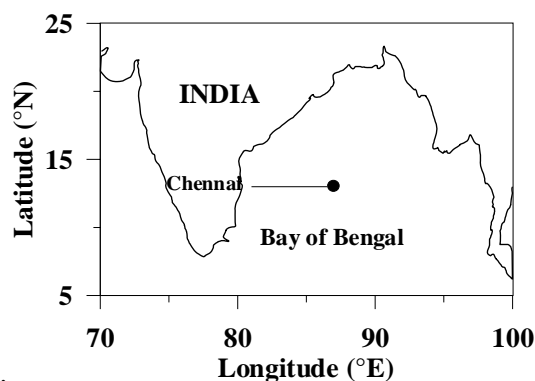


Fig.4.12 Station location during BOBMEX (line along 13°N is spatial transect (___) and dot at the end of the line is time series (.) location

**4.5.2. Data**

The research vessel INS Sagardhwani carried out a spatial survey in the southwestern Bay of Bengal (along $13^o$ N from $82^o$ E to $87^o$ E with stations at $0.5^o$ intervals) from 22 July – 30 August '99 (Fig 4.12) as a part of BOBMEX-99 experimental programme. The zonal transect along $13^o$N was repeated six times with a time gap of approximately one week covering active and weak phases of the summer monsoon. Vertical profiles of temperature and salinity were collected from each stations using mini CTD system (accuracies: temperature $\pm0.01^o$C, salinity $\pm0.02$ PSU, pressure $\pm0.02\%$ of 1000m). In between the spatial surveys, the ship also occupied a stationary position in the central Bay of Bengal ($13^o$N, $87^o$E) for time series measurements in four phases. Each phase lasted for a period of five to six days (17-22 July, 30 July - 5 August, 12-16 August and 25-28 August, 1999). At this time series location, three hourly measurements of surface marine meteorological parameters and vertical profiles of temperature and salinity were made.

**4.5.3. Results**

**4.5.3.1 Geostrophic circulation during July – August 1999 in the Bay of Bengal.**

The coastal currents are indicative of a cyclonic gyre in the Bay of Bengal except between 13°N and 17°N where it is weak northerly in July – August and by September the cyclonic gyre is well established in the Bay of Bengal (Fig. 2.7 – 2.9). The cyclonic eddy off Sri Lanka called the Sri Lanka Dome (Vinayachandran and Yamagata 1998) intensifies during this period and moves northwestward, while the cyclonic eddy off Visakhapatnam moves offshore from July to September. A weak clockwise eddy is sandwiched between these two cyclonic eddies.
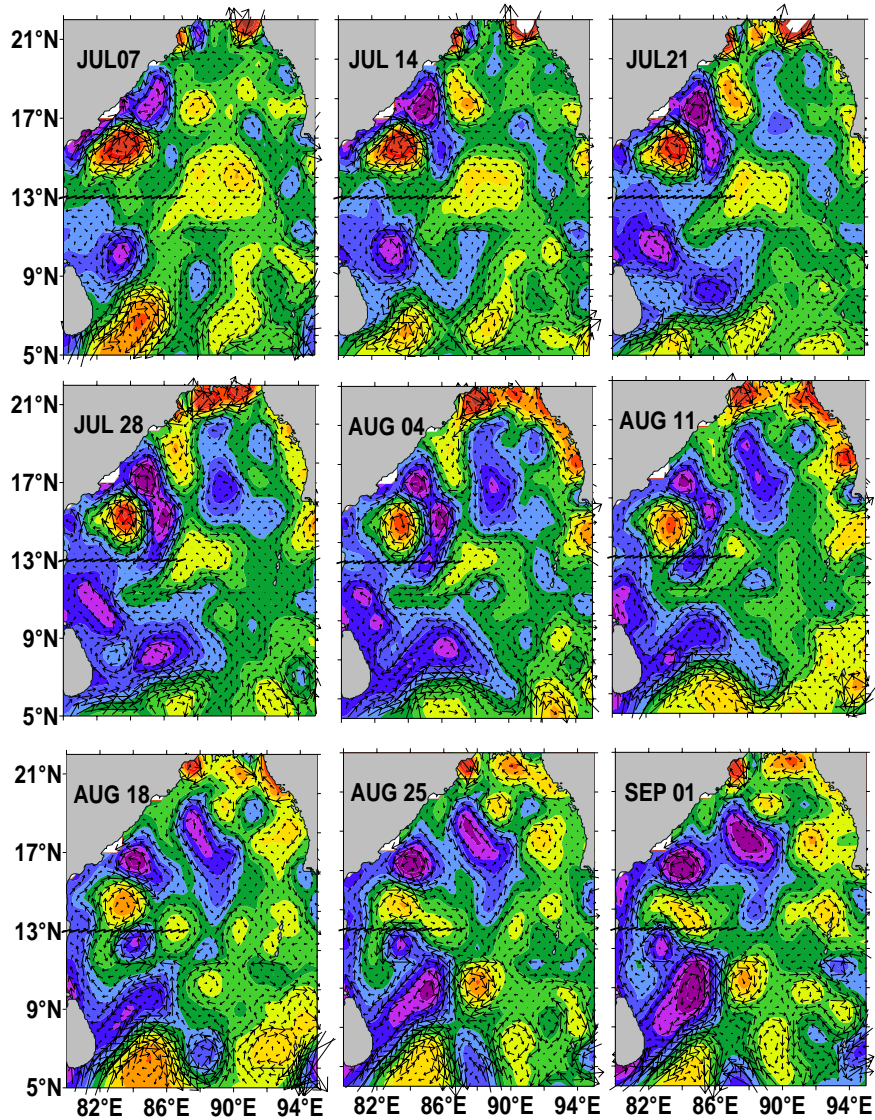
Fig.4.13 Distribution of geostrophic currents estimated from the SSH data during July-August 1999. Black lines indicate the zonal transect along $13^o$N (from coast to $87^o$E).

Utilizing SSH data, several studies (Parke et al., 1997; Gilson et al., 1998; Han and Webster, 2002) have shown that the displacements of the gyres are associated with propagating long period waves. We used SSH altimeter measurements during 1999 (Fig.4.13) to understand the basin scale variability of eddies and propagating waves in the Bay of Bengal. An interesting observation in the figure is the presence of a well developed clockwise gyre in the central Bay in the first week of July, with a tendency to move

westward. However, its westward movement was inhibited after 14 July due to the southward extension of the cyclonic gyre (VL). With the intensification of the VL, the clockwise gyre weakened, without further westward movement. Incidentally, the time series location during BOBMEX and the location of the National Institute of Ocean Technology data buoy falls in the periphery of this clockwise gyre. Therefore, the variability observed in the time series location can be due to the combined effect of the VL and clockwise gyre (Fig.4.13).

### 4.5.3.2 Spatial and temporal variability of currents

The depth-space section of temperature and salinity indicated alternate bands of warm (salinity less than 34 PSU) and cold (salinity in excess of 34 PSU) water regions (Fig. 4.14). Bands of warm and comparatively low salinity waters noticed along this transect suggested an anti-cyclonic gyre circulation. Somayajulu et al. (1987) also reported similar gyres along a section from Madras to Andaman during the summer monsoon season. During 28-30 July, two gyres were noticed along $13^o$N latitude, a cyclonic gyre between $84.5^o$E and $86.25^o$E and an clockwise gyre between $83^o$ and $84.5^o$E. When the same transect was repeated after a gap of 10 days, i.e. by 10-12 August, the core of this cyclonic gyre was noticed at $84.75^o$E, i.e. a westward shift of ~25 km compared to its position during end of July. This gyre further moved westward with the progress of time and by the end of August, i.e. by 28-30 August, the core was noticed at $83^o$E. Similar feature was also observed in the case of clockwise gyre.
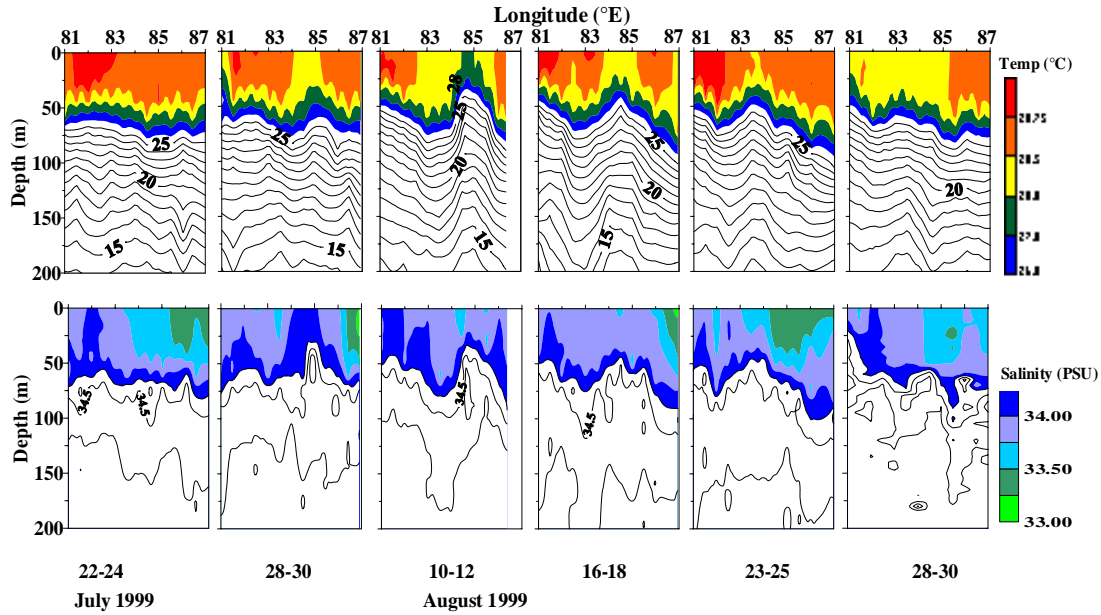
Fig.4.14 Depth-distance sections of (a) temperature and (b) salinity along 13°N. Coloured regions are temperature greater then 26°C and salinity less than 34 PSU.

To view the progressive movement of these gyres, geostrophic currents across 13° N in the thermocline region (computed with reference to 600m) is presented (Fig.4.15). The estimated geostrophic currents clearly indicated the progressive westward movement of these gyres (southerly component marked in blue colour). Across this latitude, the weak southward flow (<0.10 m/s) noticed during 22-24 July centered at 84.75°E, intensified (~0.7 m/s) subsequently and by 11 August, its core was noticed centered at 84.25°E. The core shifted further westward and by end August, it moved to 82.75°E with a reduced current strength (<0.10 m/s).This leads to the fact that the core of this cyclonic gyre, as evident from the depth-distance sections of temperature (Fig. 4.14) moved westward by ~220 km from its original position, i.e. from ~84.75°E to ~82.75°E over a period of 38 days, i.e. between 22 July and 30 August, suggesting a rate of movement of ~6.7 cm/s.
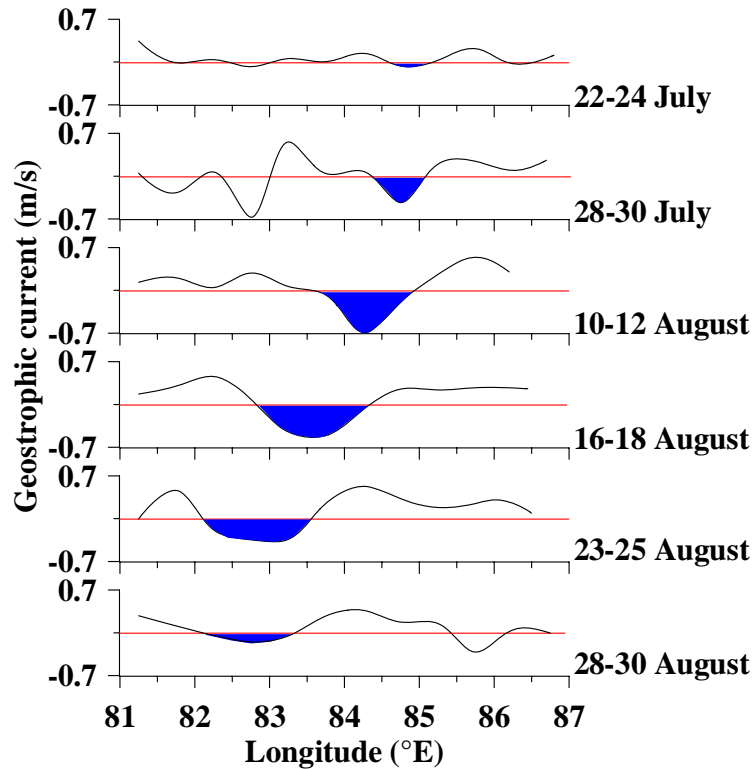
Fig.4.15 Geostrophic currents in the thermocline across 13°N (Blue highlights the southerly component of geostrophic currents)

### 4.5.3.3. Geostrophic currents from insitu measurements

Depth-time distribution of dynamic height (Fig.4.16a) indicated low and high values suggesting clockwise and anti-clockwise flow pattern. The same is evident in the geostrophic currents across 13° N (Fig.4.16), where alternate bands of southerly and northerly currents are clearly visible. These alternate bands suggested that an eddy type of circulation prevailed in this region. Similar bands are also observed in the SSH imagery as high and low sea level (Fig 4.13). This condition is conducive for horizontal current shear generation and baroclinic instability. Moreover, the geostrophic current revealed that in these bands, the flow is uni-directional in the vertical with varying magnitudes.
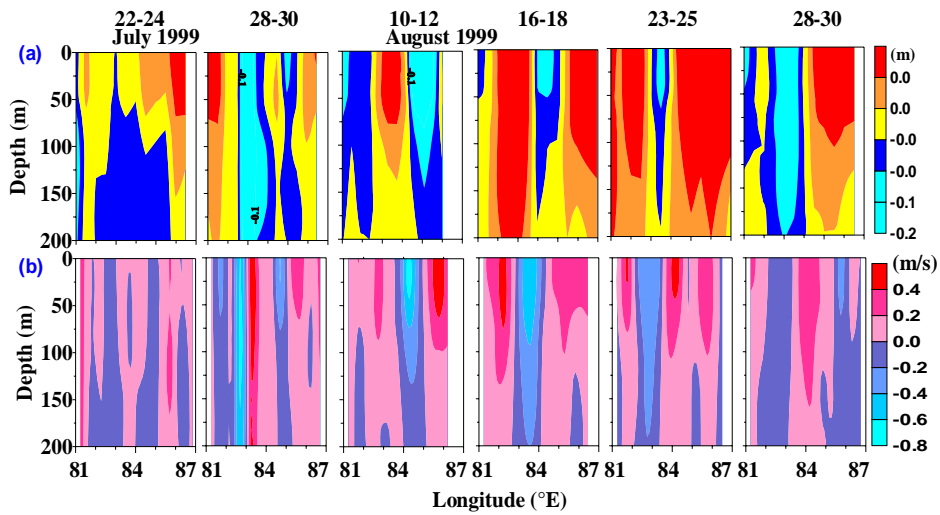
Fig.4.16 Depth-space sections of (a) dynamic height and (b) geostrophic currents across 13$^o$ N

### 4.5.3.4 Planetary wave signal in the time series data at NIOT Buoy

Direct measurements of currents are extremely sparse in the Bay of Bengal. Therefore, we have utilized the *in situ* data collected (u-v components of wind, SST, air temperature) from a moored buoy in the central Bay (13$^o$ N, 87$^o$ E) for longer duration (September 1997 to October 1998) to study the prevailing flow pattern and its relation to the local wind forcing. Time series measurements collected are subjected to FFT analysis. The dominant oscillations are found to be in the intra-seasonal band having periodicities of 10-20 days (0.004 to 0.002 cph) and 30-60 days (0.0013 to 0.001 cph) in all the fields. The dominance of 10-20 days periodicity in the SST field was also observed by Sengupta and Ravichandran (2001). Since SST and wind (U and V components) exhibited prominent peaks in the 10-20 day band, fluctuations in SST in this band can be directly forced by winds, which are well supported by the numerical simulation of McCreary et al. (2001).

According to Cane and Moore (1981), the ocean has a response mode at a period of 60 days, in the mode 3. The instability is generated when Rossby waves propagate from the eastern ocean encounter the local eastward mean flow. The cyclonic and clockwise gyres around 13$^o$N, as evident from the depth-space sections (Fig.4.12), and SSH (Fig. 4.13), can be a possible candidate to circulation in this region.

## 4.5.4. Discussion

The analysis clearly indicated the existence of cyclonic and anti-cyclonic gyres along 13°N in the Bay of Bengal, its gradual westward movement with a speed of ~6.7 cm/s and the variability with intra-seasonal periodicity.
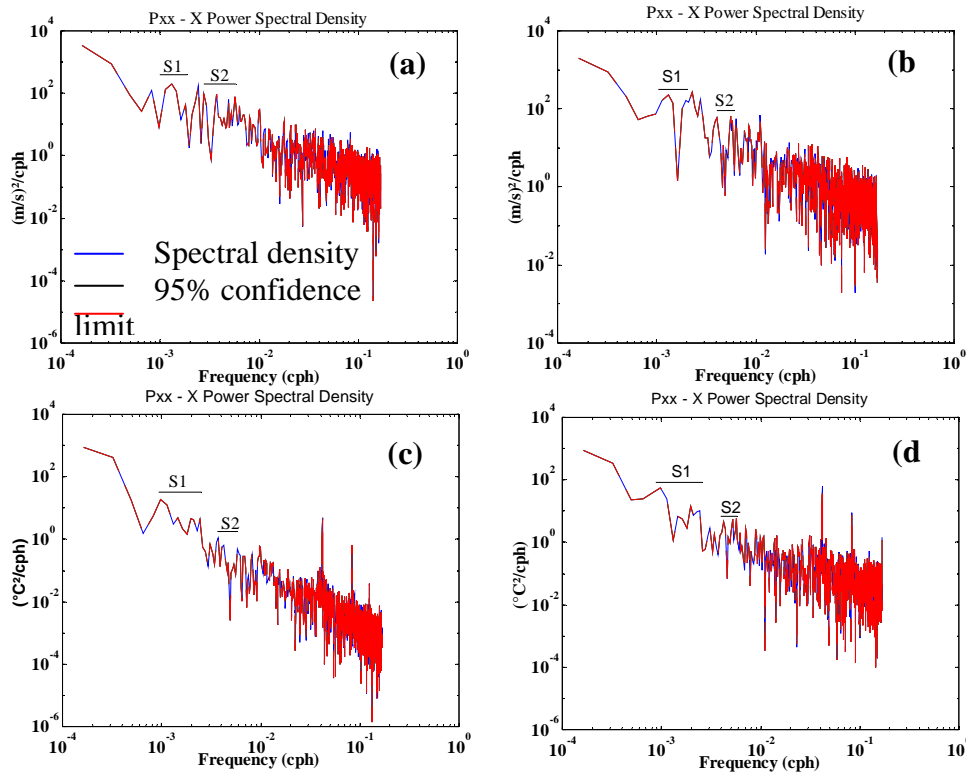


**Fig.4.17** Spectra of (a) U component wind speed, (b) V component of wind, (c) sea surface temperature and (d) air temperature. S1 and S2 correspond to intra-seasonal signal (30-60 days, i.e. 0.0013 to 0.001 cph and 10-20 days i.e. 0.004 to 0.002 cph).

The SSH and derived geostrophic currents clearly indicated the presence of a low SSH with cyclonic gyre north of 17°N off the east coast of India (Visakhapatnam Low) and an anti-cyclonic gyre south of this cyclonic gyre. The presence of cyclonic and anti-cyclonic gyres along 13°N resulted in the formation of alternate zones of convergence and divergence in the thermohaline fields (Fig.4.14a).

## Summary and Conclusions

In the present study the availability of satellite altimeter sea level data with good spatial and temporal resolution is explored to describe and understand circulation of the tropical Indian Ocean. The derived geostrophic circulations showed large variability in all scales. The seasonal cycle described using monthly climatology generated using 12 years SSH data from 1993 to 2004 revealed several new aspects of tropical Indian Ocean circulation. The interannual variability presented in this study using monthly means of SSH data for 12 years have shown large year-to-year variability. The EOF analysis has shown the influence of several periodic signals in the annual and interannual scales where the relative strengths of the signals also varied from year to year. Since one of the reasons for this kind of variability in circulation is the presence of planetary waves. This study discussed the influence of such waves on circulation by presenting two cases one in the Arabian Sea and other in the Bay of Bengal. The summary and the major results of this study are presented below.

### 5.1 Summary of Chapter I

In Chapter-1 the first three sections describe the unique geographical, geological setup and prevailing wind variability in the study region. Importance of planetary waves in altering the circulation in the study region is given in section four. After presenting the importance of studying circulation in section five, the observational background is given in section six. The criterion for selecting the area and objectives of the thesis are presented in section seven. To meet the objectives of the thesis multi-mission altimeter data is used. The details of the data and methodology for computing geostrophic currents are presented in the towards the end.

### 5.2 Summary of Chapter II

The study on SSH data and derived geostrophic currents clearly bring out many features on the seasonal variation of currents in the tropical Indian Ocean. The major findings are.

1. The East India Coastal Current and its seasonal variation is related to the formation and evolution of VH/VL and SH/SL. With the formation of the anticyclonic VH and SH the EICC starts flowing northward off Sri Lanka and north of Visakhapatnam from January. The VH and SH grows and propagate towards each other and coalesce by April – May thus producing continuous northward EICC parallel to the east coast of India. The EICC is strongest off Visakhapatnam and off Sri Lanka especially in February – April. With the onset of the summer monsoon the EICC weakens. With the formation of the cyclonic VL and SL, the EICC turns southward north of Visakhapatnam and east of Sri Lanka from May and June respectively. The VL and SL grow and move toward each other, coalesce and a continuous southward EICC develop by October – November. The southward EICC is also strong off Visakhapatnam and Sri Lanka.

2. The EBBC is in general weak compared to EICC. The EBBC turns northward after the Fall transition (by December) and turns southward after the Spring transition (May – June). The EJ and equatorial waves generated during the transition period propagating along coastal boundary may play an important role in the changes in direction of the EBBC.

3. The CBBC is well developed when the EICC is strong. During both the seasons a major part of EICC re-circulates and feeds the CBBC. During the summer monsoon the northward moving CBBC is fed by the SMC and the EICC. On the other hand during February – May the southward CBBC is fed by the EICC and the WMC. The core of the CBBC shifts westward whenever the EICC is fully developed i.e., April – May and October – November. It is interesting to note that the VH/VL and SH/SL moves meridionally during the evolution of the EICC. In the Arabian Sea it is the zonally moving LH and LL regulate the WICC. The LH forms when the WICC is northerly and the first signal of reversal of the WICC occurs off the southwest coast of India by January – February when the LH detaches from the coast. The WICC is fed mostly by the WMC which has its origin from the eastern Bay of Bengal and to a lesser extent by the EICC during this period. The WICC fully becomes southerly as the LH moves away from the coast by April – May as the core of the WICC moves to central Arabian Sea to joins CASC along the western boundary of the LH. With the

progress of the season the CASC moves further westward and then flows northward, this is also fed by the winter Somali Current. During the summer monsoon the LL forms and the WICC changes direction (northward) as the LL detaches from the coast by July – August off the southwest coast of India. The CASC becomes southward along the western boundary of the LL and is fed by waters from the western Arabian Sea by the re-circulating waters of the LL. The core of southward the CASC moves westward as he the LL moves westward with the progress of season; and reaches the Somali coast by November.

4. The summer Somali Current (northward flowing) has its origin in the southern hemisphere in May associated with a strong anticyclonic eddy off the African coast. The Somali Current crosses the equator by June and the GW is formed centered around 7°N, 52°E. the SG is a smaller gyre and not well defined from SSH data. The SSH data indicate that the zone of maximum upwelling propagates northward with the progress of the summer monsoon and by September maximum upwelling occurs off the Arabia coast. Within the upwelling region there are indications of a number of cyclonic cells of about 200km diameter, which carries the upwelled water offshore and re-circulate along its boundaries. The unusually large upwelling zone (400 km offshore – Smith and Bottero, 1977) off Arabia may be sustained by these cells.

5. On the other hand the winter Somali Current is mostly fed by the LL which moved westward. Much of the water of the winter Somali Current re-circulates within the LL which reaches the Somali coast by November – December and partly flows southward of the equator. It is interesting to note that the core of the LL when it reaches Somali coast occurs almost at the location of the GW during summer.

6. The EJ driven by the westerly winds along the equator during the transition periods cause large positive SSH and subsequent geostrophic flow indicates that on an average the Spring EJ is stronger than the Fall EJ, through observations in some years showed otherwise. However it should be noted that at least in two years (1994 and 1997) the Fall EJ was absent, and it has affected the mean values. At the eastern

Indian Ocean the waters carried by the EJ flows to northern and southern hemisphere (as northeasterly and southeasterly currents).

7.  The WMC is conspicuous in the southern Bay of Bengal from November and feeds WICC and CASC. The WMC is observed in the entire width of the north Indian Ocean during February – March and weakens by April. On the other hand the SMC appears from June and continues up to September. Both the WMC and SMC are particularly strong south of Sri Lanka. Much of the waters of the SMC flow into the Bay of Bengal via the CBBC.

8.  The ECC is preserved in the Indian Ocean from south of equator mostly as a weak eastward flow during the winter monsoon. The ECC is a continuous flow only during March – April. The SEC is observed throughout the year between 10°S and 20°S. Within the SEC, large cyclonic (February – July) and anticyclonic (July – February) gyres originate in the eastern Indian Ocean propagate as far west as 70°E (with core at about 85°E) and then dissipate. The reason for this is not clear. Associated with the anticyclonic eddy there are strong eastward currents (SECC) centered around 13°S - 15°S in the southern tropical Indian Ocean. Much weaker SECC is also seen in other parts of southern tropical Indian Ocean associated with smaller eddies.

## 5.3 Summary of Chapter III

Strong interannual variability is noticed in the tropical Indian Ocean during the two positive IOD events 1994 – 1995 and 1997 – 1998. The major features during these years.

1.  The weakening/absence of the Fall Equatorial Jet.
2.  Early onset (August) and strengthening of WMC.
3.  Strengthening of southward EBBC and strong upwelling in the northern and the eastern Bay of Bengal.
4.  Weakening of the LH/LL.
5.  Discontinuity in the southward EICC during September – December.
6.  Weakening of the winter Somali Current.
7.  Weakening of the Somali upwelling and stronger GW.

8. Weakening/absence of the ECC.

9. Northward movement of the SEC by more than 600 km.

10. Strengthening of the SEC.

11. Strong SECC in the western Indian Ocean.

12. Late onset of the Somali eddy in the southern hemisphere.


## 5.3.1 Other Major findings of interannual variability

1. Year to year variations in the onset and characteristics of the LH/LL. A number of anticyclonic/cyclonic filaments in the northward/southward WICC – its locations and dimensions vary from year to year.

2. The GW and the SG    show considerable variation in the location, and dimension also vary from year to year. The core of the GW varies by 200 – 400 km interannually reasons still to be understood.

3. The SG is maintained by at least by two processes – in some years as an anticyclonic eddy and some years as a strong offshore flow at the southern edge of a large upwelling wedge.

4. The intensity and northward propagation of upwelling wedge vary from year to year.

5. The SG and the GW coalesced to form a single gyre only in 4 of the 14 years.

6.  The Socotra eddy also has shown different locations and dimensions during different years.

7. The anticyclonic/cyclonic filaments in the current system off the Arabian coast have different dimensions and characteristics during different years even when the mean large scale circulation is maintained.

8. The CASC is modulated by several eddies with different characteristics in different years.

9. In the Bay of Bengal the VH and the SH appear as strong anticyclonic eddies in few years, though in general the SH is weaker.

10. Though the VH and the SH merge to form continuous northward EICC in many years they keep their identity within the large scale EICC.

11. Due to the presence of cyclonic eddy between VH and SH (its size and intensity vary from year to year), the EICC in some years shifts eastward from the coast. The northward EICC flows close to the coast in some years but shifts further 100 -200 km eastward in some years. Further the EICC flows northeastward and re-circulate in some years but in other years it flow eastward at its northern limit to complete the gyre.

12. The SL undergoes large spatial shifts from year to year compared to the VL. In many years the VL and SL keep their identity within the large scale southward EICC. In addition, several other smaller cyclonic eddies within the southward EICC modulate the flow regionally with varying characteristics interannually.

13. There is a weakening of the northward CBBC during strong positive IOD events and strengthening during negative IOD events (1998)

14. The strength of the EJ varies from year to year during both Spring and Fall.

15. In some years the Spring EJ is stronger but in some other years the Fall EJ is stronger. There are few years when both the EJ were strong (1998) and both were weak or absent (1994 and 1997).

16. The SEC undergoes large scale (100 – 600 km) north-south shifts in different years

17. Several eddies modulate SEC in the regional scale which vary from year to year.

18. Weaker SMC and its intrusion into the Bay of Bengal shifted westward during strong positive IOD years.

19. The westward propagation and the strength of the WMC vary from year to year in a particular month.

20. Earlier onset of the WMC during positive IOD events.

21. The dimension of the cyclonic eddy off the east African coast (May) varies from year to year. Delayed formation (June) of this eddy during 1998.


### 5.3.2 The seasonal and interannual variation of SSH

The EOF analysis on monthly climatology revealed the following

1. The first EOF mode of SSH over the Indian Ocean accounts for 41% variance and has annual periodicity with extremes during winter and summer monsoons.

2. The second EOF mode also has annual periodicity and account for 28% variance. This mode has extremes during pre-monsoon and post-monsoon and shows variability associated with evolution of currents in the Arabian Sea and the Bay of Bengal. The first two modes are not in phase.

3. The third EOF mode accounts for 19% variance and has semiannual periodicity. It is mostly accounted by the equatorial currents – the semi-annual EJ.

The EOF analysis of monthly mean SSH during 1993-2004 revealed the following interannual variability

1. The IOD (first EOF mode) events account for the maximum variance (37%) in the interannual scale with opposite maxima in the eastern and the western Indian Ocean. Time series shows 18-month periodicity with coherence in 1994 – 1995 and 1997 – 1998. The amplitudes became weaker after 2001.

2. The second EOF mode accounts for 19% and also has 18-month periodicity. The major variances occur in the equatorial Indian Ocean, off the Indian coast, the Bay of Bengal and the Arabian Sea. This mode also could be related to IOD and may be occurring with a time lag.

3. The third EOF mode accounts for 14% variance and has a periodicity of about 36 months. The maximum variance is seen in the SEC, the Arabian Sea and the Bay of Bengal.

4. Therefore the EOF analysis showed two dominant periodicities in the SSH signal on 18-month and 36-month periods in agreement with Sakova et al (2006).

5. The wavelet analysis of SSH data showed both 18 and 36 month signals with the 18 month signal particularly strong from 1994 - 2001 and again from 2006. The reason for the weakening of the 18 month signal during 2000 – 2005 is not clear.

6. Perhaps the strong IOD signals are manifestation of constructive interference of 18 month and 36-month signals as suggested by Sakova et al (2006). The El Nino signal (not very clear in wavelet analysis) also may contribute to extreme IOD events.

**5.4 Summary of Chapter IV**

In this Chapter the brief theoretical background on planetary waves is discussed. The generating mechanisms and variability in the Indian Ocean presented.

Analysis of insitu climatological from Levitus et al 1994 data revealed the signatures of propagating features along the equator and along the 9°N. The thermocline depth got modulated with the passage of the waves.

To show the effect of propagating waves on the circulation in the Indian Ocean, two case studies one in the Arabian Sea and another in the Bay of Bengal are presented. In both the cases insitu measurements are used to support the occurrence of propagating waves.

In first case the formation of Laccadive High and its westward movement is controlled by the westward moving signatures seen along 9°N Hovmoller diagrams. It is also shown that the possibility of coastally trapped waves all the way coming from eastern Equatorial Ocean as reported in the modeling studies.

In the second case, the circulation in the Bay of Bengal is linked to the propagating waves observed both in insitu and satellite data.

The two cases presented show the influence of planetary waves on circulation in the Indian Ocean.


**5.5 Future work**

The intra-seasonal and interannual variability of surface currents and circulation is one of the least understood in the Indian Ocean. The present study has shown that these scales of variability over the entire Indian Ocean. Though large scale features are mostly recurring, the mesoscale and synoptic scale variability is unique during every year. Attempts to model this variability are meager and met with limited success. Hence a through understanding of the various physical processes and improvements in the model are critical in modeling all the scales of interannual variability. Long term direct measurements and satellite data are the key in understanding interannual variability.

**References**

1    Ali, M.M., S. Rashmi,  R. Cheney (1998), An Atlas of the North Indian Ocean eddies from T/P altimeter derived sea surface height, ISRO-SAC-SP –69098.

2    Anderson, D. L. T., and D. J. Carrington (1993), Modeling inter-annual variability in the Indian Ocean using momentum fluxes from the operational weather analyses of the United Kingdom Meteorological Office and European Centre for Medium Range Weather Forecasts. .Journal of Geophysical Research., 98, 12483–12499.

3    AVISO User Handbook (1997), Sea Level Anomalies (SLAs) AVI-NT-011-312-CN, Edition 3.0, p. 23. Cent, Natl. d'Etudes Spatiales, Toulouse, France

4    AVISO/Altimetry (1996), AVISO User Handbook for Merged TOPEX/POSEIDON products, AVI-NT-02-101, Edition 3.0. Cent, Natl. d'Etudes Spatiales, Toulouse, France

5    Babu, M.T., S. Prasanna Kumar, and D.P. Rao (1991), A subsurface cyclonic eddy in the Bay of Bengal, Journal of Marine  Research, 49, 404-410.

6    Banse, K. (1968). Hydrography of the Arabian Sea shelf of India and Pakistan and effects on demersal fishes. Deep Sea Res., 15, 45-79.

7    Baquero-Bernal, A., M. Latif, and M. Legutke (2002), On dipole like variability of sea surface temperature in the tropical Indian Ocean, J. Clim., 15, 1358-1368,.

8    Basil Mathew and GS Sharma (1982), Subthermocline flow in the intertropical Indian Ocean. Bullettin, Department of Marine Sciences, 13, 64-73.

9    Basu, S., S. D. Meyers, and J. J. O'Brien (2000), Annual and interannual sea level variations in the Indian Ocean from TOPEX/POSEIDON observations and ocean model simulations., Journal of  Geophysical  Research, 105, 975–994.

10   Bhat, G.S., S. Gadgil, P. V. Hareesh Kumar,  S. R. Kalsi,  P. Madhusoodanan, V. S. N. Murty, C. V. K. Prasada Rao,  V. Ramesh Babu, L.V.G. Rao, R.R. Rao, M. Ravichandran, K. G. Reddy,  P. Sanjeeva Rao, D. Sengupta, D. R. Sikka, J. Swain, P. N. Vinayachandran (2001), BOBMEX: The Bay of Bengal monsoon experiment, Bulletin of the American Meteorological Society 82, 2217–2243.

11   Bohm, E., M. Morrison,  V. J. A. Manghani, H. S. Kim, and C. N. Flagg (1999), Remotely sensed and acoustic Doppler observations of the Ras al Hadd Jet in 1994-95. Deep-Sea Res. II, 46, 1531-1549.

12    Boyer, T.P., and S. Levitus (1994), Quality control and processing of historical temperature, salinity and oxygen data. NOAA Technical Report NESDIS 81. U.S. Department of Commerce, Washington, DC, USA,65 pp.

13    Brandt, P., L. Stramma, F. Schott, J. Fischer, M. Dengler, and D. Quadfasel (2002), Annual Rossby waves in the Arabian Sea from TOPEX/POSEIDON altimeter and in-situ data. Deep-Sea Res. II, 49 (7),1197-1210.

14    Brink, K., R. Arnone, P. Coble, C. Flagg, B. Jones, J. Kindle, C. Lee, D. Phinney, M. Wood, C. Yentsch, and D. Young (1998), Monsoons boost biological productivity in Arabian Sea. EOS 79 (165), 168 - 169.

15    Bruce, J. G. (1968). Comparison of near surface dynamic topography during the two monsoons in the western Indian Ocean. Deep- Sea Research, 15, 665–667.

16    Bruce, J. G., D. R. Johnson, and J. C. Kindle (1994), Evidence for eddy formation in the eastern Arabian Sea during the northeast monsoon, Journal of Geophysical Research., 99, 7651–7664.

17    Bruce, J. G., J. C. Kindle, L. H. Kantha, J. L. Kerling, and J. F. Bailey (1998), Recent observations and modeling in the Arabian Sea Laccadive High region, Journal of Geophysical. Res., 103, 7593– 7600.

18    Bruce, J. G., M. Fieux and J. Gonella (1981), A note on the continuance of the Somali eddy after the cessation of the Southwest monsoon. Oceanologica Acta, 4, 7–9.

19    Busalacchi, A. J., and M. A. Cane (1988), The effect of varying stratification on low frequency equatorial motions. Journal of Physical Oceanography, **18**, 801–812.

20    Cane, M. A., (1980),  On the dynamics of equatorial currents, with application to the Indian Ocean. Deep Sea Research., **27**, 525–544.

21    Cane, M., and D. Moore (1981), A note on low frequency equatorial basin modes, Journal of Physical Oceanography, 11, 1578-1584,.

22    Carrington, D. J. and D. L. T. Anderson (1993), using an ocean model to validate ECMWF heat-fluxes. Quarterly Journal of the Royal Meteorological Society, 119, 1003- 1022.

23    Cipollini, P., D. Cromwell, M.S. Jones, G.D. Quartly and P.G. Challenor (1997), Concurrent altimeter and  infrared observations of Rossby wave propagation near 34°N in the northeast Atlantic", Geophysical Research Letters., **24**, 889- 892.

24    Clarke, A. J., and X. Liu (1994), Interannual Sea Level in the Northern and Eastern Indian Ocean. Journal of Physical Oceanography, 24, 1224–1235.

25    Colborn, J. G., (1975), Thermal Structure of the Indian Ocean, IIOE Oceanogr. Monogr., vol. 2, 173 pp., Univ. of Hawaii Press, Honolulu.

26    Cutler, A.N., and J.C. Swallow (1984), Surface currents of the Indian Ocean (to 25°S, 100°E): Compiled from historical data archived by the Meteorological Office, Bracknell, UK, Rep. 187, 8pp., 37 charts, Inst. of Oceanogr., Wormley, England,.

27    Darbyshire M. (1967), The surface waters off the coast of Kerala, southwest India. Deep-Sea Research, 14295-. 320.

28    DaSilva, A., A. C. Young, and S. Levitus (1994), Atlas of surface marine data 1994, volume 1.: Algorithms and procedures, Tech. Rep. 6, U.S. Department of Commerce, NOAA, NESDIS.

29    Defant, A. (1961), Water bodies and stationary current conditions at boundary surfaces, Physical Oceanography, Pergamon. New York, 1, 451–475.

30    Donguy, J. R., and G. Meyers (1995), Observation of geostrophic transport variability in the western tropical Indian Ocean. Deep-Sea Research **42**(6), 1007–28.

31    Dorandeu, J. and P.Y. Le Traon (1999), Effects of Global Mean Pressure variations on Sea Level changes from TOPEX/POSEIDON, Journal of Atmosphere, Oceanic Technol.,16, 1279-1283.

32    Ducet, N., P.-Y. Le Traon, and G. Reverdin (2000), Global high resolution mapping of ocean circulation from TOPEX/Poseidon and ERS-1/2, Journal Geophysical. Research, 105, 19,477–19,498.

33    Dueing, W. and F. Schott (1978), Measurements in the source region of the Somali Current during the monsoon reversal. Journal of Physical Oceanography, 8, 278–289.

34    Duing, W., (1970), The monsoon regime of the currents in the Indian Ocean. East west Centre Press, university of Hawai, Honolulu, 68pp.

35    Duing, W., and A. Leetma (1980), Arabian Sea cooling: A preliminary heat budget, Journal of Physical Oceanography, 10, 307-312.

36    Eigenheer, A., D. Quadfasel (2000), Seasonal variability of the Bay of Bengal circulation inferred from TOPEX/Poseidon altimetry, Journal of Geophysical Research 105, 3243–3252.

37    Elliot, A. J.,  and G. Savidge (1990), Some features of the upwelling off Oman. Journal of Marine Research, 48, 319–333.

38    Eriksen, C. C., (1979), An equatorial transect of the Indian Ocean, Journal of Marine Research, 37, 215–232,.

39    Eriksen, C. C., M. B. Blumenthal, S. P. Hayes, and P. Ripa (1983), Wind-generated equatorial Kelvin waves observed across the Pacific Ocean. Journal of Physical Oceanography, **13,** 1622–1640.

40    Evans, R. H., and O. B. Brown (1981), Propagation of thermal fronts in the Somali Current system. Deep-Sea Research, 28A, 521–527.

41    Fang, W., J. Guo, P. Shi  and Q. Mao (2006), Low frequency variability of South China Sea surface circulation from 11 years of satellite altimeter data, Geophysical Research Letters,. 33, L22612, doi:10.1029/2006GL027431,

42    Ffield, A., (1997), GRL special section: WOCE Indian Ocean expedition. Geophysical Research Letters 24, 2539–2540.

43    Fieux, M., H. Stommel (1977), Onset of the southwest monsoon over the Arabian Sea from marine reports of surface winds: structure and variability, Monthly Weather Review 105, 231-236.

44    Findlater, J., (1971), Mean monthly airflow at low levels over the western Indian Ocean. Geophysical Memoirs 115, 55–58.

45    Fischer, J., F. Schott, L. Stramma (1996), Currents and transports of the Great Whirl-Socotra Gyre system during the summer monsoon; August 1993, Journal of Geophysical Research, 101, 3573–3587

46    Flagg, C. A., and H.-S. Kim (1998),  Upper ocean currents in the northern Arabian Sea from shipboard ADCP measurements collected during the 1994–1996 U.S. JGOFS and ONR Programs. Deep-Sea Research II, 45, 1917–1959.

47    Fu, L., EJ Christensen, CA Yamarone, M. Lefebvre, Y. Menard, M. Dorrier and P. Escudier (1994),TOPEX/POSEIDON mission overview, Journal of Geophysical. Research, 99, 24,633-24642,.

48    Gent, P. R., K. O'Neill, and M. A. Cane, (1983), A model of the semiannual oscillation in the equatorial Indian Ocean. Journal of Physical Oceanography, **13,** 2148–2160.

49    Gill, A. E., and B. A. King, (1985), The effect of a shoaling thermocline on equatorially-trapped Kelvin waves. Dynamical Climatology, DCTN 27, 28 pp.

50    Gill, A.E., (1982), Atmosphere-Ocean dynamics, Academic press, 662 pp,.

51    Gilson, J. D. Roemmich, B. Cornuelle, and L.L. Fu (1998), Relationship of TOPEX/Poseidon altimetric height to steric height and circulation in the North Pacific, Journal of Geophysical Research, 103, 27947-27965,.

52    Gopalakrishna, V. V., S. M. Pednekar and V. S. N. Murty (1996), T-S variability and volume transport in the central Bay of Bengal during southwest monsoon, Indian Journal of Marine Sciences, 25:50–55.

53    Gopalan, A.K.S., V.V. Gopala Krishna, M.M. Ali and Rashmi Sharma (2000), Detection of Bay of Bengal Eddies from TOPEX and sea truth observation. Journal of Marine. Research, 58, 721-734.

54    Hacker, P., E. Firing, J. Hummon, A.I. Gordon and J.C. Kindle (1998), Bay of Bengal currents during the northeast monsoon. Geophysical Research Letters, 25(15), 2769-2772.

55    Han, W. and J.P. McCreary (2001), Modeling salinity distributions in the Indian Ocean, J.Geophys. Res., **106**, 859–877.

56    Han, W. and P.J. Webster (2002), Forcing mechanisms of sea level inter-annual variability in the Bay of Bengal, Journal of Physical Oceanography, 32, 216-239.

57    Han, W., (1999), Influence of salinity on dynamics, thermodynamics and mixed-layer physics in the Indian Ocean. Ph.D. thesis, Nova Southeastern University, Dania, FL, USA.

58    Han, W., D. M. Lawrence, P.J. Webster (2001), Dynamical response of equatorial Indian Ocean to intraseasonal winds: zonal flow, Geophysical Research Letters 28 (22), 4215–4218.

59    Han, W., J. P. McCreary, and K. Kohler (2001), Influence of precipitation minus evaporation and Bay of Bengal rivers on dynamics, thermodynamics, and mixed-layer physics in the upper Indian Ocean, J. Geophys.Res., 106, 6895–6916.

60    Han, W., J.P. McCreary, D.L.T. Anderson and A.J. Mariano, (1999), Dynamics of the eastward surface jets in the equatorial Indian Ocean. Journal of Physical Oceanography, 29(9), 2191-2209.

61    Hareesh Kumar PV and KV Sanilkumar (2004), Long period waves in the coastal region of North Indian Ocean,. Indian J Mar Sci, 33, 150-154.

62  Hareesh Kumar, P. V., and B. Mathew (1997), Salinity distribution in the Arabian Sea, Indian Journal of Marine Science., 26, 271– 277.

63  Hastenrath S., and L. L. Greischar (1991), The monsoonal current regimes of the tropical Indian Ocean. Observed surface flow fields and their geostrophic and wind driven components. Journal of Geophysical Research, 96:12619–12633,.

64  Howden, S. D., and R. Murtugudde (2001), Effect of river inputs into the Bay of Bengal. Journal of Geophysical Research, 106, 19825–19843.

65  Hughes, T. J., G.H. Denton, B.J. Andersen D.H. Schilling J.L. Fastook and C.S. Lingle, (1981), The last great ice sheets: a global view. In: G. H. Denton and T. J. Hughes (Editors), The Last Great Ice Sheets. Wiley--Interscience, New York, N.Y., pp. 263--317

66  Jacobs, G.A., R.H. Preller, S.K. Riedlinger and W.J. Teague, (1998), Coastal wave generation in the Bohai Bay and Propagation along the Chinese coast, Geophysical Research Letters, **25**, 777-780.

67  Jensen, T. G., (1993), Equatorial variability and resonance in a wind-driven Indian Ocean model. Journal of Geophysical Research, **98**, 22533–22552.

68  Kalyanidevasena., C. and S.P. Subramanian (1995), Study of seasonal current variability in the Arabian Sea using Geosat altimeter data, International Journal of Remote Sensing, , 65,14, 2691-2701.

69  Kantha, L.H., (1999), Monitoring the oceans using data-assimilative models: Implications for integrated in-situ and remote observing systems, In: Abstract, 3rd Symposium on Integrated Observing Systems, 79th AMS Annual Meeting, January 11–15, , Dallas, TX.

70  Kantha, L.H., J.-K. Choi, K. J. Schaudt, C. K. Cooper ( 2005),  A regional data-assimilative model for operational use in the Gulf of Mexico. In: Sturges, W. (Eds.), AGU Monograph on Recent Developments in the Circulation of the Gulf of Mexico.

71  Kantha, L.H., J.-K. Choi, R. Leben,  C. Cooper, M. Vogel, J. Feeney (1999), Hindcasts and real-time nowcast/forecasts of currents in the Gulf of Mexico, In: Offshore Technology Conference, May 3–6, 1999, Houston, TX.

72  Kantha,, T Rojsiraphisal , J Lopez (2008), The North Indian Ocean circulation and its variability as seen in a numerical hindcast of the years 1993–2004, Progress in Oceanography, 76 ,111–147

73  Kapala, A., K. Born, and H. Flohn (1994), Monsoon anomaly or an El Nin˜o event at the equatorial Indian Ocean? Catastrophic rains 1961/62 in East Africa and their teleconnections. In

Proceedings of the International Conference on monsoon variability and prediction (pp. 119–126). Trieste, Italy: WMO.

74 Kim, H.-S., N. Flagg and S. D. Howden (2001), Northern Arabian Sea variability from TOPEX/Poseidon altimetry data: an extension of the US JGOFS/ONR shipboard ADCP study. Deep-Sea Research II, 48, 1069–1096.

75 KNMI ATLAS (Koninklijk Nederlands Meteoroiogisch Institut) (1952) Indische Ocean Oceanographische en meteorologische gegevens, 2 edn. Publication no. 135.

76 Knox, R. (1976). On a long series of measurements of Indian Ocean equatorial currents near Addu Atoll. Deep-Sea Research, 23, 211–221.

77 Knox, R. A. and D. Halpern, (1982), Long range Kelvin wave propagation of transport variations in Pacific Ocean equatorial currents. Journal of Marine Research, **40**,329-339.

78 Kumar, S. P. and A. S. Unnikrishnan, (1995), The seasonal cycle of temperature and associated wave phenomena in the Bay of Bengal. Journal of Geophysical Research,**100**, 13585–13593.

79 La Fond, E. C., (1957), Oceanographic studies in the Bay of Bengal. Proc. Indian Acad. Sci.(B), 46(1):1-46

80 Le Traon, P.-Y. and F. Ogor (1998), ERS-1/2 orbit improvement using TOPEX/POSEIDON: the 2 cm challenge. Journal of Geophysical Research, 103, 8045-8057.

81 Le Traon, P.-Y., F. Nadal, and N. Ducet (1998), An improved mapping method of multisatellite altimeter data, J. Atmos. Oceanic Technol., 15, 522-534.

82 LeBlond, P.H., and L.A. Mysak (1978), Waves in the Ocean, Elsevier, pp 602.

83 Legeckis, R., (1987), Observation of a western boundary current in the Bay of Bengal. Journal of Geophysical Research, Vol. 92, 12974-12978.

84 Levitus, S., and T. P. Boyer, (1994), Temperature. Vol. 4, World Ocean Atlas 1994, NOAA Atlas NESDIS 4, 117 pp.

85 Levitus, S., R. Gelfeld, T. Boyer, and D. Johnson (1994), Results of the NODC Oceanographic Data and Archaeology and Rescue Project. Key to Oceanographic Records Documentation; 19–73.

86 Lukas, R., S. P. Hayes and K. Wyrtki (1984) Equatorial sea level response during the 1982–83 El Ni~no. Journal of Geophysical Research, **89**, 10,425–10,430.

87    Luther, M. E. (1999). Interannual variability in the Somali Current 1954–1976. Nonlinear Analysis. Theory, Methods and Applications. An International Multidisciplinary Journal, 35, 59–83.

88    Luther, M. E., and J. J. O'Brien (1985). A model of the seasonal circulation in the Arabian Sea forced by observed winds. Progr. Oceanogr., 14, 353–385.

89    Luyten, J. R., and J. C. Swallow (1976), Equatorial undercurrents. Deep-Sea Research, 23, 999–1001.

90    Luyten, J.R., D.H. Roemmich (1982), Equatorial currents at semiannual period in the Indian Ocean. Journal of Physical Oceanography 12, 406–413.

91    Luyten, J.R., Fieux, M., J. Gonella (1980), Equatorial currents in the western Indian Ocean. Science 209, 600–603.

92    Martin, J.M., J.D. Burton and D. Eisma(Eds.) (1981)  River inputs to ocean systems, 384 pp, United Nation Press, Geneva,.

93    Masumoto, Y., and G. Meyers (1998), Forced Rossby waves in the southern tropical Indian Ocean. Journal of Geophysical Research, 103, 27589–27602.

94    McClean, J. L., D. P. Ivanova and J. Sprintall (2005), Remote origins of interannual variability in the Indonesian throughflow region from data and a global Parallel Ocean Program simulation, Journal of Geophysical Research, 110, C10013, doi:10.1029/2004JC002477.

95    McCreary J. P. and P. Kundu (1988), A numerical investigation of the Somali current during the southwest monsoon. Journal of Marine Research, 46:25–58,

96    McCreary Jr., J.P., P.K. Kundu, R.L. Molinari (1993), A numerical investigation of dynamics, thermodynamics and mixed layer processes in the Indian Ocean, Progress in Oceanography 31, 181–244.

97    McCreary, J. P., and P. K. Kundu (1988). A numerical investigation of the Somali Current during the Southwest Monsoon. Journal of Marine  Research, 46, 25–58.

98    McCreary, J. P., K. E. Kohler, R. R. Hood, S. Smith, J. Kindle, A. S. Fischer, and R. A. Weller (2001), Influences of diurnal and intraseasonal forcing on mixed-layer and biological variability in the central Arabian Sea, Journal of Geophysical Research, 106, 7139–7155.

99    McCreary, J.P., W. Han, D. Shankar and S.R. Shetye (1996), Dynamics of the east India coastal current. 2. Numerical solutions, Journal of Geophysical Research, 101, 13993-14010,.

100  McPhaden, M. (1982), Variability in the central Indian Ocean. Part I: Ocean dynamics. Journal of Marine Research, 40, 157–176.

101  Meehl, G. A., and J. M. Arblaster (2002), Indian monsoon GCM sensitivity experiments testing tropospheric biennial oscillation transition conditions, Journal of Climatology, 15, 923-944.

102  Molinari, R. L., D. Olson and G. Reverdin (1990), Surface current distributions in the tropical Indian Ocean derived from compilations of surface buoy trajectories. Journal of Geophysical Research, 95, 7217–7238.

103  Moore, D.W. and S. G. H. Philander (1977), Modeling of the tropical oceanic circulation. In The Sea, E. D. Goldberg, I. N. McCave, J. J. O'Brien and J. H. Steele, Eds., Vol. 6, pp. 319–361, Wiley Interscience, New York.

104  Morrow, R. and F. Birol (1998), Variability in the southeast Indian Ocean from altimetry: forcing mechanisms for the Leeuwin Current Journal of Geophysical Research, 103(C9), 18529-18544.

105  Murthugudde, R., J.P. McCreary Jr., A.J. Busalacchi  (2000), Oceanic processes associated with anomalous events in the Indian Ocean with relevance to 1997–1998. Journal of Geophysical Research ,105, 3295–3306.

106  Murty, C.S., and V.V.R. Varadachari (1968), Upwelling along the east coast of  India, Bull. Nat. Inst. Sci. India, 36, 80-86.

107  Murty, V. S. N., M. S. S. Sarma, B. P. Lambata, V. V. Gopalakrishna, S. M. Pednekar, A. S. Rao, A. J. Luis, A. R. Kaka, and L. V. G. Rao (2000), Seasonal variability of upper-layer geostrophic transport in the tropical Indian Ocean during 1992–1996 along TOGA-I XBT tracklines. Deep-Sea Research I, 47, 1569–1582.

108  Murty, V. S. N., Y. V. B. Sarma, D. P. Rao, and C. S. Murty (1992), Water characteristics, mixing and circulation in the Bay of Bengal during southwest monsoon, Journal of Marine Research,  **50,** 207–228.

109  Narayana Pillai V, P.K. Vijayarajan and A. Nandakumar (1980) Oceanographic investigations off the southwest coast of India. FAO/UNDP Report, (FAO, Rome), pp 51.

110  Pankajakshan, T. and D. V. Rama Raju (1987), Intrusion of Bay of Bengal water into Arabian Sea along the west coast of India during north east monsoon.. In Contributions in Marine Sciences (eds Rao, T. S. S., Natarajan, R., Desai, B. N., Swami, G. N. and Bhat, S. R.), Dr S. Z.

Qasim Sastyabdapurti felicitation volume, National Institute of Oceanography, Goa, India, , pp. 237–244

111 Parke, M., G. Born, R. Leben, C. McLaughlin, and C. Tierney (1997), Altimeter sampling haracteristics using a single satellite, Journal of Geophysical Research, 103, 10513,.

112 Pedloskey , J, Geophysical Fluid Dynamics, Springer-Verlag pp 624, 1979.

113 Perigaud, C. and P. Delecluse (1992), Annual sea level variations in the southern tropical Indian Ocean from geosat and shallow water simulations. Journal of Geophysical Research, **97**, 20169–20178.

114 Pond, S., and G.L. Pickard, (1983), Introductory Dynamical Oceanography, - 2nd ed., Pergamon Press, 329pp.

115 Potemra, J. T., M. E. Luther and J. J. O'Brien (1991), The seasonal circulation of the upper ocean in the Bay of Bengal. Journal of Geophysical Research, 96, 12667–12683.

116 Prasanna Kumar, S., H. Snaith, P. Chellenor, and H.T. Guymer (1998),  Seasonal and inter-annual sea surface height variations of the northern Indian Ocean from the TOPEX/POSEIDON altimeter, Indian  Journal of Marine Science. , 27, 10-16.

117 Quadfasel, D., and F. Schott (1983), Southward subsurface flow below the Somali Current. Journal of Geophysical Research, 88, 5973–5979.

118 Raghunadha Rao A., P.G.K. Murty, and Basil Mathew (2001), Geostrophic currents using Topex/Poseidon altimeter data in the Indian ocean, ISRS -2001.

119 Ramasastry A.A., and P. Myrland (1959), Distribution of temperature, salinity and density in the Arabian Sea along the South Malabar coast (south India) during the post-monsoon season. Indian Journal of Fisheries, 6, 223-255.

120 Rao, A.S., (1998),  Rossby waves in the Bay of Bengal: observations and simulations. Ph.D. thesis, Andhra University, Vishakhapatnam, India.

121 Rao, K. H., M. K. Antony, C. S. Murty, and G. V. Reddy (1986), Gyres in the NW Bay of Bengal-Some observed evidences, Indian Journal of Marine Science, 16,9-14,.

122 Rao, R.R., R.L Molinari, and J.F. Festa (1991), Surface meteorological and near surface oceanographic Atlas of the tropical Indian Ocean, US Govt. printing press, 59.

123 Rao, R.R., R.L. Molinari, and J.F. Festa, (1989), Evolution of the climatological near-surface thermal structure of the tropical Indian Ocean. Part 1: Description of mean monthly mixed-layer

depth and sea-surface temperature, surface current and surface meteorological fields. Journal of Geophysical Research, 94(C8), 10801-10815.

124 Rao, S. A., S. K. Behera, Y. Masumoto, and T. Yamagata (2002), Interannual subsurface variability in the tropical Indian Ocean with a special emphasis on the Indian Ocean Dipole, Deep Sea Res., Part II, 49, 1549-1572.

125 Rao, Y.P. (1981), The climate of the Indian subcontinent. In: world survey of climatology, vol 9: Climates of southern and western Asia, K. Takahashi and H. Arakawa (eds.), Elsevier Scientific, Amsterdam,67-119,.

126 Reppin, J., F. Schott, A. J. Fischer, and D. Quadfasel (1999), Equatorial currents and transports in the upper central Indian Ocean. Journal of Geophysical Research, **104**(C7), 15495–514.

127 Ripa, P. and S. P. Hayes (1981), Evidence for equatorial trapped waves at the Galapagos Islands. Journal of Geophysical Research, **86**, 6509-6516.

128 Saji, N. H., B. N. Goswami, P. N. Vinayachandran, and T. Yamagata, (1999). A dipole in the tropical Indian Ocean. Nature, London,401, 360–363.

129 Sakova I. V, G Meyers , R. Coleman (2006), Interannual variability in the Indian Ocean using altimeter and IX1-expendable bathy-thermograph (XBT) data: Does the 18-month signal exist?, Geophysical Research Letters, 33, L20603, doi:10.1029/2006GL027117,

130 Sanilkumar, K.V., T.V. Kuruvilla, D. Jogendranath and R.R. Rao (1997), Observations of the western boundary current of the Bay of Bengal from a hydrographic survey during March 1993. Deep Sea Res., 44, 135-145.

131 Saunders, P.M., and B.A. King (1995), Oceanic fluxes on the WOCE A11 section, Journal of Physical Oceanography, **25**, 1942-1958.

132 Scharroo, R. and P. Visser (1998), Precise orbit determination and gravity field improvement for the ERS satellites. Journal of Geophysical Research, 103, 8113-8127.

133 Schott, F. (1983), Monsoon response of the Somali Current and associated upwelling. Progress in Oceanography, 12, 357–381.

134 Schott, F., and D. Quadfasel (1982), Variability of the Somali Current and associated upwelling. Progress in Oceanography, 12, 357–381.

135 Schott, F., and J. Fischer (2000), Winter monsoon circulation of the northern Arabian Sea and Somali Current. Journal of Geophysical Research, 105, 6359– 6376.

136  Schott, F., and J. P. McCreary (2001), The monsoon circulation of the Indian Ocean. Progress in Oceanography, 51, 1–123.

137  Schott, F., J. C. Swallow, and M. Fieux (1990), The Somali Current at the equator: annual cycle of currents and transports in the upper 1000 m and connection to neighboring latitudes. Deep-Sea Res., 37, 1825–1848.

138  Schott, F., J. Fischer, U. Garternicht, and D. Quadfasel (1997), Summer monsoon response of the Northern Somali Current (1995), Geophysical Research Letters, 24, 2565–2568.

139  Schott, F., J. Reppin, and J. Fischer (1994), Currents and transports of the Monsoon Current south of Sri Lanka, Journal of Geophysical Research, **99**(C12), 25127–41. .

140  Schott, F., J. Reppin, J. Fischer, and D. Quadfasel (1994), Currents and transports of the Monsoon Current south of Sri Lanka. Journal of Geophysical Research, 99, 25127–25141.

141  Schott, F., J.P. McCreary (2001), The monsoon circulation of the Indian Ocean. Progress in Oceanography 51, 1–123.

142  Schott, F., M. Fieux, J. Kindle, J. Swallow and R. Zantopp (1988), The boundary currents east and north of Madagascar. Part 2: Direct measurements and model comparisons. Journal of Geophysical Research, 93, 4963-4974.

143  Sengupta, D. and R. Ravichandran (2001), Oscillations of Bay of Bay of Bengal SST during 1998 summer monsoon, Geophysical Research Lettters., 28, 2033-2036.

144  Sengupta, D., B.N. Goswami and R. Senan (2001), Coherent intra-seasonal oscillations of ocean and atmosphere during Asian summer monsoon, Geophysical Research Letters, 28, 4127-4130.

145  Shankar D (2000), Seasonal cycle of sea level and currents along the coast of India, Cur Sci, 78, 279-288.

146  Shankar, D. and S.R. Shetye (1997), On the dynamics of the Lakshadweep high and low in the southeastern Arabian Sea. Journal of Geophysical Research, **102**, 12551–12562.

147  Shankar, D. P. N. Vinaychandran, and A.S. Unnikrishnan (2002), The monsoon currents in the North Indian Ocean , Progress in Oceanography, 52(1),63 120.

148  Shankar, D., (1998), Low-frequency variability of sea level along the coast of India. Ph.D. thesis, Goa University, Goa, India.

149 Shankar, D., and S. R. Shetye (1999), Are interdecadal sea level changes along the Indian coast influenced by variability of monsoon rainfall? Journal of Geophysical Research, 104, 26031–26042.

150 Shankar, D., J.P. McCreary, W. Han and S.R. Shetye (1996), Dynamics of the East India Coastal Current: 1. Analytic solutions forced by interior Ekman pumping and local alongshore winds. Journal of Geophysical Research, **101**, 13975–13991.

151 Shankar, D., P. N. Vinayachandran, and A. S. Unnikrishnan (2002), The monsoon currents in the north Indian Ocean. Progress in Oceanography., **52**, 63–120.

152 Shenoi S. S. C.,  D. Shankar, and S. R. Shetye (1999b), On the sea surface temperature high in the Lakshadweep Sea before the onset of the southwest monsoon, Journal of Geophysical Research, 104, 15703–15712.

153 Shenoi S. S. C., P. K. Saji1 and A. M. Almeida (1999a), Near-surface circulation and kinetic energy in the tropical Indian Ocean derived from Lagrangian drifters, Journal of Marine Research, 57, 885–907.

154 Shetye, S. R., A. D. Gouveia, S. S. C. Shenoi, D. Sundar, , G. S. Michael, A. M. Almeida, and K. Santanam (1990), Hydrography and circulation off the west coast of India during the Southwest Monsoon 1987. Journal of Marine Research., 48, 359–378.

155 Shetye, S. R., A. D. Gouveia, S. S. C. Shenoi, D. Sundar, , G. S. Michael,  and G. Nampoothiri, (1993), The western boundary current of the seasonal subtropical gyre in the Bay of Bengal. Journal of Geophysical Research, 98, 945–954.

156 Shetye, S.R., A.D. Gouveia, D. Shankar, S.S.C. Shenoi, P.N. Vinaychandran, D. Sunder, G.S. Michael, and G. Nampoothiri (1996), Hydrography and circulation in the western Bay of Bengal during the Northeast monsoon, Journal of Geophysical Research, 101, 14,011-14,025.

157 Shetye, S.R., A.D. Gouveia, S.S.C. Shenoi, D. Sunder, G.S. Michael, A.M. Almeida, and K. Santanam, (1991), The coastal current of western India during the northeast monsoon, Deep Sea Res., Part A, 38,1517-1529,.

158 Shi, W., J. M. Morrison, E. Bo¨hm, and V. Manghnani (1999), Remotely sensed features in the US JGOFS Arabian Sea Process Study. Deep-Sea Res. II, 46, 1551–1575.

159 Smith, R.L. and J.S. Bottero (1977), On upwelling in the Arabian Sea. In: A Voyage of Discovery, M. ANGEL, editor, Pergamon, New York, 291-304.

160 Somayajulu, Y.K, T.V.R Murthy, S.P. Kumar and J.S. Sastry (1987), Hydrographic characteristics of central Bay of Bengal during SW monsoon, Indian Journal of Marine Science., 16, 207–217.

161 Sprintall, J., A. Gordon, R. Murtugudde, and D. Susanto (2000), A semiannual Indian Ocean forced Kelvin wave observed in the Indonesian Seas in May 1997. Journal of Geophysical Research, 105, 17217-17230.

162 Stanley, H.R (1979), The Geos-3 Project, Journal of Geophysical Research, **84**, 3779-3783,.

163 Stramma, L., J. Fischer, and F. Schott (1996), The flow field off southwest India at 8°N during the southwest monsoon of August 1993. Journal of Marine Research., 54, 55–72.

164 Stramma, L., J.R.E. Lutjeharms (1997), The flow field of the subtropical gyre of the South Indian Ocean, Journal of Geophysical Research 102, 5513–5530.

165 Subrahmanyam, B., I. S. Robinson, J. R. Blundell and P. G. Challenor (2001), Rossby Waves in the Indian Ocean from TOPEX/POSEIDON altimeter and model simulations, International Journal of Remote Sensing, 22, 141–167.

166 Swallow JC., (1981), Evolution of near-surface features in the Somali Current. In : Recent Progress in Oceanography, JP McCreary, DW Moore and JM Witte (Eds.), Nova University/NYIT Press, 381-306.

167 Swallow, J. C., F. Schott, and M. Fieux (1991), Structure and transport of the East African Coastal Current, Journal of Geophysical Research, 96, 22254–22267.

168 Swallow, J. C., M. Fieux, and F. Schott (1988), The boundary currents east and north of Madagascar, Part I: Geostrophic currents and transports. Journal of Geophysical Research, 93, 4951–4962.

169 Swallow, J. C., R. L. Molinari, J. G. Bruce, O. B. Brown, and R. H. Evans (1983), Development of near-surface flow pattern and water mass distribution in the Somali Basin in response to the southwest monsoon of 1979, Journal of Physical Oceanography, 13, 1398-1415.

170 Swallow, J.C. and J.G. Bruce (1966), Current measurements off the Somali coast during the southwest monsoon of 1964. Deep-Sea Res., 13(5), 861-888

171 Tapley, B.D., D.P. Chambers, C.K. Shum, R.J. Eanes, J.C. Ries, and R.H. Stewart (1994), Accuracy assessment of the large-scale dynamic topography from TOPEX/POSEIDON altimetry, Journal of Geophysical Research., 99, 24605--24617,.

172  Tourre, Y. M., and W. B. White (2003), Patterns of Coherent Climate Signals in the Indian Ocean during the 20th Century, Geophysical Research Letters, 30(23), 2224, doi:10.1029/2003GL018476.

173  Unnikrishnan, A. S., S.P. Kumar and G.S., Navelkar (1997),  Large-scale processes in the upper layers of the Indian Ocean inferred from temperature climatology. Journal of Marine  Research., **55**, 93–115.

174  Unnikrishnan, A. S., V. S. N. Murty, M. T. Babu, C. K. Gopinathan, and R. J. K. Charyulu (2001), On the anomalous current structure in the eastern equatorial Indian Ocean during southwest monsoon of 1994. Marine and Freshwater Research, 52, 727–734.

175  Varadachari, V. V. R. and G. S. Sharma (1967), Circulation of the surface waters in the north Indian Ocean, Journal of Indian Geophysical Union, , **IV**, 61–73.,

176  Varkey, M.J., V.S.N. Murty, and A. Suryanarayana (1996), Physical Oceanography of the Bay of Bengal and Andaman Sea, Oceangr. and Mar. Biology: an annual review, **34**, 1-70.

177  Vinayachandran P. N., J. Kurian, C. P. Neema (2007), Indian Ocean response to anomalous conditions in 2006, Geophysical Research Letters, 34, L15602, doi:10.1029/2007GL030194.

178  Vinayachandran, P. N. and T. Yamagata (1998),  Monsoon response of the sea around Sri Lanka: generation of thermal domes and anticyclonic vortices. Journal of  Physical Oceanography, **28**, 1946–1960.

179  Vinayachandran, P. N., S.R. Shetye, D. Sengupta and S. Gadgil (1996), Forcing mechanisms of the Bay of Bengal circulation. Curr. Sci., **71**, 753–763.

180  Vinayachandran, P. N., Y. Masumoto, T. Mikawa, and T. Yamagata (1999), Intrusion of the Southwest Monsoon Current into the Bay of Bengal. Journal of Geophysical Research, 104, 11077–11085.

181  Warren, B., Stommel, H , Swallow, J C. (1966), Water masses and patterns of flow in the Somali Basin during the southwest monsoon of 1964. Deep Sea Res. 13, 825-860

182  Webster, P. J A. M. Moore, J. P. Loschnigg, and R. R. Leben (1999), Coupled ocean–atmosphere dynamics in the Indian Ocean during 1997–98. Nature, **401,** 356–360.

183  Webster, P. J. (2002), The JASMINE pilot study, Bull. Am. Meteorol. Soc., 83, 1603-1630,

184  Wirth A., J. Willebrand and F. Schott (2002),Variability of the Great Whirl from observations and models, Deep Sea Research Part II: Topical Studies in Oceanography, Volume 49, Issues 7-8, Pages 1279-1295.

185  Wunsch, C., (1993), Physics of the ocean circulation, in F. Sansò and R. Rummel, eds., Oceanography

186  Wyrtki, K (1971), Oceanographic Atlas of the International Indian Ocean Expedition, National Science foundation, Washington, D.C., 531

187  Wyrtki, K. (1973), An equatorial jet in the Indian Ocean, Science, 181, 262–264.

188  Yu , L., J.J. O'Brien, J. Yang (1991), On the remote forcing of the circulation in the Bay of Bengal, J. Geophys. Res., **96**, 20449-20454.